INTERCOMPARISON OF GRACE-BASED GROUNDWATER LEVEL CHANGE AND IN-SITU MEASUREMENTS OVER CENTRAL ANATOLIA BASINS, TURKEY

A THESIS SUBMITTED TO
THE GRADUATE SCHOOL OF NATURAL AND APPLIED SCIENCES
OF
MIDDLE EAST TECHNICAL UNIVERSITY

BY

İPEK GÜL KARASU

IN PARTIAL FULFILLMENT OF THE REQUIREMENTS
FOR
THE DEGREE OF MASTER OF SCIENCE
IN
CIVIL ENGINEERING

AUGUST 2019

Approval of the thesis:

INTERCOMPARISON OF GRACE-BASED GROUNDWATER LEVEL CHANGE AND IN-SITU MEASUREMENTS OVER CENTRAL ANATOLIA BASINS, TURKEY

submitted by **İPEK GÜL KARASU** in partial fulfillment of the requirements for the degree of **Master of Science in Civil Engineering Department, Middle East Technical University** by,

Prof. Dr. Halil Kalıpçılar
Dean, Graduate School of **Natural and Applied Sciences** _____

Prof. Dr. Ahmet Türer
Head of Department, **Civil Engineering** _____

Assoc. Prof. Dr. M.Tuğrul Yılmaz
Supervisor, **Civil Engineering, METU** _____

Examining Committee Members:

Prof. Dr. Elçin Kentel Erdoğan
Civil Engineering, METU _____

Assoc. Prof. Dr. M.Tuğrul Yılmaz
Civil Engineering, METU _____

Prof. Dr. İsmail Yücel
Civil Engineering, METU _____

Assoc. Prof. Dr. Yakup Darama
Civil Engineering, Atılım University _____

Assist. Prof. Dr. Gülizar Özyurt Tarakcıoğlu
Civil Engineering, METU _____

Date: 27.08.2019

I hereby declare that all information in this document has been obtained and presented in accordance with academic rules and ethical conduct. I also declare that, as required by these rules and conduct, I have fully cited and referenced all material and results that are not original to this work.

Name, Surname: İpek Gül Karasu

Signature:

ABSTRACT

INTERCOMPARISON OF GRACE-BASED GROUNDWATER LEVEL CHANGE AND IN-SITU MEASUREMENTS OVER CENTRAL ANATOLIA BASINS, TURKEY

Karasu, İpek Gül
Master of Science, Civil Engineering
Supervisor: Assoc. Prof. Dr. M.Tuğrul Yılmaz

August 2019, 118 pages

The purpose of this study is to validate the satellite- (GRACE) and hydrological model- (GLDAS) based groundwater storage (GWS) change information using in-situ groundwater level observations and investigate the accuracy of Gravity Recovery and Climate Experiment (GRACE) retrievals over Central Anatolia. In this study, GRACE-derived GWS changes from January 2003 to December 2015 are compared with in-situ groundwater level observations from five basins comprising Central Anatolia Basin. The basin areas range between 7,605 km^2 and 233,929 km^2 which are relatively small according to the footprint of GRACE. It is expected that as the basin area increases the accuracy of GRACE-based GWS variations increase. Also, GRACE is skillful to monitor the large mass changes. The highest correlation between GRACE-based GWS and in-situ observations are found between 0.48 and 0.66 and widely ascribed to the seasonal component. Although Akarçay Basin has the lowest surface area, it has a correlation value about 0.53 which is higher than the correlation value of Central Anatolia Basin ($r \approx 0.45$). Especially, in Konya Closed Basin, where groundwater levels are significantly decreasing, the correlation coefficient becomes 0.44. This implies that Global Land Data Assimilation System (GLDAS) estimates and GRACE signals do not represent the ground conditions precisely. Despite these

results, GRACE-derived terrestrial water storage variations agreed well with the droughts occurred over Turkey in between 2007-2009 and 2014.

Keywords: Central Anatolia, GLDAS, GRACE, Groundwater, Terrestrial Water Storage

ÖZ

GRACE UYDU GÖZLEMLERİNE DAYANAN YERALTI SUYU SEVİYE DEĞİŞİMİ VERİSİNİN ORTA ANADOLU HAVZALARI ÜZERİNDE YER GÖZLEM VERİLERİ İLE KARŞILAŞTIRILMASI

Karasu, İpek Gül
Yüksek Lisans, İnşaat Mühendisliği
Tez Danışmanı: Doç. Dr. M.Tuğrul Yılmaz

Ağustos 2019, 118 sayfa

Bu çalışmanın amacı uydu ve modele dayalı yeraltısuyu rezervi değişim verisini yer gözlemleri ile doğrulamak ve Gravity Recovery and Climate Experiment (GRACE) uydusundan elde edilen tahminlerin Orta Anadolu üzerindeki hassasiyetini araştırmaktır. Bu çalışmada, GRACE'den elde edilen yeraltısuyu rezervindeki değişim verisi Ocak 2013 ile Aralık 2015 arasında Orta Anadolu'yu kapsayan beş havzadaki yeraltı suyu seviye gözlemleri ile kıyaslanmıştır. Bu havzaların alanları 7,605 km^2 ve 233,929 km^2 arasında değişmektedir. Bu alanlar GRACE uydusunun mekansal çözünürlüğüne göre nispeten küçüktür. Havza alanı arttıkça GRACE'den elde edilen yeraltısuyu miktarındaki değişimin doğruluğunun artması beklenmektedir. Ayrıca, kütledeki büyük değişimler GRACE tarafından algılanmaktadır. GRACE'e dayalı yeraltısuyu rezervi değişimi ile yer gözlem verileri arasındaki en yüksek korelasyon değerleri 0.48 ile 0.66 arasında değişmektedir ve bu değişim sezonsal bileşenden kaynaklanmaktadır. Akarçay Havzası en küçük yüzey alanına sahip olmasına rağmen korelasyon değeri 0.53 civarındadır. Bu değer ise Orta Anadolu Havzası'nın korelasyonundan ($r \approx 0.45$) büyüktür. Özellikle, yeraltısuyu seviyelerinin önemi ölçüde azaldığı Konya Kapalı Havzası'nda korelasyon değeri 0.44'tür. Bu durum GLDAS model tahminleri ve GRACE sinyallerinin yüzeydeki şartları doğru

temsil etmediği anlamı taşımaktadır. Bu sonuçlara rağmen, GRACE karasal su deposundaki değişimler 2007-2009 ve 2014 yılları arasında Türkiye'de gerçekleşen kuraklıklarla örtüşmektedir.

Anahtar Kelimeler: Orta Anadolu, GLDAS, GRACE, Yeraltı Suyu, Karasal Su Deposu

To my beloved parents and in memory of my grandmother Makbule Kalkanlı with love and respect

ACKNOWLEDGEMENTS

This thesis is a product of collaborative work supported by many people in their own ways. First of all, I would like to thank my supervisor Assoc. Prof. Dr. M. Tuğrul Yılmaz for encouraging me to work on such an interesting subject and for his suggestions and comments. I would also like to thank Assoc. Prof. Dr. Koray Yılmaz who shared his knowledge and guidance.

I would like to thank MGM, DSİ and NASA for providing data.

I am also grateful to my friends: Burak Bulut, Mahdi Hesami Afshar, Muhammad Amjad, Kaveh Patakchi Yousefi, Ali Ulvi Galip Şenocak and Eren Düzenli for their support, vision and joyful conversations. I would especially thank my dearest friend Eren Düzenli for his guidance and valuable friendship.

I would like to thank my home mates Zarife and Kaplan which are the best cats in the world.

I am grateful to my cousin Duygu Kalkanlı and my friend Heval Ataş for their friendship, guidance and advice.

My special thanks to my precious sister Nazlı Barçın Doğan for her endless support and lifelong friendship. I know that I will always become stronger when she is beside me.

I would like to thank Serbaycan Metin who supported me patiently and was always there for me; his presence means a lot to me.

I would also like to thank my grandmother Zahide Karasu and my aunt Gülsen Karasu for their wisdom and endless support.

I would like to express my deepest thanks to my father Atalay Karasu and my mother Ayşe Kalkanlı Karasu for their endless patience, support and confidence in me throughout my life.

I would like to thank the loving memory of Nurcan Ersoy.

I would like to thank my grandmother Makbule Kalkanlı with all my respect and longing.

TABLE OF CONTENTS

LIST OF TABLES

TABLES

LIST OF FIGURES

FIGURES

LIST OF ABBREVIATIONS

AGRMET: Air Force Weather Agency's AGRicultural METeorological Model

AVHRR: Advanced Very High Resolution Radiometer

CDFM: Cumulative Deviation from Mean

CLM: Common Land Model

CMAP: Climate Prediction Center Merged Analysis of Precipitation

CSR: Center for Space Research

CWC: Canopy Water Content

DLR: Deutsches Zentrum für Luft- und Raumfahrt

DSİ: General Directorate of State Hydraulic Works of Turkey

ENSO: El Niño–Southern Oscillation

EWH: Equivalent Water Height

EWT: Equivalent Water Thickness

GDAS: NCEP's Global Data Assimilation System

GFZ: GeoForschungsZentrum Potsdam

GLDAS: Global Land Data Assimilation System

GPCP: Global Precipitation Climatology Project

GPSS: Global Navigation Satellite System

GRACE: Gravity Recovery and Climate Experiment

GSFC: Goddard Space Flight Center

GWS: Groundwater Storage

JPL: Jet Propulsion Laboratory

KCB: Konya Closed Basin

KMB: Kırşehir Massive Block

LSM: Land Surface Model

MGM: Turkish State Meteorological Service

MODIS: Moderate Resolution Imaging Spectroradiometer

MTA: General Directorate of Mineral Research and Exploration

NAO: North Atlantic Oscillation

NASA: National Aeronautics and Space Administration

NCAR: National Center for Atmospheric Research

NCEP: National Centers for Environmental Prediction

NDVI: Normalized Difference Vegetation Index

NOAA: National Oceanic and Atmospheric Administration

NOAH: The National Centers for Environmental Prediction (NCEP)/Oregon State University/Air Force/Hydrologic Research Lab Model

RMS: Root Mean Square

scPDSI: Self-calibrating Palmer Drought Severity

SH: Spherical Harmonics

SM: Soil Moisture

SW: Surface Water

SWE: Snow Water Equivalent

Sy: Specific Yield

SZB: Sakarya Zone Block

TAB: Tauride-Anatolide Block

TRMM: Tropical Rainfall Measuring Mission

TWS: Terrestrial Water Storage

VIC: Variable Infiltration Capacity

CHAPTER 1

INTRODUCTION

Water is an essential element to maintain the existence of civilizations for centuries. Groundwater reservoirs are regarded as important alternatives for surface water resources as fresh water. Globally, 43% of the irrigation water is supplied from groundwater (Siebert et al., 2010), while this ratio is around 20-25% over Turkey (Kibaroglu et al., 2011). The stresses on water supplies aggravated by climate change as well as the increase in the population become an unpredictable problem. Especially, the excessive amount of groundwater extraction becomes a global issue. So, maintaining the sustainability of this natural resource is critically essential for the countries' economic development. Therefore, it is important to quantify the changes in groundwater storage.

There are many types of groundwater monitoring methods such as conceptual modeling, observation well sampling, geophysical and remote sensing techniques. Although conceptual model specify the consequences of abstraction or remediation scenarios, it should be validated with well samplings. Also, models require too many parameters that are often not practical to obtain particularly at 3D, hence may involve high uncertainties. In addition, geophysical data is obtained from surface and well measurements. However, these are not time and cost effective tasks especially in basin-scale studies because of the network installation, instrumentation, personnel and sampling costs. Hence, instruments such as Gravity Recovery and Climate Experiment (GRACE) enable us to make regional estimates of total mass of water and its components by the contribution from hydrological models. It relies on the relationship between gravity and surface mass, rather than empirical methods and calibrations with in-situ measurements. For this reason, it is useful in areas where in-situ measurements are scarce and undergo maintenance and sustainability problems.

Spatio-temporal changes in subsurface storage can be monitored by GRACE satellites. The primary objective of the GRACE mission is to measure the Earth's gravity field and it's time variability. The final processed product of GRACE is expressed in terms of terrestrial water storage (TWS). The cause of fluctuations in Earth's gravitational field is the movement of water over Earth's surface. The estimates of TWS serve for climate change, weather predictions, biological and agricultural productivity, flooding and drought predictions, etc. Over the ocean TWS is interpreted as ocean bottom pressure and on land it is the the sum of groundwater, soil moisture, surface water, snow and ice. The secondary objective of the GRACE mission is to obtain precise measurements of globally distributed vertical temperature and humidity profiles of the atmosphere using the radio transmissions from Global Navigation Satellite System (GPSS).

Data provided by GRACE has been used to study for a variety of subjects such as mass distribution of polar ice caps/sheets, water movement on and beneath the land, global sea level change as a result of temperature and water mass change and for tracking the forces that generate the Earth's geomagnetic field that result in earthquakes and eruptions. It has been applied in many hydrologic problems such as groundwater storage (GWS) changes (Feng et al., 2013; Long et al., 2013; Rodell et al., 2007; Strassberg et al., 2007; Voss et al., 2013), floods (Chen et al., 2010), the loss of ice mass from ice sheets (Velicogna, 2009), ocean currents and sea level rise (Nicholls & Cazenave, 2010), and the changes in the solid Earth (Han et al., 2008).

Consequently, GRACE dataset has improved the understanding of how mass is distributed globally and the knowledge of climate change estimates in terms of seasonal and inter-annual magnitudes and tendency since it is launched in March, 2002. The spatial resolution of GRACE is given as about 150,000 km^2. According to Longuevergne et al. (2013) the spatial resolution is 200,000 km^2 while it is 100,000 km^2 for Landerer and Swenson (2012). It is stated that the changes in TWS could be detected over an area of ~200,000 km^2 if the change exceed 1.5 cm of equivalent water height (EWH) (Rodell & Famiglietti, 1999). This precision allows detection of ~3 km^3

of TWS change. Also, Swenson and Wahr (2003) reported that GRACE can detect changes in TWS to an accuracy of about 0.7 cm equivalent water thickness (EWT) for a basin area of 400,000 km^2, and an accuracy of 0.3 cm EWT for an area of about 4,000,000 km^2.

Using GRACE data, many studies were conducted at large areas and investigated the utility of GRACE and related water balance models. In recent years, interest in using GRACE datasets has been expanding to smaller basins. However, there is a challenge in applying GRACE products to areas with spatial coverage which is less than the GRACE footprint. Huang et al. (2015) stated that the large mass changes allow the storage changes to be detected by GRACE despite the area of the regions is relatively small according to the spatial resolution of GRACE. This confirms the studies of Famiglietti et al. (2011) and Scanlon et al. (2012) who found that the groundwater mass changes in the California Central Valley (~52,000 km^2) were detected by GRACE. Also, Huang et al. (2015) investigated the potential of GRACE to detect groundwater storage variations at two regions of 54,000 km^2 and 86,000 km^2 in the North China Plain. They found a good agreement between GRACE-derived groundwater storage variations and in-situ groundwater level measurements. The R-square correlation values in these two basins were 0.91 and 0.75, respectively. Liesch and Ohmer (2016) compared the groundwater levels with GRACE data and found a good agreement (R-square between 0.55 and 0.75) at five groundwater basins (1,500 to 18,000 km^2) in Jordan. Proulx et al. (2013) applied GRACE data to evaluate the dynamics of TWS in two basins which are Prairie Coteau (PC) (38,000 km^2) and Northern Glaciated Plains (NGP) (66,000 km^2). The agreement between GRACE TWS and the combination of ground observations of groundwater and surface water and modeled changes in hydrologic components became as $r^2 = 0.75$ and $r^2 = 0.64$, respectively for PC and NGP. These studies show that there is still a need for more groundwater validation studies at smaller scale, especially for heterogeneous aquifer systems.

Most of the GRACE studies conducted in Turkey are focused on modelling the geoid surface and analysis of Earth's gravity field (Atayer & Aydın, 2012; Avsar & Ustun, 2012; Simav, Yıldız, & Arslan, 1989). Avsar and Ustun (2012) investigated time-dependent changes of gravity for an area including Turkey and its neighbourhood by using data obtained from GRACE measurements. The study highlighted a significant decline in gravity around Caspian Sea coast.

Additionally, Ahi and Jin (2019) used GRACE observations to predict agricultural and hydrological drought conditions in Turkey. The study compared results of several models such as Global Land Data Assimilation System (GLDAS) and Tropical Rainfall Measuring Mission (TRMM)-3B43, drought indices such as self-calibrating Palmer Drought Severity (scPDSI), El Niño–Southern Oscillation (ENSO) and North Atlantic Oscillation (NAO), and GRACE observations. The results of this study revealed that GRACE could be a better tool for prediction of agricultural and hydrological drought 9 months before.

This study focuses on analyzing GWS changes in small basins with different scales that cover Central Anatolia. Especially in Konya Closed Basin, precipitation rates within the basin have drastically decreased below the average and the effect of climate change as well as population growth increase the demand for water in recent years. So, water used for irrigation, domestic consumption and industry needs have been increasing day by day. These demands are mostly met from groundwater reservoirs which are poorly managed and thus have been under increasing stress (WWF-Turkey, 2014). After the drought occurred in 2007, the government institutions have given the priority to long-term and economic management plans.

The main objective is to monitor the changes in groundwater storage by using the satellite- and GLDAS Land Surface Models (LSMs)-based information and to investigate the accuracy of GRACE retrievals at small basins and at acceptable scale (Central Anatolia Basin) by comparing with ground measurements. Also, variables of GLDAS LSMs are compared with each other. Additionally, different methods of

basinwide estimation of GWS changes are examined. This study is significant because, for the first time, the ground-based estimates of groundwater level changes are compared with the satellite estimates over Turkey in Central Anatolia.

CHAPTER 2

DESCRIPTION OF THE STUDY AREA

2.1. Geographical Setting and Climate

The study area is comprised of five basins of Turkey which are Akarçay Basin, Kızılırmak Basin, Konya Closed Basin (KCB), Sakarya Basin, and Yeşilırmak Basin (Figure 2.1). The study area is located in the northern and central parts of Turkey. The region covers approxiamately a total area of 233,929 km^2. The area of each basin comprising the study region separately shown in Table 2.1.

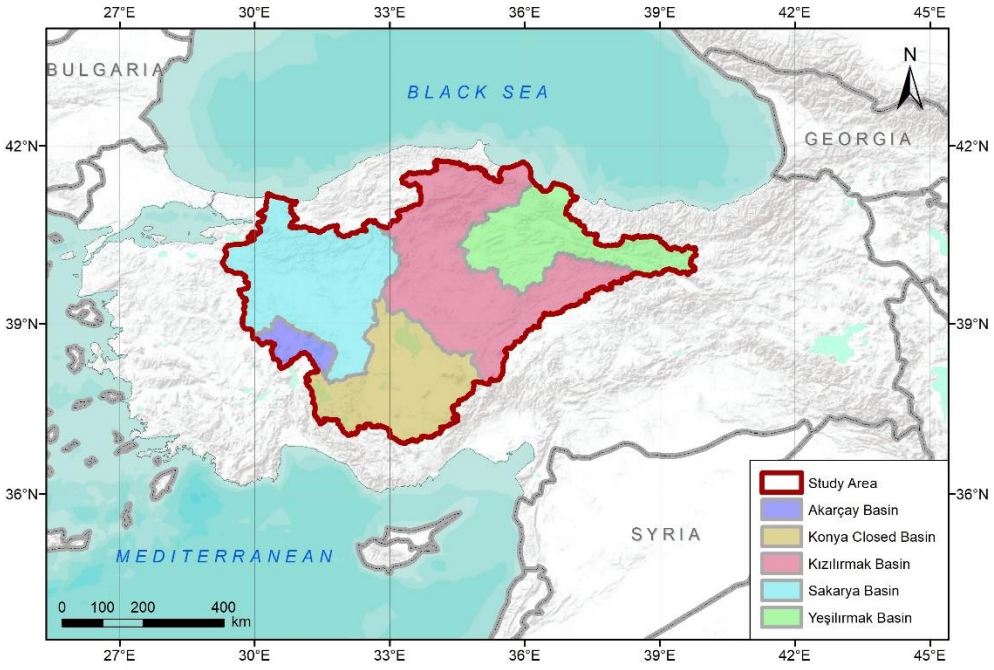

Figure 2.1. Map of the study area

Table 2.1. Catchment areas

	Basin	Catchment Area (km^2)
1	Kızılırmak	78,180
2	Sakarya	58,180
3	Konya	53,850
4	Yeşilırmak	36,114
5	Akarçay	7,605
6	Central Anatolia Basin	233,929

The topographic elevation of the study area ranges between 891 and 3404 m above sea level (Figure 2.2). The study region is covered with mountains parallel to the coasts at the northern and southern parts. So, it has different climate types as a result of various landforms that affect meteorological conditions and climate control factors. The precipitation amounts also vary in the region. It has the characteristics of the Black Sea precipitation regime in the north and Central Anatolia in the south. The mountains hold the rain clouds, and therefore the coastal areas have milder climate while the areas in the inland Anatolia plateau experience terrestrial climate (hot summers, cold winters) (Sensoy, Demircan, Ulupınar, & Balta, 2008).

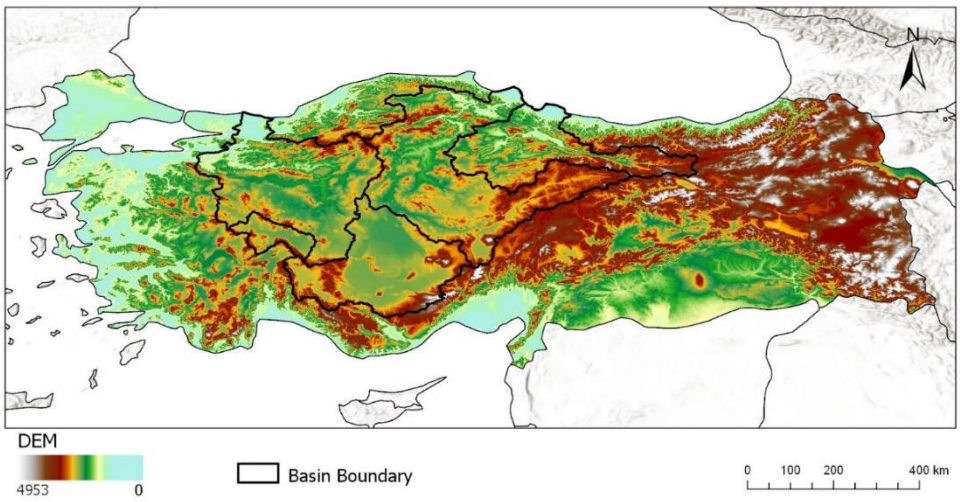

Figure 2.2. SRTM Digital Elevation Model (DEM) of the study area

Especially, KCB is investigated in detail because the basin is a semi-arid basin which has experienced huge non-renewable groundwater abstraction for irrigation over the past few decades (Bayari et al., 2009). Konya has been known as the main grain producer of Turkey and in such water limited areas groundwater is the most dependable water resource. One of the reasons of excessive groundwater abstraction is the significant increase in the planting areas of corn, sunflower, sugar beet which require high amount of water. Based on the observations of the groundwater wells operated by DSİ 4th Regional Directorate, groundwater levels have decreased more than 28 meters across the basin since 1980 (Göçmez & İşçioğlu, 2004). Also, formations of sinkholes (locally called Obruk) prove this alarming situation (Bayari et al., 2008).

In recent years, agricultural lands have increased in KCB and it can be seen from Normalized Difference Vegetation Index (NDVI) maps. NDVI is also used for quantifying crop productivity. Monthly Moderate Resolution Imaging Spectroradiometer (MODIS) – NDVI maps are generated for 2002 – 2006, 2007 – 2011, 2012 – 2016 and are given in Figures 2.3, 2.4 and 2.5, respectively. The pixels having NDVI values greater than 0.4 represents vegetation cover. Since 2002, the increase in agricultural production was observed. The highest NDVI value was recorded in May and the crops were harvested in June or July. It has been observed that NDVI values and the density of the harvested areas have increased when compared with the prevous years.

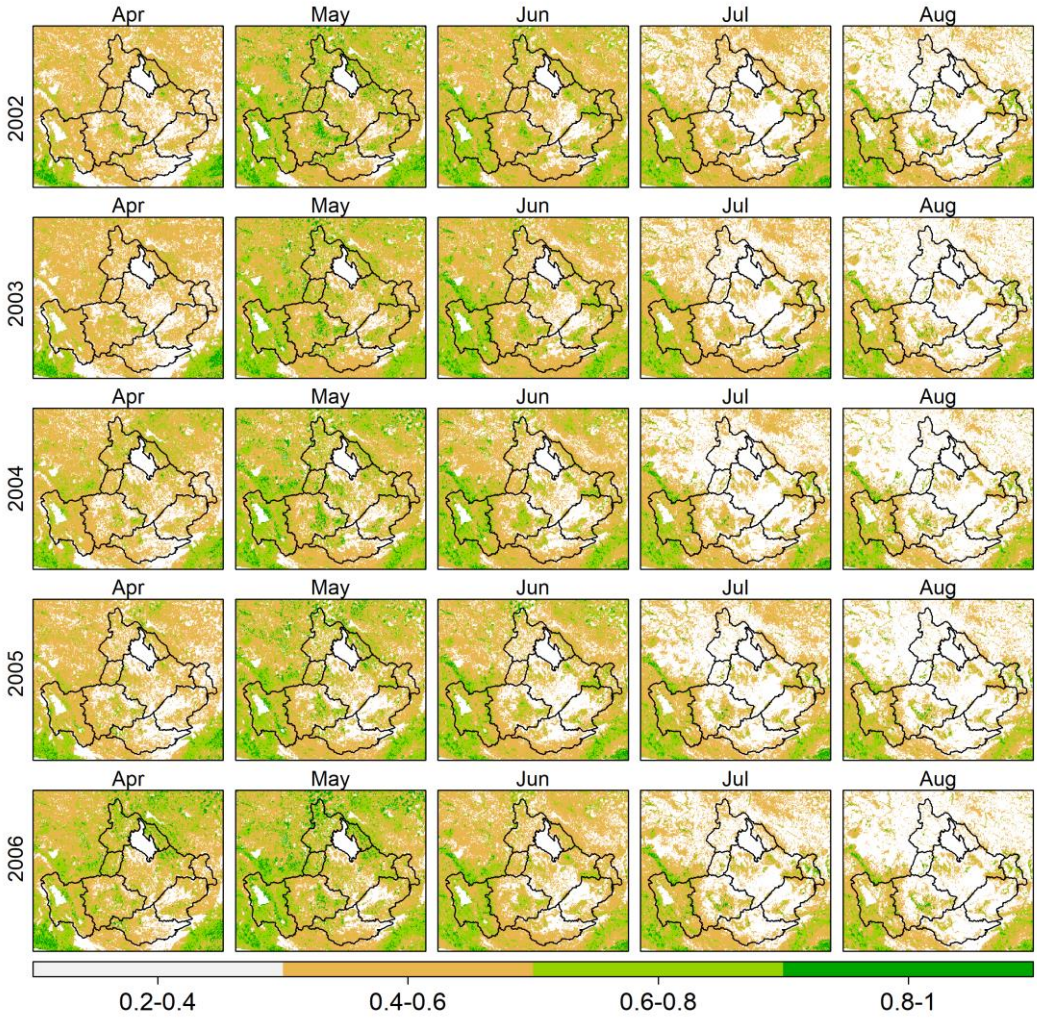

Figure 2.3. Monthly MODIS (MOD13Q1)-NDVI maps of 2002 – 2006 years over KCB

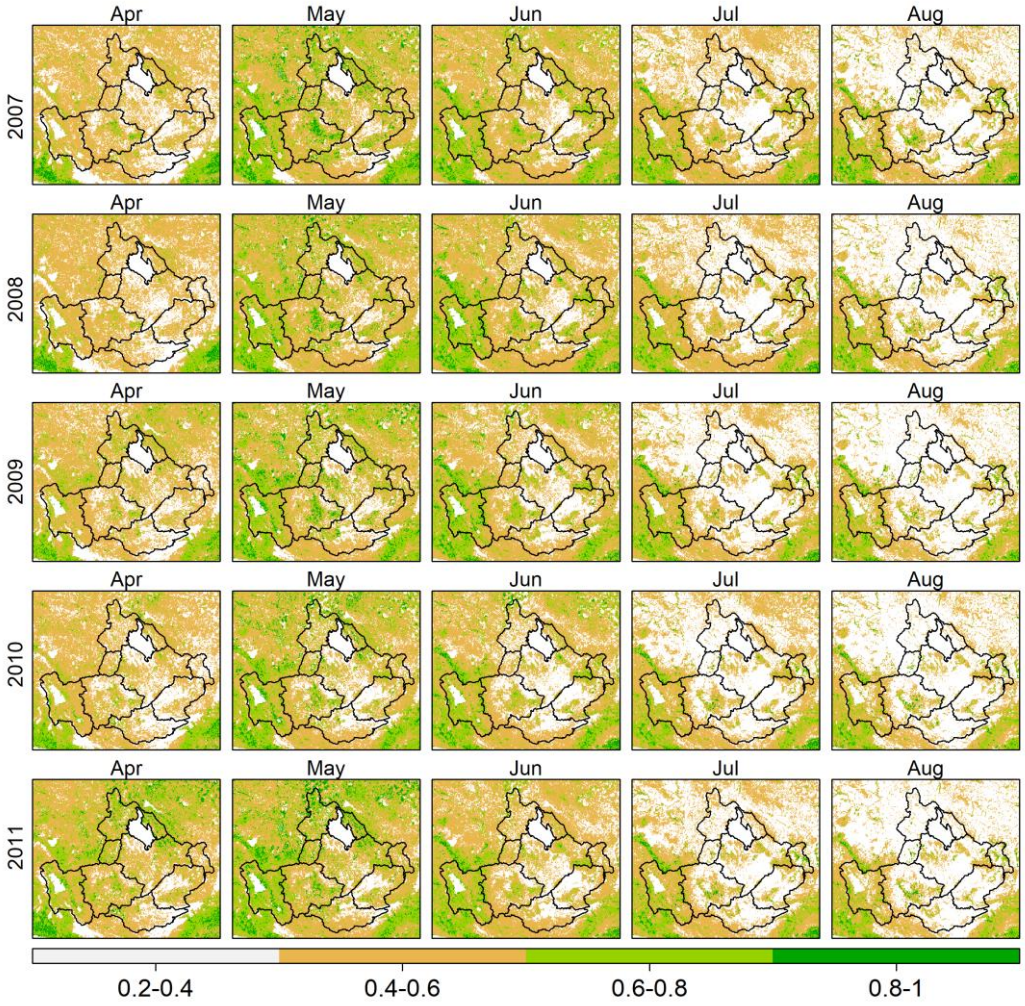

Figure 2.4. Monthly MODIS (MOD13Q1)-NDVI maps of 2007 – 2011 years over KCB

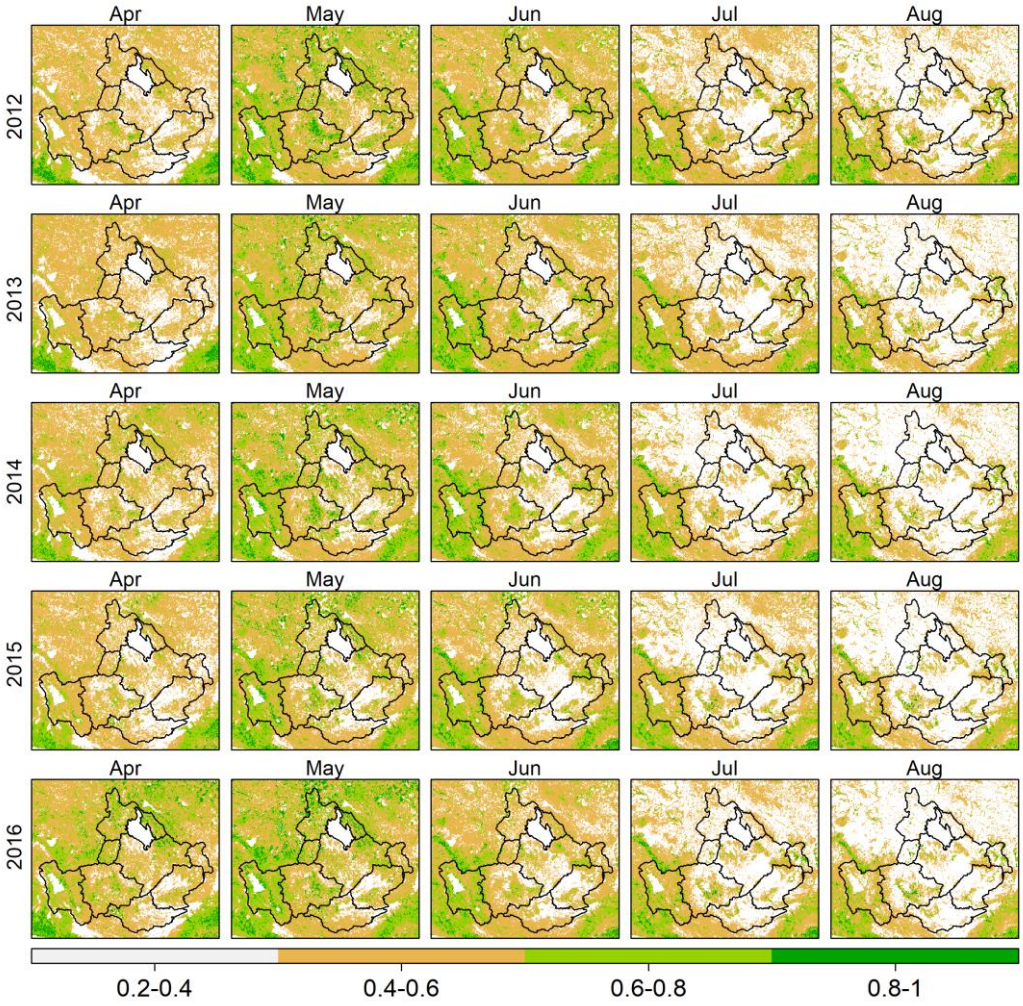

Figure 2.5. Monthly MODIS (MOD13Q1)-NDVI maps of 2012 – 2016 years over KCB

2.2. Geology

2.2.1. Regional Geology of Konya Closed Basin

Throughout Late Cretaceous to Late Tertiary, the basement of KCB emerges from the closure of Neo-Tethys Ocean where Tauride-Anatolide Block (TAB), Sakarya Zone Block (SZB) and Kırşehir Massive Block (KMB) were converged into a single landmass (Bayari et al., 2009; Okay & Tüysüz, 1999). The TAB, which forms the bulk of the southern Turkey, was formed between Early Paleozoic and Late Mesozoic. It comprised of mainly with detrital and marine carbonates. At the bottom, the SZB starts with a Triassic subduction-accretion complexes which comprise the characteristics of Sakarya Zone. It is followed upwardly with Jurassic to Cretaceous clastics and carbonates, and end up with Paleogene rocks at the top. The three blocks are overlain by Paleogene and younger rock units. The Paleogene series of TAB and SZB are comparable and composed of clastics and marine carbonate rocks. Toward the top, marine limestone and volcaniclastics overlie the turbiditic sandstone and shale alternation. Through the top of the Eocene deposits, irregularly seated evaporitic rocks were constituted. The overlying Oligo-Miocene stratigraphy are comprised of continental clastics, tuffs, limestone and evaporites at the bottom. The top of the sequence was composed of gypsum-shale alternation. The Neogene (Late Miocene to Late Pliocene) stratigraphy was made of a basal conglomerate. It follows with lacustrine carbonates that alternate with weakly cemented marl in the upper parts. Plio-Quaternary deposits are represented by paleolake sediments and alluvial fans that concordantly overlies Miocene deposits. The Quaternary deposits which are characterized by shoreline landforms surround the margins of the plain (Orhan et al., 2019). In the Late Tertiary, Central Anatolia is affected by a neotectonic regime with compressional and extensional tectonics. In this region, extensional tectonism results in asthenospheric intrusion underneath the upper crust. It leads to thinning of the lithosphere that causes volcanic activity within and around the KCB occasionally until the Late Holocene. The generalized stratigraphic columnar section of KCB is shown in Figure 2.6 and the geological map of KCB is provided in Figure 2.7.

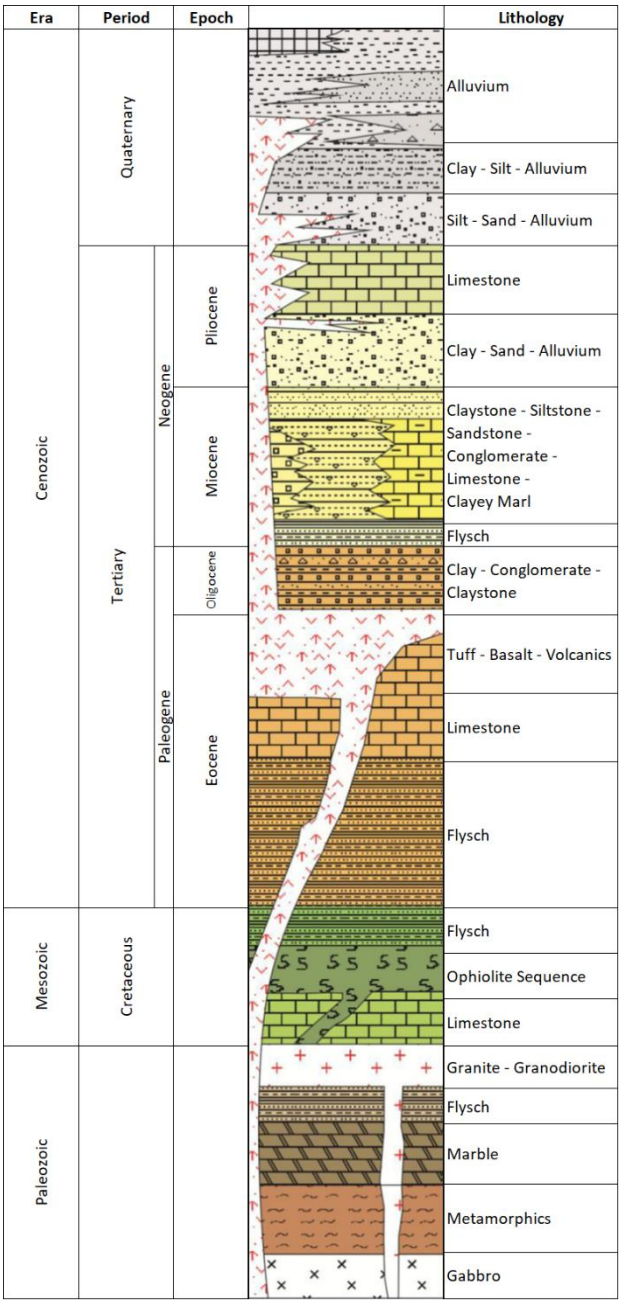

Figure 2.6. Generalized stratigraphic columnar section of KCB (DSİ, 2015).

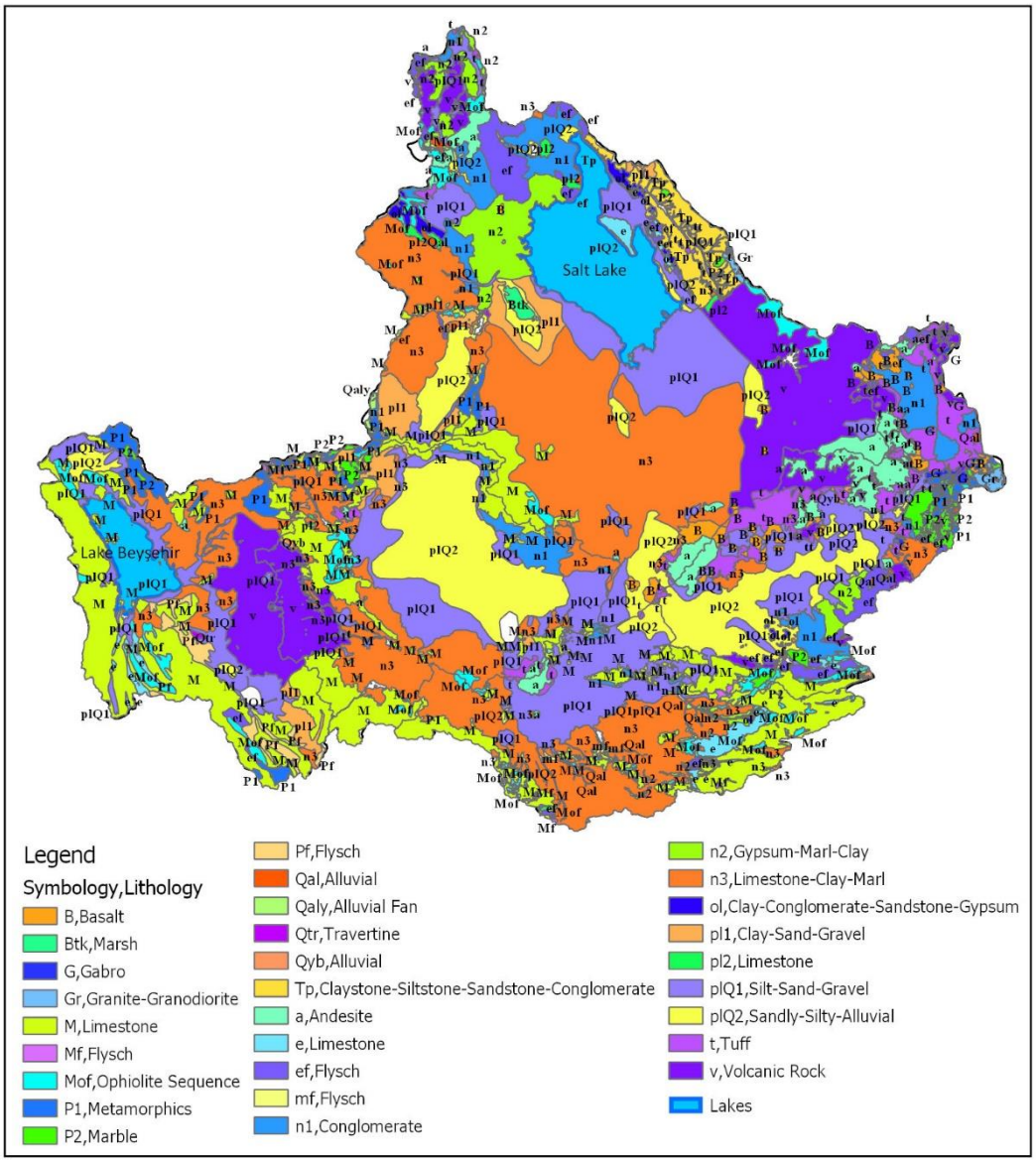

Figure 2.7. Geological map of KCB (modified from MTA, 2002).

2.2.2. Regional Hydrogeology of Konya Closed Basin

The groundwater hydrology of the KCB is described by Bayari et al. (2008). According to the simplified conceptual hydrogeologic model (Figure 2.8), there exits two main aquifer systems as shallow and deep aquifers. The deep, confined and thermal aquifer is composed of TAB and SZB units which are overlain by the weakly

permeable Paleogene units whereas the shallow, fresh water aquifer is comprised of Neogene units and covered with the Quaternary Paleolake Sediments (QPS) (Bayari et al., 2009). The Paleogene and QPS units constitute the aquitard systems. The groundwater flows fed up the aquifers from the footprints of Taurus Mountains at the south which is the main recharge area towards the Salt Lake which is the discharge area at the north (Bayari et al., 2008).

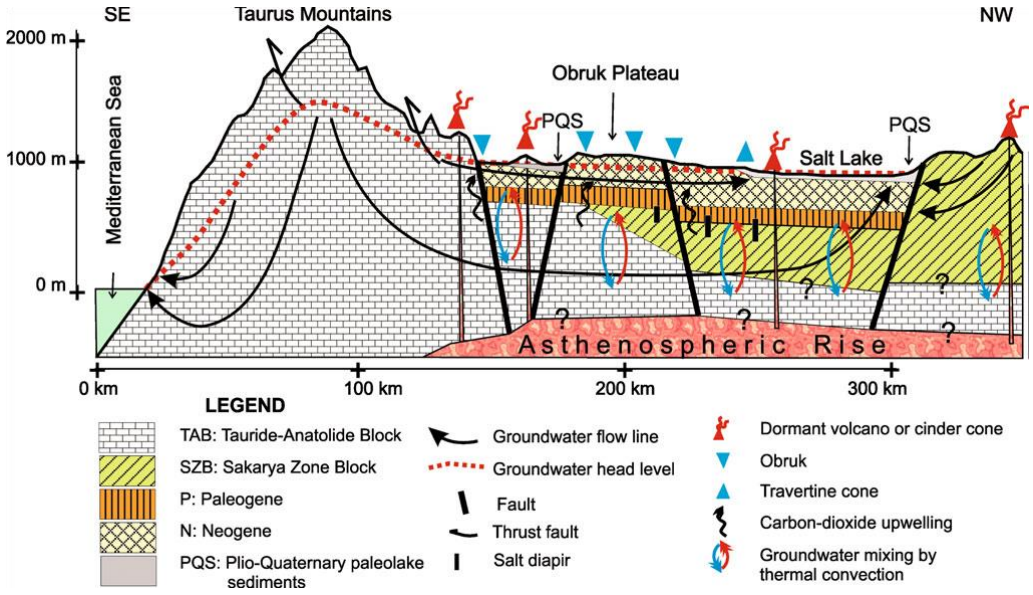

Figure 2.8. Schematic representation of regional groundwater flow system (retrieved from Bayari et al., 2008).

A large portion of the basin is covered with cool and fresh groundwater bearing Neogene aquifer. It has a highly developed karst feature composed of Neogene Limestone which has many dissolved pores with fractures and forms a very productive aquifer. The aquifer is confined at the northern and southern parts of the basin where it is overlain by Plio-Quaternary sediments. The unconfined conditions prevail mainly at the Obruk Plateau where the aquifer is exposed at the surface and can be fed by infiltration. Also, the Paleozoic age SZB and Paleozoic-Mesozoic karstric carbonates of TAB outcrops are observed in Bozkır, Hadim, Seydişehir, Akören, Ahırlı, Beyşehir,

Doğanhisar and Kadınhanı regions where the groundwater can be replenished. The deep flow of groundwater in SZB and TAB aquifers is warm and saline because it is exposed to heat flux from magmatic intrusions and is enriched in terms of ionic composition (Bayari et al., 2009). The thick Paleogene aquitard that underlies the shallow aquifer prevents the mixing of groundwater and the upwelling of hypogenic gas toward the surface. Although the basin lacks any surface outlet and the removal of water is controlled mainly by evaporation, the groundwater outflow occurs through the karstic features directed towards Lake Beyşehir and Lake Suğla and to the Mediterranean Sea through the cavities and the dolines.

CHAPTER 3

DATASETS AND METHODS

3.1. DATASETS

3.1.1. GRACE

GRACE is a mission that tracks the Earth's gravity field, managed by the collaboration between National Aeronautics and Space Administration (NASA) and Deutsches Zentrum für Luft- und Raumfahrt (DLR). The twin spacecraft were launched on March 17, 2002 to provide extremely valuable information about the dynamic structure of the Earth.

3.1.1.1. Basic Theory of GRACE

Newton proposed in his Law of Universal Gravitation that the gravitational force is directly proportional to the product of two point masses. The force exists between any two masses, including the planet Earth and any object under the attraction of the Earth's gravity field. The magnitude of the attractive force between these masses is given by Equation (1).

$$F = G\frac{Mm}{r^2} \tag{1}$$

where F is force of gravity between two masses, G is the universal gravitational constant, M is the mass of the Earth and m is the mass of the object, and r equals to the distance seperating the objects' centers. Additionally, the Newton's Second Law of Motion states that for a point mass, m, the magnitude of the gravitational force is given by Equation (2).

$$F = mg \tag{2}$$

where g is the acceleration due to gravity at the Earth's surface.

The gravitational acceleration can be calculated by combining both Equations (1) and (2).

$$g = G\frac{M}{r^2} \tag{3}$$

The Earth is not a uniform sphere. The value of gravity field vary locally because of the bulges at the equator, changes in topography and rocks that have different densities.

The two identical satellites of GRACE follow each other in the same near-polar orbit. As the satellites approach a greater mass concentration, the leading satellite is affected first and pulled away from the trailing satellite. So, the distance between the satellites increases. After the front satellite passes over, the trailing satellite is pulled towards and speeds up. So, the distance between the satellites decreases. As it passes the area of higher density it slows down as well which does not affect the leading satellite. Finally, the distance comes back to its standard separation. The changes in the gravity field are determined by measuring the distance varying between the satellites themselves (Figure 3.1).

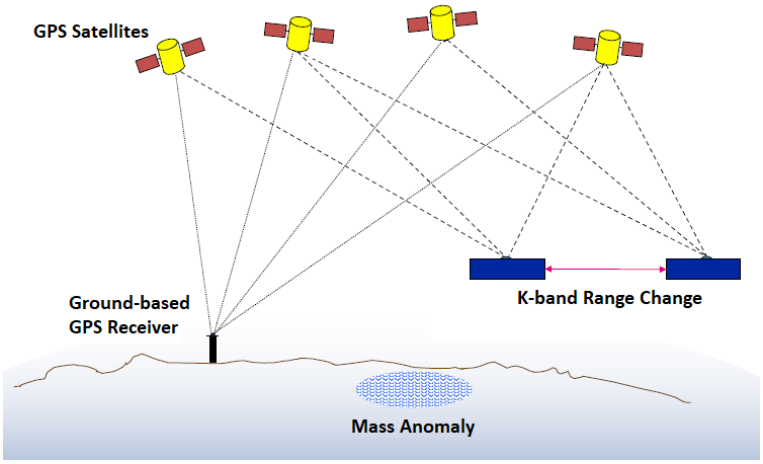

Figure 3.1. GRACE mission concept (retrieved from Bettadpur, 2016).

The importance of GRACE is that using a microwave K-band microwave ranging system which gives much more sensitive and precise measurements than any other gravity field observations, such as ground-based measurements or single satellites. The ranging system can detect the rate of change of separations as small as 10^{-3} millimeters (1 μm) over an approximate distance of 220 kilometers.

GRACE has no vertical resolution (Wahr et al., 2006). It cannot directly provide the absolute water storage and its components. It is used to detect and quantify the mass changes. To convert this to mass anomalies, a time-mean gravity field is subtracted. The time-mean gravity field is known as static field which represents the Earth's spatially varying but constant in time reference field and it is removed in the processing step. The output is expressed as TWS anomaly in a unit of cm of EWT or EWH. The variations in TWS are calculated by their deviations from a specific time period. The period represents the mean gravity field which is assumed as the average of all months from January 2004 to December 2009. The remaining signals vary around zero. While the positive changes indicate an increase in mass amount, the negative changes indicate mass losses. So, it helps us to monitor the water movements and how it is varying over time.

Due to battery management, GRACE data has some gaps, especially in recent years. So, the study is conducted from January 2003 to December 2015 (13 years). The data are processed independently in three centres CSR, GFZ and JPL to generate the GRACE products. The GRACE data is divided into three levels (Bettadpur, 2016).

Level 1-A & Level 1-B: The raw data includes all the necessary inputs and calibrated in non-destructive sense. The intersatellite range rate, range acceleration and pointing estimates etc. are included.

Level 2: The Level 1-B products are processed to produce the monthly gravity estimates in form of spherical harmonics coefficients.

Level 3: The geophysically corrected, smoothed and filtered gravity field products are ready-to-use data provided as mass anomalies.

3.1.1.2. Spherical Harmonics Solution

In this study, GRACE Tellus Level-3 Release 5 (RL05) Land Grids Version datasets from CSR, GFZ and JPL centers are used. The datasets are publicly available at http://grace.jpl.nasa.gov, supported by the NASA MEaSUREs Program. The data is processed according to Spherical Harmonics (SH). The products from three centers similarly capture the variations and the differences between the products are very small (Sakumura et al., 2014). Therefore, the simple arithmetic mean of three products is taken.

Wahr et al. (2006) demonstrated that the data is noisy, so filtering with spatial integration is required. Although the Gaussian filtering which is a smoothing operation reduces the signal leakage, the spatial and temporal bias increase as the signal loss decreases (Klees et al., 2007). The dataset provides mass grids at a temporal resolution of 1 month and a spatial resolution of 1° at a global scale. There are 360 longitude points (0.5° to 359.5°) and 180 latitude points (-89.5° to 89.5°) in the solution data set. Although the mass products are analyzed at 1° grids, gridded products do not represent the actual resolution of the GRACE observations. In the post-processing step, spatial filtering is used to smooth the data by reducing the noise within the data. Nearby grid cells are dependent on each other because the Gaussian filtering is applied. Some of the signals are lost while reducing the noise. Thus, scaling coefficients are used to restore the signal amplitudes to compare the GRACE TWS with LSMs as well as to estimate GWS change from GRACE. These factors are dimensionless and provided for each 1° x 1° grid cells in the downloaded datasets. The GRACE TWS is multiplied with the scaling factor as follows:

$$g'(x,y,t) = g(x,y,t) \times SF(x,y) \quad (4)$$

where $g(x,y,t)$ represents each grid point for each month, $SF(x,y)$ is the scaling factor at each grid and $g'(x,y,t)$ is the gain-corrected time series.

The scaling factors (or gain factors) are independent of the GRACE signals and derived from National Center for Atmospheric Research (NCAR)'s Common Land

Model (CLM) 4.0 Model. Although anthropogenic conditions such as surface water and groundwater usage (especially for irrigation) are not taken into account, LSMs are assumed to represent the actual mass changes (Longuevergne et al., 2013; Scanlon et al., 2012). The magnitude of scaling factors over Turkey are shown in Figure 3.2.

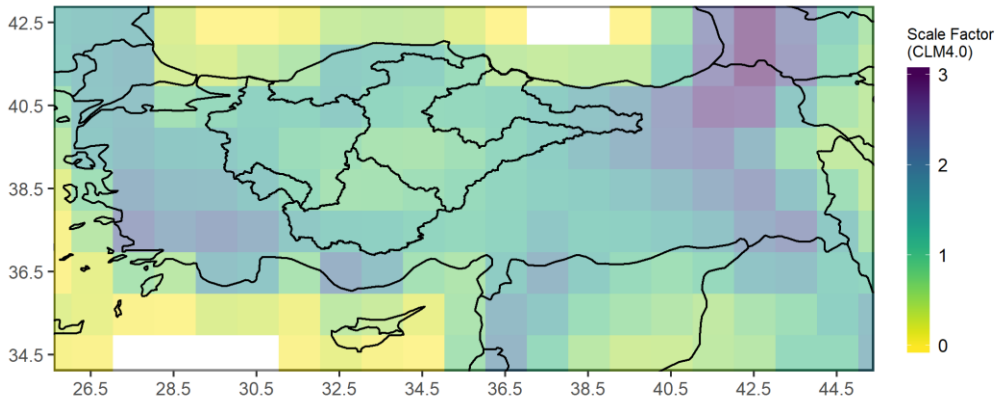

Figure 3.2. Scale factors over Turkey

The gain factor is obtained by applying least square regression to minimize the difference between the model's unfiltered (ΔST) and filtered (ΔSF) signals (Landerer & Swenson, 2012). The filters applied to the GRACE data are also applied to the LSM to compute the filtered signals.

$$M = \sum (\Delta S_T - k\Delta S_F)^2 \tag{5}$$

where M is the function to be minimized, k is scaling factor, ΔS_T and ΔS_F are the model's unfiltered and filtered TWS anomalies, respectively. In this study, scale factors which are taken from the provided dataset are applied to the corresponding grids of GRACE TWS.

3.1.1.3. Error Estimation

Error estimation is necessary for assessing the accuracy of GRACE as well as improving the LSMs if GRACE is used as an diagnostic tool. The estimates of TWS

variations are affected by measurement and processing errors that cause signal degradation (Landerer & Swenson, 2012; Wahr et al., 2006). These SH errors, which are described as measurement and leakage errors, are the residuals after post-processing and rescaling to attain the actual TWS signals. The error components correspond to the expected uncertainty are provided in the datasets. According to Wahr et al. (2006), the measurement errors (Figure 3.3) are calculated by using the residuals of TWS variations after eliminating the annual and interannual signals with the long-term trend. The residuals are the amount of inaccuracies within the gravity field solutions. This approach overestimates the errors because the residuals may include interannual and subseasonal signals or contain signals that are not considered as noise. The grid cell measurement errors are previously scaled with the gain factors (Landerer & Swenson, 2012). The mass errors vary every month and are normally distributed when adjusted. It depends on latitude, smoothing radius and the size of the region. It increases near the equator and decreases toward the higher latitudes as well as decreases as the smoothing radius and the area of the region increases.

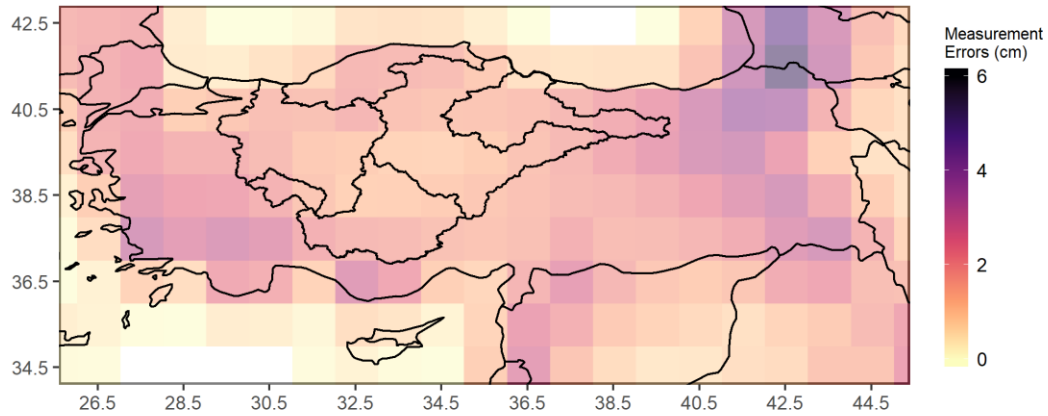

Figure 3.3. Measurement errors over Turkey

Leakage errors are quantified as residuals which are estimated by the root-mean-square (RMS) difference between the filtered TWS from GRACE and unfiltered

signals of TWS estimates simulated by the LSMs. Then, the grid cell leakage errors are scaled by the ratio of the RMS variability of the filtered GRACE and one of the LSM time series to reduce the error estimations.

The scale component is applied to reduce the discrepancies between the amplitudes of the signals. In Level-3 TWS leakage error calculations, CLM 4.0 model is used.

$$LE_{grid} = RMS(\Delta S_T - k\Delta S_F)\frac{RMS_{GRACE}}{RMS_{Model}} \tag{6}$$

where LE_{grid} is the leakage error at each grid point and ΔS_T and ΔS_F are expressed in Equation (6). The leakage errors over Turkey are shown in Figure 3.4.

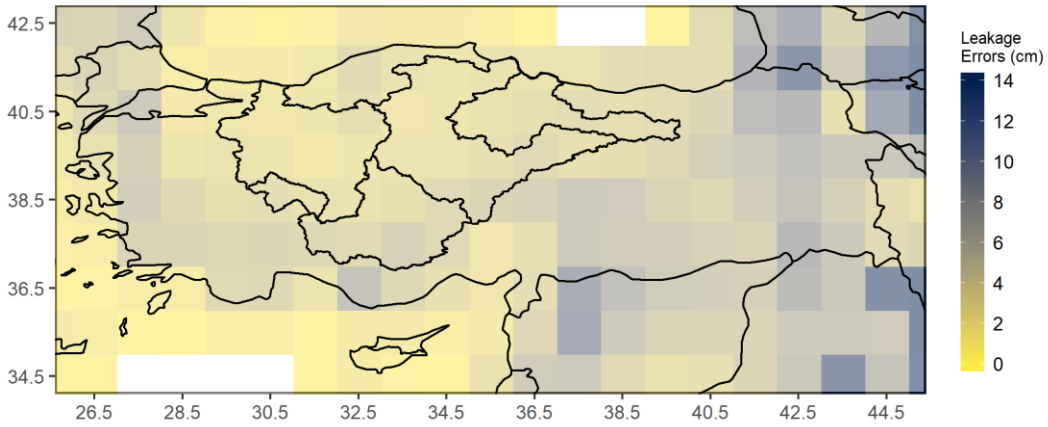

Figure 3.4. Leakage errors over Turkey

The uncertainty estimates are time independent and provided by GRACE Tellus. For each grid point, the total error in TWSA is calculated by taking the quadrature sum of the error components.

$$Total\ TWS\ Error_{grid} = \sqrt{(ME_{grid})^2 + (LE_{grid})^2} \tag{7}$$

The error shown in Figure 3.5 reflects the uncertainty in the TWS anomaly time series of each grid over the study region.

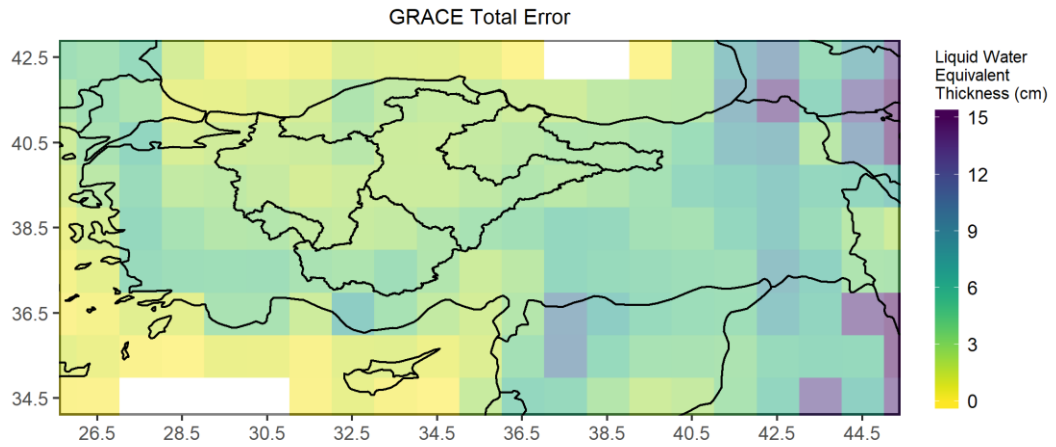

Figure 3.5. Gridded total error over Turkey

The errors in adjacent cells are highly correlated and cannot be averaged at basin scale. To calculate the uncertainty in a region, the error covariance is taken into consideration following the approach described by (Landerer & Swenson, 2012).

$$d_{i,j} = \frac{\pi}{180} A \sqrt{[(long(i) - long(j))\cos(lat(i))]^2 + [(lat(i) - lat(j)]^2} \tag{8}$$

$$Cov(x_i, x_j) = \sigma_i \sigma_j \exp\left(\frac{-d_{ij}^2}{2d_0^2}\right) \tag{9}$$

$$var = \sum_{i=1}^{N}\sum_{j=1}^{N} w_i w_j Cov(x_i, x_j) \tag{10}$$

where i and j represent two different grid points, A is the radius of the Earth assumed as 6371 km, *long* and *lat* indicate longitude and latitude of each grid cell, respectively. $d_{i,j}$ is the distance between two grid points on a sphere, d_0 is a decorrelation length scale which is taken as 300 km for measurement error and 100 km for leakage error. Cov is the covariance between two grid cells, σ is the standard deviation of the error components which in turn to provided error data, N is the number of grid cells, w is the area weight at each grid cell and simplified to $1/N$ by assuming each grid cell has equal contribution to the basin. var is the error variance of a regional mean TWS.

By means of Equation (11), the variance of leakage error and measurement error are calculated. The total error within the basin is calculated by summing the measurement error (σ_m) and leakage error (σ_l) in quadrature.

$$Error_{total} = \sqrt{(\sigma_m)^2 + (\sigma_l)^2} \quad (11)$$

3.1.2. GLDAS Land Surface Models

GRACE only provides estimates of terrestrial water storage change information. To infer the groundwater change, some components of terrestrial water storage should be removed from TWS. However, estimation of these components using remote sensing or ground observations is not trivial. In this study, these estimates are obtained from model estimates, more specifically using GLDAS simulations.

3.1.2.1. General Information

GLDAS is developed jointly by NASA - Goddard Space Flight Center (GSFC) and National Oceanic and Atmospheric Administration (NOAA) - National Centers for Environmental Prediction (NCEP). The provided data from satellite observations and ground-based hydrological data are integrated to generate outputs of land surface states and fluxes in global scale. These parameters are simulated by four LSMs which are Mosaic (Koster & Suarez, 1996), The National Centers for Environmental Prediction (NCEP)/Oregon State University/Air Force/Hydrologic Research Lab Model (NOAH) (Ek et al., 2003), CLM (Bonan et al., 2002) and Variable Infiltration Capacity (VIC) (Liang et al., 1994). The GLDAS simulations are performed on a 1° × 1° grid resolution. Besides, a 0.25° × 0.25° grid data products are generated for NOAH model, covering 2000 to present. The temporal resolution for the GLDAS products is 3-hour. The monthly datasets are generated by temporal averaging of the 3-hourly products on that month. In this study, monthly 1° × 1° outputs are used by considering the GRACE resolution.

There are two versions of GLDAS which are GLDAS-1 and GLDAS-2. GLDAS-1 has generated 40 years of data from January 1979 to present. The simulation is forced by a combination of three atmospheric forcing datasets that are model derived NCEP's Global Data Assimilation System (GDAS) atmospheric analysis fields, disaggregated NOAA Climate Prediction Center Merged Analysis of Precipitation (CMAP) fields, and satellite observation derived using the method of the Air Force Weather Agency's AGRicultural METeorological Model (AGRMET).

GLDAS Version 2 has two components as GLDAS-2.0 and GLDAS-2.1. For the period between January 1948 and December 2010, GLDAS-2.0 has generated 63 years of improved and climatologically consistent data using the updated Princeton Global Meteorological Forcing Dataset (Sheffield et al., 2006). Princeton Forcing Datasets provides meteorological data to drive the LSMs and other terrestrial modeling systems. On the other hand, GLDAS-2.1 simulation started on January 2000 and still continues. It is generated by using the combination of NOAA-NCEP's GDAS fields of atmospheric analysis, spatially and temporally disaggregated GPCP precipitation fields, and satellite observations derived using the method of the AGRMET. Only GLDAS-2 NOAH LSM is publicly accessible. The updated NOAH is named as NOAH Version 3.3.

The objective of GLDAS-2.1 is to have climatologically corrected datasets. Throughout the data record of GLDAS-1, the source of forcing data was changed several times. It is resulted in some discontinuities that introduced highly uncertain fields in 1995-1997. Due to the fact that these intervals are not within the study period, GLDAS-1 LSMs are used. In addition, version of land surface models are upgraded and the observations are derived from Advanced Very High Resolution Radiometer (AVHRR) base parameters for GLDAS-1, and from MODIS based land surface parameters such as land cover, land mask and vegetation maps for GLDAS-2.

CLM was developed according to the concepts of ecological climatology that studies the terrestrial ecosystems. The terrestrial ecosystems have a great effect on physical,

chemical and biological processes that are the determinants of climate. CLM can be run as a stand-alone 1-D model in a coupled and uncoupled to the atmosphere.

Like CLM, NOAH is a stand-alone, 1-D model that can run both uncoupled and coupled.

Mosaic is developed for the NASA's Global Climate Change. Like CLM and NOAH, Mosaic is a stand-alone, 1-D model that can be run uncoupled or it can run coupled to the atmospheric models. The 1° x 1° grid cells can be divided into a Mosaic of tiles based on the distribution of vegetation types within the cell.

The VIC model is developed at the University of Washington. It is a calibrated hydrological model and gives comprehensive outputs by solving water and energy balance at the same time. Unlike Mosaic, NOAH and CLM, VIC is an uncoupled. It is running at macro-scales like continental and global scales, so it may increase the error in small scales.

GLDAS's hydrological data are used for the improvements of climate research and forecasting. Also, these output fields provide valuable information on TWS.

3.1.2.2. Model Parameters

The GLDAS model outputs are in NetCDF format and were downloaded from GES DISC (https://disc.gsfc.nasa.gov/). In GLDAS LSMs, TWS is approximately calculated as the sum of the parameters which are soil moisture (SM), snow water equivalent (SWE), and canopy water content (CWC). Also, this study takes into account these geophysical parameters. As shown in Table 3.1, the units of LSMs parameters and GRACE TWS are different. The model parameters are represented in terms of kg/m^2, or mm. Conversely, the unit of TWS is centimeter. To get a consistent data, the units are converted to the same unit of measure.

Table 3.1. *Characteristics of GLDAS Dataset*

Characteristics of GLDAS Dataset						
Land Surface Models	Parameters	Unit	Spatial Resolution	Spatial Extent	Temporal Resolution	Time Span
CLM 2.0 MOSAIC NOAH 2.7 VIC	Soil Moisture (SM)	kg/m^2 (mm)	1° × 1°	180°W - 180°E 90°N - 60°S	Monthly Average	Jan 2003 - Dec 2015
	Snow Water Equivalent (SWE)	kg/m^2 (mm)	1° × 1°	180°W - 180°E 90°N - 60°S	Monthly Average	Jan 2003 - Dec 2015
	Canopy Water Storage (CWS)	kg/m^2 (mm)	1° × 1°	180°W - 180°E 90°N - 60°S	Monthly Average	Jan 2003 - Dec 2015

SM is calculated as the ratio of the mass of water within a unit of soil to a unit volume of soil (kg/m^2). The number of horizontal layers and depths for soil moisture are model specific. Table 3.2 summarizes the depths of soil layers of GLDAS LSMs. Accordingly, CLM model is divided into 10 layers with a smaller depth range. It has the most dynamic soil column than the other LSMs.

Table 3.2. *Vertical Range of Soil Moisture Content*

Vertical Range of Soil Moisture Content (cm)			
Noah	**Mosaic**	**VIC**	**CLM**
4 Layers	3 Layers	3 Layers	10 Layers
0 - 0.1	0 - 0.02	0 - 0.1	0 - 0.018
			0.018 - 0.045
			0.045 - 0.091
0.1 - 0.4	0.02 - 1.50	0.1 - 1.6	0.091 - 0.166
			0.166 - 0.289
0.4 - 1.0			0.289 - 0.493
			0.493 - 0.829
1.0 - 2.0	1.5 - 3.50	1.6 - 1.9	0.829 - 1.383
			1.383 - 2.296
			2.296 - 3.433

SWE data is taken from GLDAS LSMs. During the simulations, the modeled SWE is constrained and adjusted by the snow cover data derived from the MODIS sensors. If the model do not have snow cover but the MODIS snow cover within the pixel is greater than 40%, a quantity about 10 mm SWE is added (Rodell & Houser, 2004). Also, if the MODIS indicates a snow cover less than 10%, the snow within the model pixels are removed (Fang et al., 2008).

The third variable used in this study is CWC which represents the amount of water that is kept within the vegetation cover and is taken from GLDAS LSMs.

3.1.3. Station Based Data

In this study, groundwater level and precipitation observations obtained from ground stations are used. Groundwater level records of the monitoring wells which are collected at monthly intervals are taken from the General Directorate of State Hydraulic Works of Turkey (DSİ) and daily precipitation datasets are obtained from Turkish State Meteorological Service (MGM).

Unfortunately, there is no information about the aquifer properties of the wells. Only the aquifer type representing the well is specified. However, the well-screens may be placed within different aquifers. So, groundwater flows through different layers at different depths. Also, specific yield values are not available because the results of pump tests are not attainable and the tests were not conducted for each aquifer.

3.1.4. Specific Yield Estimations

The GRACE-derived GW is expressed as the equivalent heights of water relative to a time-mean from 2004 to 2009. In order to compare the in-situ levels with GRACE derived GW, the groundwater level observations are converted into GWS changes by multiplying the level changes with specific yield (Sy) for the unconfined aquifers or storativity for the confined aquifers.

The definition of Sy is the amount of water that can be drained from an unconfined aquifer under gravity. Sy values are dimensionless and calculated as the ratio of the

amount of water to the unit change in the water table height. The GWS change for each well can be calculated as:

$$\Delta GWS = S_y \Delta H_{GW} \quad (12)$$

where S_y is the specific yield and ΔH_{GW} is the change in water table as calculated in Section 3.2.2. The accurate predictions of water levels depend on the reliable estimates of Sy. The Sy values mainly vary according to the aquifer properties and geological structures. Also, it is difficult to obtain the Sy values using field pumping tests due to karstic characterization of aquifers in the KCB. As a result, there are not liable Sy observations available. Hence, the Sy values used in this study are chosen based on a literature review, and represented in Table 3.3.

Table 3.3. *Specific yield values for geological materials from the literature*

Aquifer Material		(Morris & Johnson, 1967)		(Johnson, 1967)	(Health, 1983)
		Sy Range (%)	**Average Specific Yield (%)**		
Siltstone		0.9 - 32.7	12		
Clay		1.1 - 17.6	6	2	2
Silt		1.1 - 38.6	20	8	
Loess			18		
Tuff		2.0 - 47	21		
Limestone		0.2 - 35.8	14		18
Schist			26		
Basalt					8
Fine	Sand	1.0 - 45.9	33	21	22
Medium		16.2 - 46.2	32	26	
Coarse		18.4 - 42.9	30	27	
Fine	Sandstone	2.1 - 39.6	21		6
Medium		11.9 - 41.1	27		
Fine	Gravel	12.6 - 39.9	28	25	19
Medium		16.9 - 43.5	24	23	
Coarse		13.2 - 25.2	21	22	

However, Todd & Mays (2005) state that experimental methods may be disturbed because the range of the results is very large. The Sy estimates used in this study are

ranged from 0.08 to 0.021. For confined aquifers, Sy values is selected as $5x10^{-4}$ (Todd & Mays, 2005). In Section 3.2.2., an average Sy value is chosen as 0.10 for Method 2 and applied to all wells.

3.2. METHODS

3.2.1. Study Area Masking

The study area does not fit perfectly with the 1° x 1° grids. So, the grid cells where the study region covers more than 20% of the cell are taken into account. In this way, the areas that are not part of the study area are not included. To find the values representing the basin, the area weighted average of the selected grids is calculated.

3.2.2. Groundwater Data Analysis

Monitoring wells are used to investigate the variations in groundwater levels. Active pumping wells are not considered because the head values of these wells are affected from pumping and other anthropogenic stresses (Sun et al., 2010).

There are 294 observation wells where groundwater level measurements are taken in the study area. The data have been recording since the early 1950s. However, temporal gaps caused by malfunction of the measuring equipment, field conditions and dryness of the wells, data were not collected and not complete for every month. Therefore, an extensive well elimination is required and the selected subset of groundwater wells must have a sufficient amount of data to minimize the uncertainty in the groundwater storage time-series.

The quality control is conducted in two steps. Firstly, the quality of the well records are checked manually. Based on the suggestions of DSİ, unreliable records due to human-made mistakes are excluded from the time series (DSİ, personal communication, July 3, 2019). Secondly, the amount of well data less than 36 months (3 years) out of 156 are eliminated. The reason is to ensure that the amount of data in each well is reasonable. The final output of the quality control process yields a total of 120 wells (out of 294) and the attributes of groundwater monitoring wells for each

basin can be seen in Appendix A. The distribution of pumping wells (available data), weather stations and monitoring wells used in this study are shown in Figure 3.6.

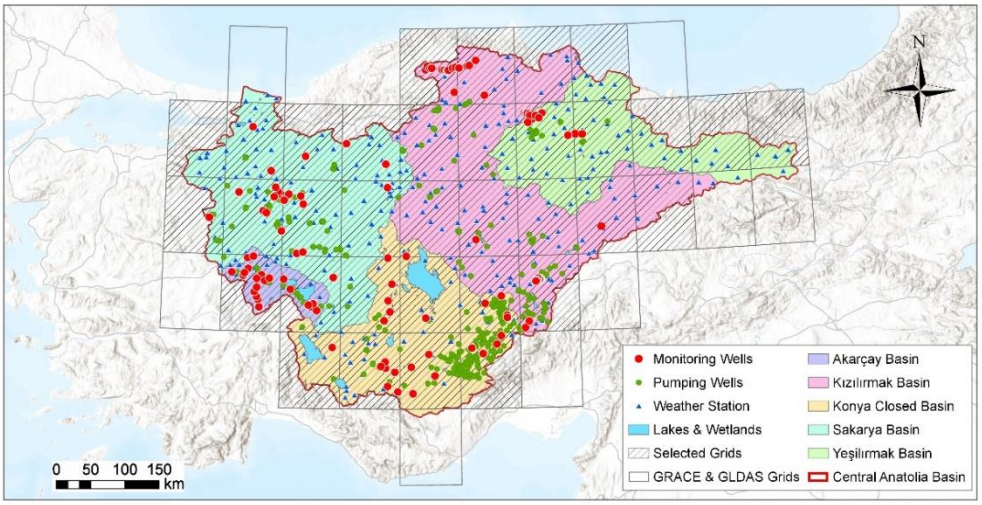

Figure 3.6. Location of weather stations, monitoring wells used in this study, and pumping wells over the selected grids

The standardized range of groundwater levels at each monitoring station over the study region are shown in Figure 3.7. For rescaling, Z-score standardization is used.

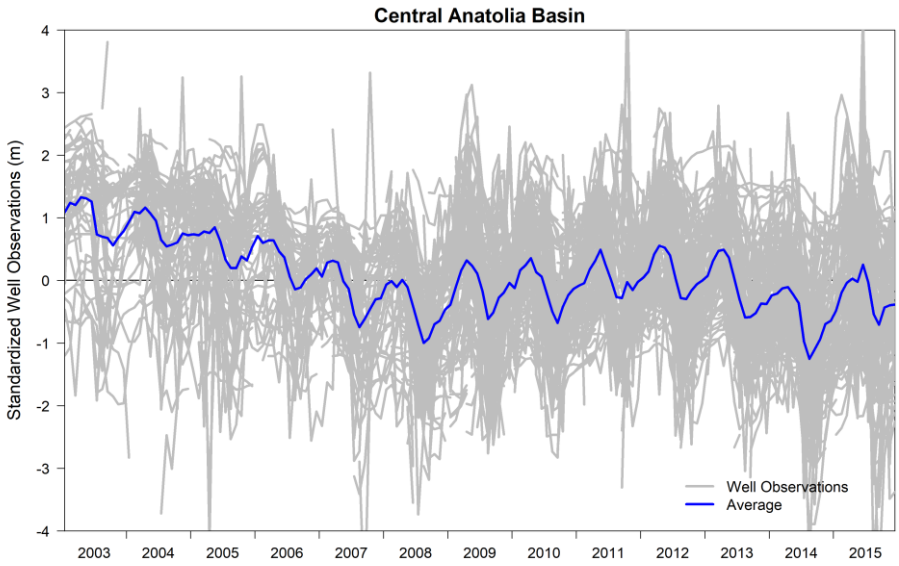

Figure 3.7. Standardized well levels (in grey) and average of all the well levels (in blue) in Central Anatolia Basin

The anomaly of groundwater levels are calculated to compare the groundwater storages with GRACE-derived estimates (Figure 3.8).

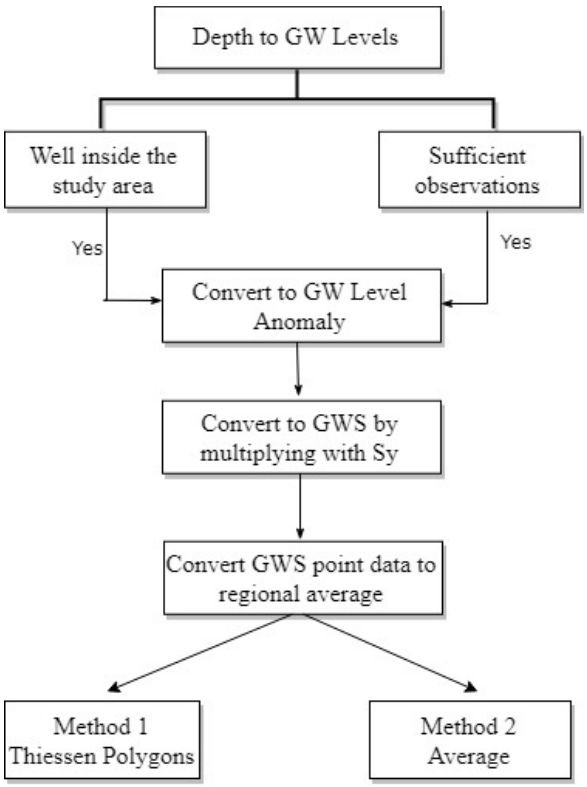

Figure 3.8. A flowchart to estimate the groundwater storage anomalies

In order to calculate an average hydraulic head value for each well, the total historical record should be considered (Scanlon et al., 2012). However, it is not applicable because of the lack of the monitoring well data which varies in each groundwater well. Therefore, the groundwater head changes are estimated for each well by subtracting the long-term average of 13 years from the value of each month, unlike the GRACE time-mean period (2004-2009).

$$\Delta H_{GW} = Depth_{GW} - \overline{Depth_{2003 \rightarrow 2015}} \quad (13)$$

where ΔH_{GW} is the change in groundwater well level, $Depth_{GW}$ is the depth to the groundwater level from the surface, $\overline{Depth_{2003 \rightarrow 2015}}$ is the average well level during 2003-2015.

It is difficult to establish monthly groundwater level fluctuations representing the basin. In general, there are three different methods (Thiessen, IDW, Average) implemented and for this study, two different approaches are employed for estimating a representative groundwater level change values for the catchment.

Firstly, Thiessen polygons are constructed for each month according to the availability of the well observations. Then, area weighted basin average time series are calculated (Rodell et al., 2007).

$$\Delta GWS = \frac{1}{C}\sum_{i}^{N} S_{yi} \times C_i \times \Delta H_i \tag{14}$$

$$C = \sum_{i}^{N} C_i \tag{15}$$

where S_i is the specific yield for unconfined aquifers or storativity value for confined aquifers. N is the number of subareas or subbasins. C_i represents the areas of the subbasins and C is the total area of the subbasins which equals to the basin area. The areas of subbasins or Thiessen polygons are used to distribute the specific yield values of each well that represents each aquifer type.

For the second method, the groundwater level anomaly values of all the wells are averaged (Frappart & Ramillien, 2018; Strassberg et al., 2009) and multiplied with a constant Sy value. In this method, the constant value of Sy acts as a normalizing constant.

3.2.3. Anomaly and Uncertainty Expression

The TWS anomaly data were previously processed with respect to a time-mean baseline which is the average of all months from January 2004 to December 2009. Hence, a new baseline did not needed to be calculated again for the 13 years of the study. So, the monthly anomaly values of each variable at every grid cell are calculated

by taking their deviation according to the reference period of GRACE, as shown in the Equation (16).

$$\Delta TWS_{i,j,k} = TWS_{i,j,k} - \sum_{k=1}^{n} \frac{TWS_{i,j,k}}{n} \quad (16)$$

where *i,j* represents the location of the grid cell. *n* is the number of months averaged (between 2004 and 2009).

The model outputs between January 2003 and December 2015 period are used in accordance with the availability of the GRACE and in-situ well data. The simulated TWS is approved as the sum of the anomalies of GW, SM, SWE, CWC and calculated by using the Equation (17) for each grid.

$$\Delta TWS = \Delta GW + \Delta SM + \Delta SWE + \Delta CWC \quad (17)$$

where TWS is total water storage, GW is groundwater storage, SM is the sum of soil moisture content in all soil layers, SWE is snow depth water equivalent, and CWC is plant canopy surface water storage.

To estimate the monthly groundwater storage variations using GRACE, the monthly change in the hydrological components of the LSMs are subtracted from GRACE TWS for each grid by using Equation (18).

$$\Delta GW = \Delta TWS - \Delta SM - \Delta SWE - \Delta CWC \quad (18)$$

The results are averaged over the basin area by taking the area weight of the selected grids. There have been no error estimates made for GLDAS data in any publication. So, the sum of the standard deviations of the model parameters are taken into account as the effect of the error estimates in groundwater. Using Equation (19), the total error on GWS change can be estimated as:

$$\sigma_{GW} = \sqrt{(\sigma_{TWS})^2 + (\sigma_{SM})^2 + (\sigma_{SWE})^2 + (\sigma_{CWS})^2} \quad (19)$$

3.2.4. Cumulative Deviation from Mean Precipitation

Cumulative Deviation from Mean (CDFM) is a simple arithmetic technique that is used for rainfall evaluation (Emelyanova et al., 2013; Yesertener, 2008) and is applied to groundwater studies (Ferdowsian et al., 2001). It assumes that rainfall can explain the changes in the groundwater levels in unconfined aquifers. The deviations from the average rainfall are plotted cumulatively using Equation (20).

$$CDFM_t^M = \sum_{i=1}^{t} (M_{i,j} - \bar{M}_j) \tag{20}$$

where $M_{i,j}$ is rainfall in month i which is a sequential index of time at corresponding j-th month of the year, $\bar{M}_j$ is the mean monthly rainfall for the jth month of the year, and t is the total number of months in the dataset.

3.2.5. Deseasonalization

Seasonal and Trend Decomposition using Loess (STL) is used to decompose the time-series into three components; seasonality, trend and remainder.

$$Y_t = S_t + T_t + R_t \tag{21}$$

where Y_t is data, S_t is seasonal component, T_t is trend and R_t is remainder at period t.

It is used to extract the seasonal pattern from the original data and uses iterative loess smoothing which is a locally weighted regression technique to obtain an estimate of the trend (Cleveland et al., 1990). It is a non-parametric technique that enables detection of non-linear patterns in long-term trends (Cleveland & Loader, 1996). This method is conducted because the weighting reduces the effect of outliers, which affects the direction and slope of the best fit line, and handles any type of seasonality. A smoothing function reduces the noise by capturing general patterns in the time series. So, it can assess the relationship between two variables where trends are difficult to visualize.

3.2.6. Trend Analysis

In order to estimate yearly drawdowns, Leave-One-Out Cross Validation (LOOCV) method is performed by fitting a linear model based on simple linear regression. It is used to prevent overfitting the predictive accuracy of the model and get unbiased estimate. In this cross-validation technique, a sample is removed for once and the remaining data are trained to fit a regression line. Then, the fitted model is used to predict the value of retained data points. This procedure is repeated for every data point.

Additionally, to test the significance of a trend, modified Mann-Kendall trend test is applied because the datasets are serially correlated (Humphrey et al., 2016; Liesch & Ohmer, 2016; Scanlon et al., 2013). The reason why a non-parametric test is used is that the tests do not depend on the knowledge of the distribution.

3.2.7. Inter-Comparison

To estimate the strength of linear relationship between two variables Pearson's correlation analysis is conducted.

$$r_{x,y} = \frac{1}{n-1} \frac{\sum_{i=1}^{n}(X_i - m_X)(Y_i - m_Y)}{\sigma_X \sigma_Y} \tag{22}$$

where *r* is Pearson correlation coefficient that gives the correlation between X and Y, *n* is sample size, *m* is mean value and σ represents standard deviation.

The cross-correlation between X_t and Y_{t+k} are conducted by using the Equation (23).

$$r_k = \frac{\sum_{i=1}^{n-k}(X_i - m_X)(Y_{i+k} - m_Y)}{\sqrt{\sum_{i=1}^{n}(X_i - m_X)^2 \sum_{i=1}^{n}(Y_i - m_Y)^2}} \tag{23}$$

where *k* is the time lag. It can be either positive or negative representing the direction.

Additionally, RMS Error is used to evaluate the difference between GRACE-based groundwater levels and monitoring well levels.

$$RMSE = \sqrt{\frac{\sum_{i=1}^{n}(Y_i - X_i)^2}{n}} \tag{24}$$

where Y_i is the predicted groundwater level change values and X_i values are in-situ groundwater level data.

CHAPTER 4

RESULTS AND DISCUSSION

GRACE TWS datasets are used along with GLDAS model datasets to obtain groundwater estimates, which are later validated using the ground station based datasets. However, it is necessary to investigate the GRACE TWS datasets so that the groundwater validation results could better be understood. There are various aspects of the TWS datasets: TWS datasets are obtained mainly from three processing centers, while these time series have different slowly/fast varying components (i.e., trend, seasonality, anomaly) that have different responses to different hydrometeorological variables (i.e., precipitation) and have different relations with model datasets used to obtain groundwater datasets.

Accordingly, TWS time series from different centers and mean TWS estimates are investigated over the study regions to see whether or not the datasets greatly vary from each other. Then, the components of TWS time series are analyzed to see which component of TWS dominates the GRACE TWS signal. Later, TWS estimates are examined for their relationship with the hydrometeorological variables and hydrological model datasets to better understand the impact of climate and the consistency of the datasets. Finally, the groundwater estimates obtained as the combination of GRACE TWS and GLDAS datasets are validated using groundwater well level observations. The workflow is visualized in Figure 4.1.

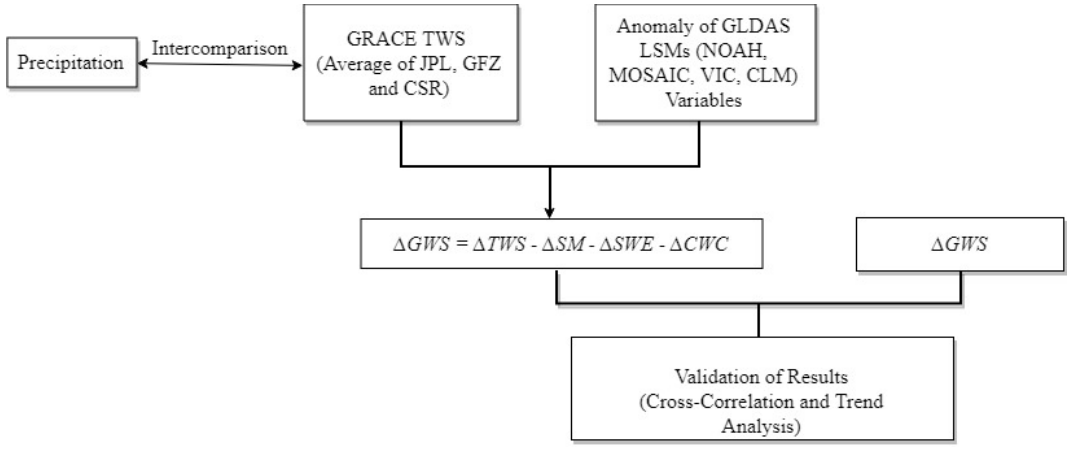

Figure 4.1. A flowchart describing the methodology

4.1. GRACE TWS Solutions

There are multiple sources providing GRACE datasets utilizing different methods to obtain TWS solutions. In this study, the datasets provided by three official data processing centers (JPL, GFZ, CSR) are used. Even though these estimates from three centers are different, in general the dominant linear signal in these datasets are the same. As an example the linear relationship (i.e., correlation coefficient) between these datasets over Central Anatolia Basin are given in Figure 4.2, where the correlations vary between the datasets are very high (0.95 – 0.98). The correlations between the datasets for smaller sub-basins (Akarçay, Kızılırmak, Konya, Sakarya and Yeşilırmak) are given in Appendix B.

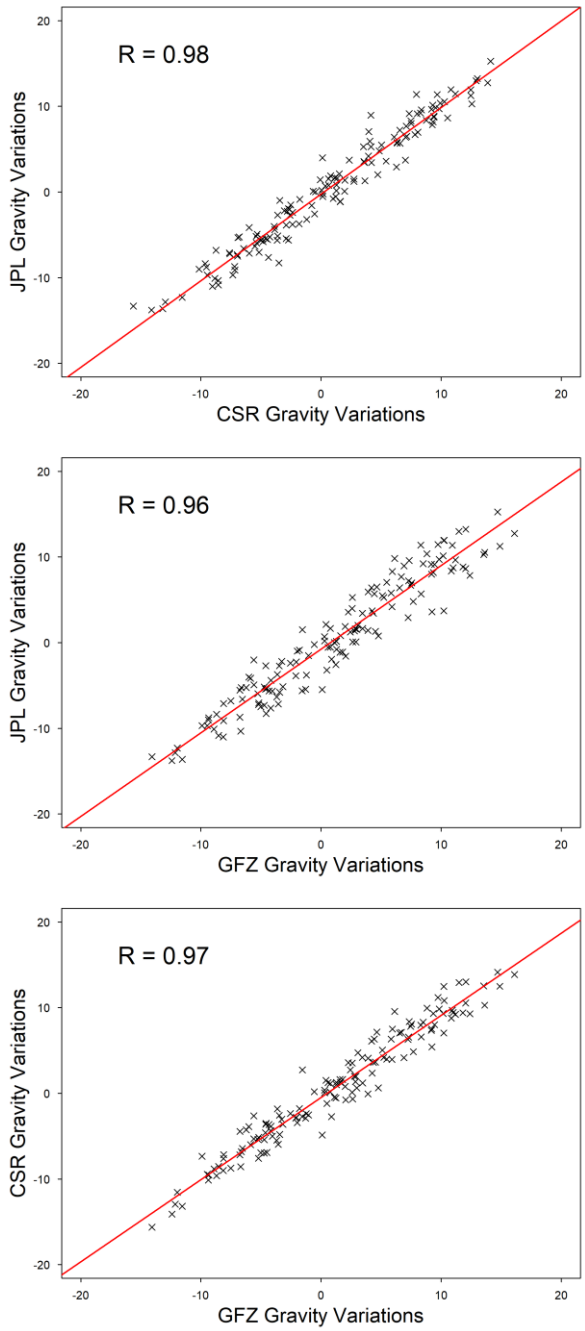

Figure 4.2. Comparison of TWS solutions from JPL, CSR, and GFZ over Central Anatolia Basin

The time series of TWS datasets obtained from three data centers and their average over Central Anatolia Basin are given in Figure 4.3. The data gaps are due to battery management. Overall, there is only marginal difference between the time series of

these datasets over the inflection points, otherwise the time series almost overlap at other times (Figure 4.3). In terms of dataset selection, literature generally takes the average of these different estimates to acquire GRACE time series that are used in their final analysis (Sakumura et al., 2014; Seyoum & Milewski, 2016; Xiao et al., 2015). Accordingly, these three different GRACE solutions are also averaged (Figure 4.3), where this averaged time series is used in the entire study.

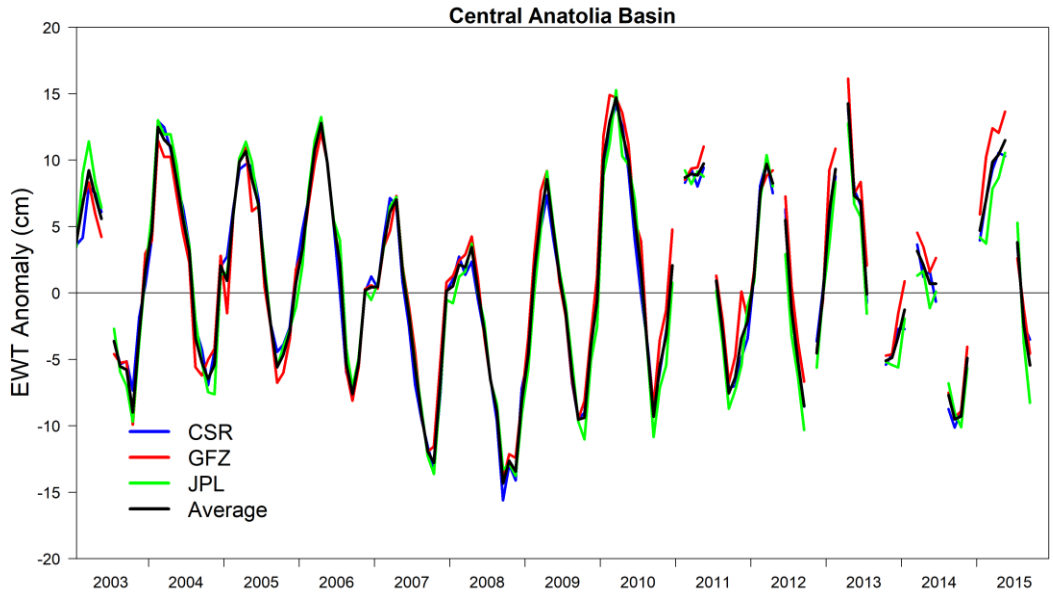

Figure 4.3. Time series of TWS from 3-centers over Central Anatolia Basin

Again following the recommendations of data providers (Wahr et al., 2006), the GRACE TWS data is multiplied by the scaling factor to avoid signal loss. The final scaled GRACE TWS time-series used in this study and the unscaled original TWS time series for the Central Anatolia Basin are given in Figure 4.4, and the scaled TWS time series for all sub-basins are given in Figure 4.5.

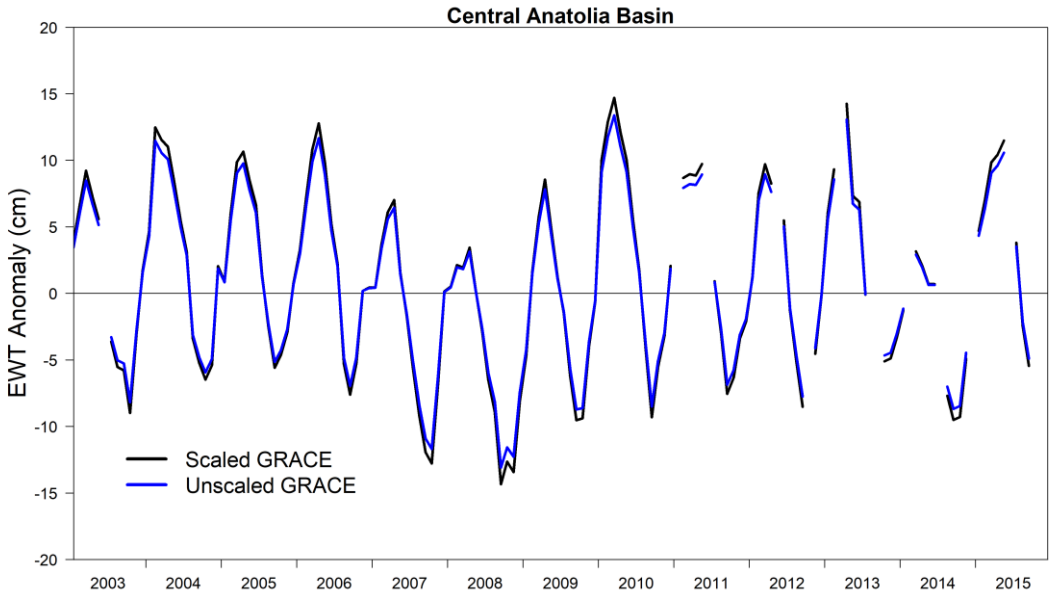

Figure 4.4. Time series comparison of scaled and unscaled GRACE TWS over Central Anatolia Basin

There are only marginal differences between the scaled and the unscaled original GRACE TWS time series, implying the impact of this scaling step is only minimal and other factors dominate the temporal variability of the GRACE TWS estimates. Similar results are also obtained for the other sub-basins of Central Anatolia Basin (shown in Appendix C) that scaling coefficient impact the temporal variability of the TWS estimates only marginally. This implies the GRACE TWS temporal variability are more impacted from the change of other factors (e.g., precipitation, climate) than local signal leaks

The time series comparisons of GRACE TWS of the basins show nearly identical patterns. Figure 4.4 shows that the peaks and valleys occur almost at the same time intervals. The magnitudes of the datasets are almost in the same range and agree well with each other.

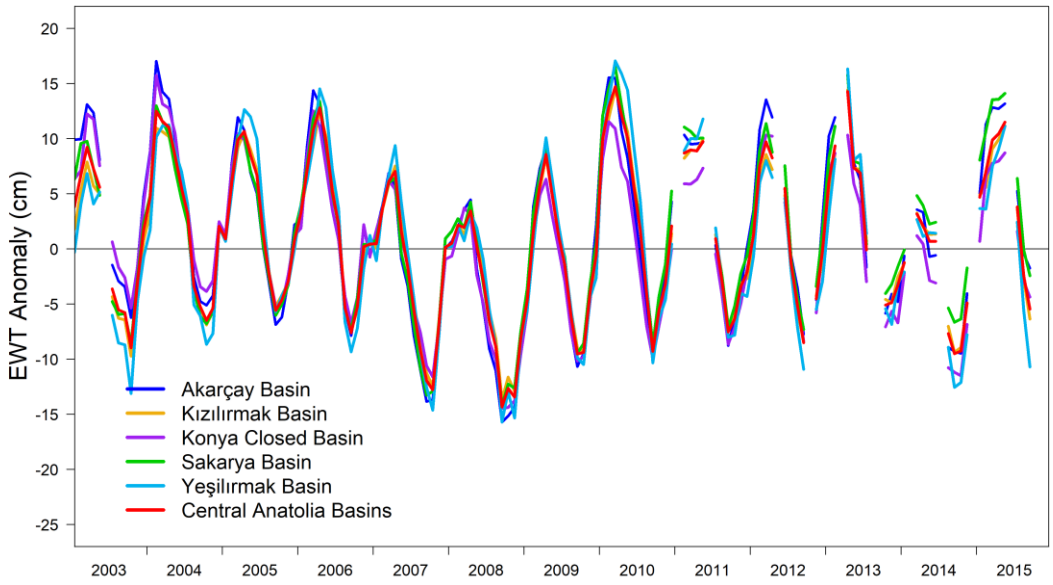

Figure 4.5. Comparison of GRACE TWS time series of the basins

Once the GRACE TWS estimates are obtained for each basin separately, then modified Mann-Kendall trend test is conducted over Central Anatolia Basin and sub-basins to test the existence of trend in GRACE TWS variations. The values of Kendall's tau related with the test are between -0.16 and 0.04 for the study region, where only the downward trend in KCB is significant (p-value < 0.01). The negative trend stresses the total water storage decrease persistently over the KCB.

4.2. GRACE TWS Time Series Decomposition

In general, the GRACE time series show strong seasonality, while the deviations from the seasonal means during the dry and the wet periods (i.e., anomaly) is primarily important for many studies. Hence, the seasonality information is subtracted from the GRACE solutions initially, so that these solutions could be compared against the other datasets (i.e. precipitation).

The decomposed components of GRACE TWS over the Central Anatolia Basin are given in Figure 4.6, while the decomposed time series for the individual sub-basins are given in Appendix D.

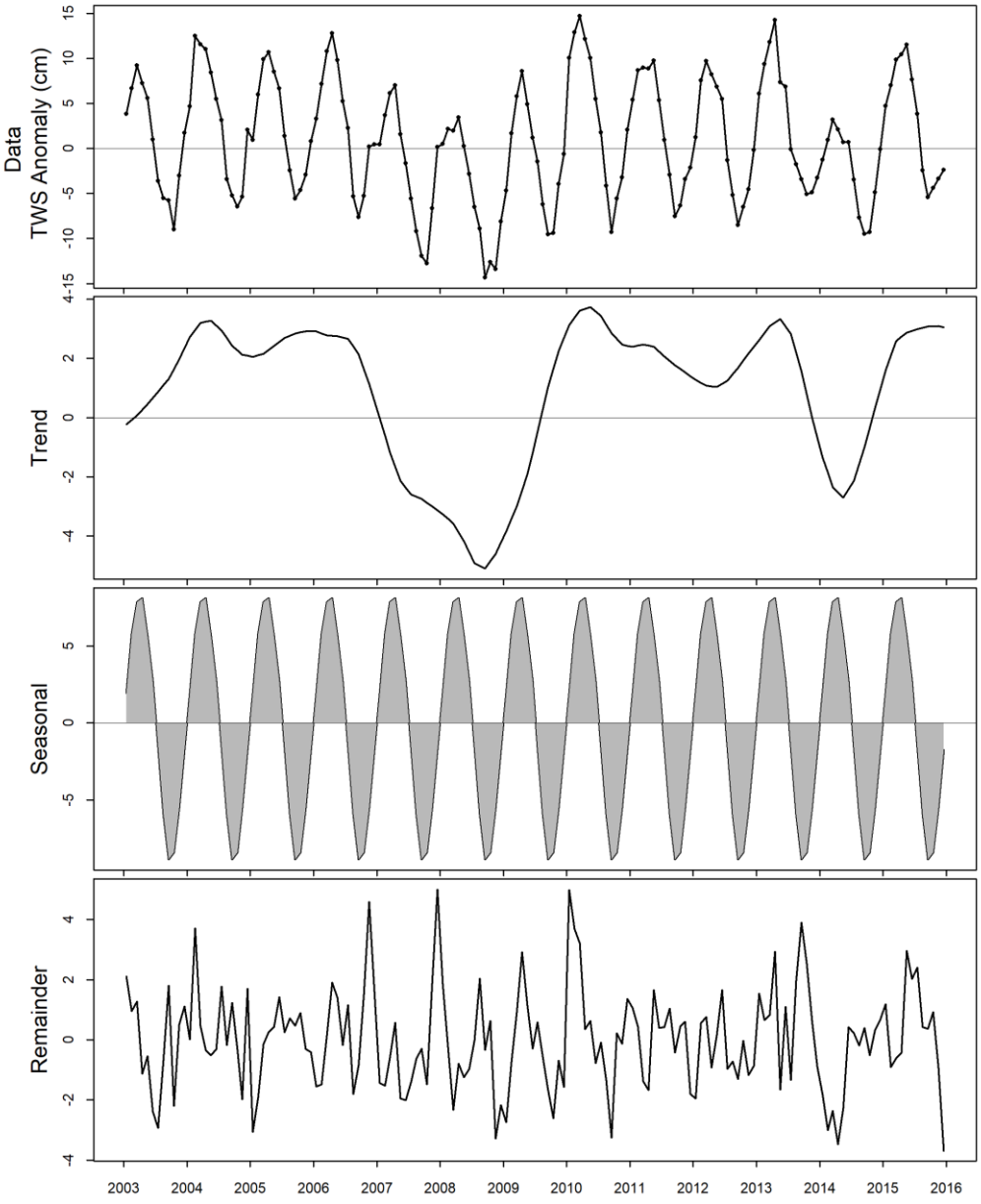

Figure 4.6. Decomposition of GRACE TWS time series of Central Anatolia Basin

Overall the seasonal component has the highest variability measured by standard deviation (Table 4.1), while the trend and anomaly remainder components have much less variability. The TWS time series are dominated by long-term signals. The trends show the TWS has a rapid decline between 2006 and 2009, which is consistent with the drought conditions observed in the area (Bulut & Yılmaz, 2016).

Even though the water storages recover after the year 2009, they again start to decrease rapidly after 2013 until mid-2014, which is again consistent with another drought period over the area.

Table 4.1. *Standard deviations of GRACE TWS time series components over Central Anatolia Basin and 5 basins.*

	Basin	Total	Seasonal	Trend	Random
GRACE TWS	Akarçay	7.63	6.53	3.12	2.00
	Kızılırmak	6.49	5.78	2.26	1.65
	Konya	6.73	5.67	2.92	1.67
	Sakarya	6.99	6.08	2.74	1.86
	Yeşilırmak	7.55	6.69	2.62	2.01
	Central Anatolia Basin	6.74	5.98	2.41	1.68

4.3. GRACE TWS and Precipitation

The TWS time series obtained for different basins have great similarity over the regions investigated in this study (Figure 4.5). This implies either GRACE TWS estimates are impacted from a much wider region or the overall region is under the same dominant climatic variability so that different basins investigated in this study have similar dry/wet period transition. To have better confidence about the variability observed in this study, GRACE TWS observations are compared against precipitation datasets.

Cumulative monthly residual precipitation may give insight about the accuracy of GRACE TWS signals. Here, because TWS estimates have heavy seasonality, the seasonality information is removed before they are compared against the CDFM. The seasonally adjusted GRACE TWS time series and CDFM precipitation time series over Central Anatolia Basin are shown in Figure 4.7 and the graphs of each basin can be seen in Appendix E.

These two time series show very consistent variability that 2007-2008 and 2013-2014 are the driest periods between 2002 and 2015 (Bulut & Yılmaz, 2016), while the Central Anatolia Basin region starts to recover from these severe drought conditions in 2009 and 2015 respectively for these two periods.

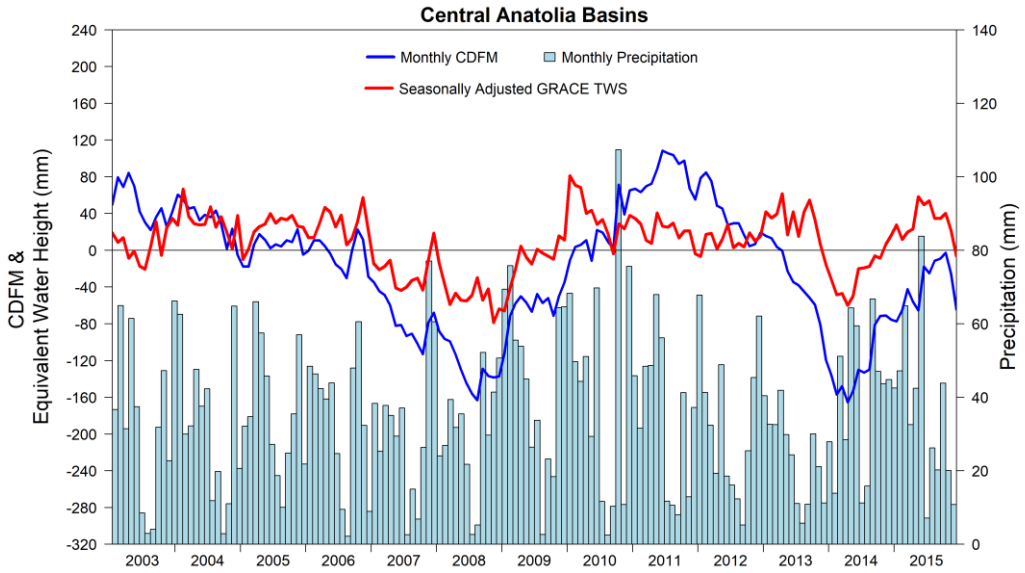

Figure 4.7. Comparison of monthly CDFM and deseasonalized GRACE TWS over Central Anatolia Basin

The linear relation between CDFM and GRACE TWS over Central Anatolia Basin and its sub-basins without any lag is measured via the correlation coefficient given in Table 4.2. Overall, the correlations vary between 0.42 and 0.71. Estimation of the drought periods over the same region similarly using two independent variables increases the confidence of the events over the regions.

Table 4.2. *Correlations between CDFM and seasonally adjusted GRACE TWS*

	Basin	Catchment Area (km^2)	Pearson's Correlation (r)
1	Akarçay Basin	7,605	0.57
2	Kızılırmak Basin	78,180	0.56
3	Konya Closed Basin	53,850	0.71
4	Sakarya Basin	58,180	0.56
5	Yeşilırmak Basin	36,114	0.42
6	Central Anatolia Basin	233,929	0.65

In addition to the analysis between the CDFM and TWS, the performance of TWS is also tested independently using the Salt Lake extent over KCB. Because precipitation over KCB contributes significantly to the Salt Lake water storage, any drought event occurring over the basin also strongly impact the extent of the lake. According the Salt Lake extent data, obtained from the study of Ceyhan (2016), is used as an independent dataset (Landsat images) to validate the GRACE TWS estimates. Ceyhan (2016) calculated the water extent values of the Salt Lake based on the lake extent of June 2011 which is the maximum outline of the study period between 2000 and 2015. The extent anomalies are calculated based on the GRACE time-mean baseline. The average of lake extent values between 2004 and 2009 are assumed to be the mean extent and the monthly extent values are subtracted from the mean. Accordingly, GRACE TWS time series and Salt Lake extent has been compared in Figure 4.8. The average correlation coefficient values between the Salt Lake extent and GRACE grids (GRACE Grid-1 and Grid-2) overlapping Salt Lake is 0.61, implying GRACE TWS estimates capture a good portion of the variability of the Salt Lake extent and the water storage over the basin.

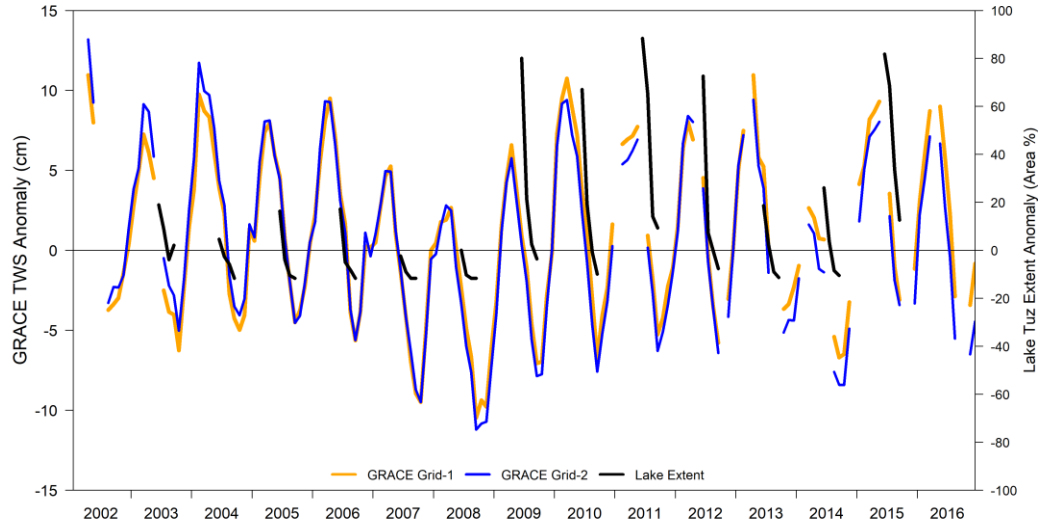

Figure 4.8. Monthly estimates of TWS from GRACE (left axis) and area extent anomaly for Salt Lake (right axis)

4.4. GRACE TWS and Hydrological Models

Similarly, to better understand the sources of the errors of groundwater change estimates, it is important to investigate the TWS and the other components (i.e., model-based datasets). Hence, TWS- and hydrological model (GLDAS)-based dataset relations are investigated separately.

GLDAS LSM-based datasets are used to obtain the GWS change information using the TWS datasets (Equation (18)). However, there are multiple GLDAS versions (GLDAS-1 and GLDAS-2) obtained using different models (NOAH, VIC, MOSAIC, CLM) forced by different datasets. Accordingly, the TWS estimates obtained from each of these models vary among each other as well as GRACE satellite. The TWS time series of different models and GRACE are investigated over Central Anatolia Basin. In Figure 4.9, TWS from every GLDAS LSMs are compared with GRACE TWS, and the relationship between LSMs-derived and GRACE-derived TWS are

examined by Pearson's correlation coefficient in Table 4.3 for the Central Anatolia Basin and its subbasins.

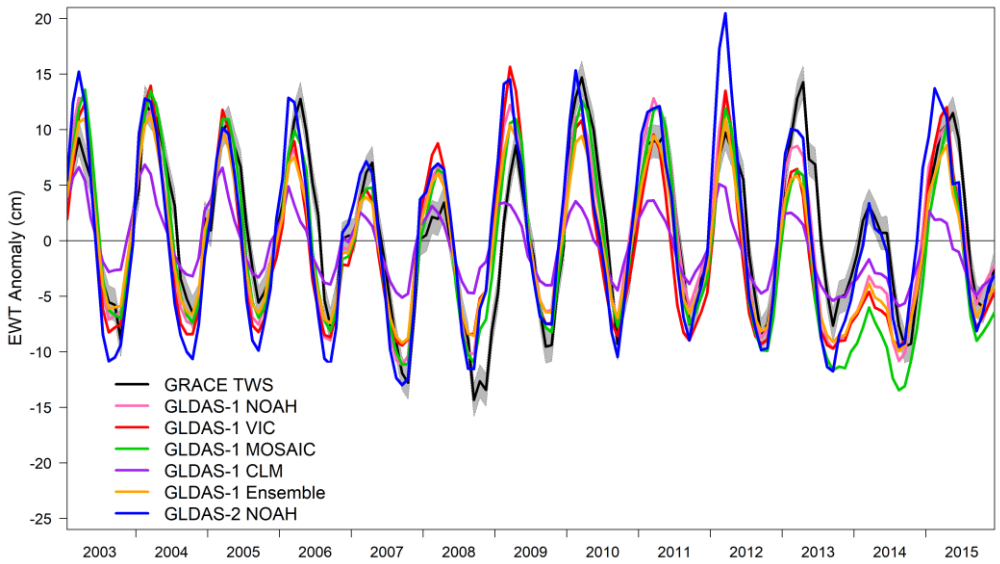

Figure 4.9. Comparison of GRACE TWS anomaly with GLDAS derived TWS anomaly over Central Anatolia Basin

Overall, GRACE TWS and GLDAS TWS are highly correlated with each other. Among all the LSMs, CLM has the lowest amplitude while GLDAS-2 NOAH has the highest amplitude.

Table 4.3. *Correlation between LSM-derived TWS and GRACE TWS over the basins*

			GRACE TWS					
			Akarçay	Kızılırmak	Konya	Sakarya	Yeşilırmak	Central Anatolia Basin
TWS	GLDAS-1	NOAH	0.91	0.85	0.89	0.88	0.78	0.87
		VIC	0.83	0.79	0.81	0.83	0.77	0.82
		MOSAIC	0.91	0.85	0.91	0.89	0.82	0.89
		CLM	0.85	0.74	0.84	0.78	0.62	0.77
		Ensemble	0.90	0.84	0.89	0.87	0.79	0.86
	GLDAS-2 NOAH		0.85	0.83	0.82	0.85	0.81	0.85

The monthly SM variations from GLDAS LSMs are shown in Figure 4.10. From the results, SM variations are highly correlated with TWS. The variations from MOSAIC gives the highest correlation with GRACE TWS. Also, GLDAS-1 NOAH and GLDAS-1 Ensemble SM variations are strongly correlated with GRACE TWS.

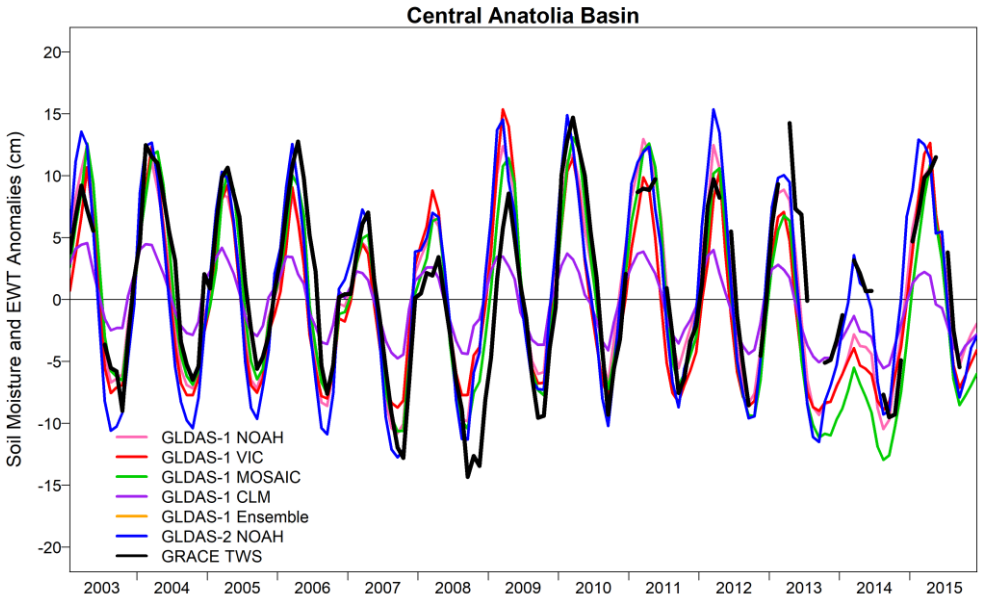

Figure 4.10. Soil moisture anomalies derived from GLDAS LSMs vs GRACE TWS over Central Anatolia Basin

The monthly SM, SWE, CWC variations from GLDAS LSMs are investigated over Central Anatolia Basin (Figures 4.10 – 4.12) and its subbasins (Appendix F).

The model-based variables in each model used for the estimation of the GWS vary as a result of the physics used by different models and the utilized different forcing datasets. On the other hand, other variables are not as much correlated with TWS as SM does. To emphasize the relative importance of the variables, the variance of each component is compared with respect to the variance of the TWS. Except CLM, the relative variances indicate that SM is the main component explaining most of the variance in the time series (Table 4.1 and Table 4.4).

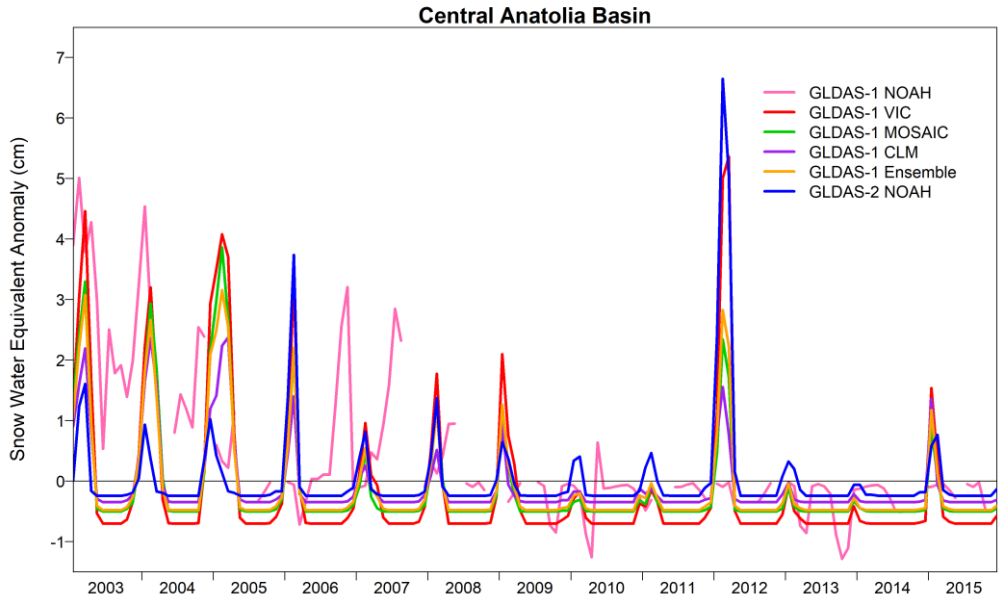

Figure 4.11. Snow water equivalent anomalies derived from 5 GLDAS LSMs over Central Anatolia Basin

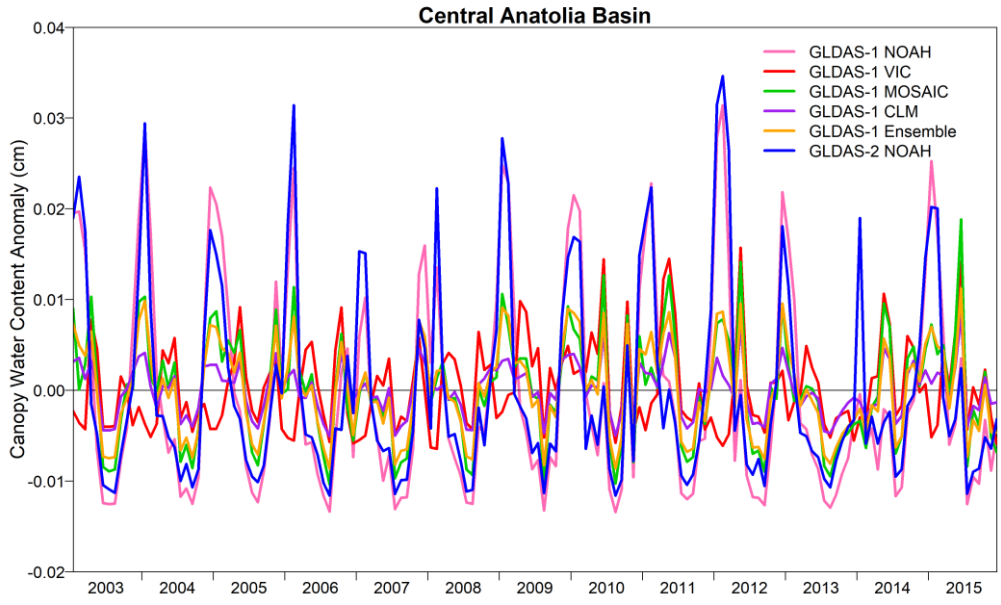

Figure 4.12. Canopy water content anomalies derived from 5 GLDAS LSMs over Central Anatolia

Table 4.4. *Standard deviations of SM, SWE, and CWC from different GLDAS LSMs*

		Akarçay Basin		
		σ_{SM}	σ_{SWE}	σ_{CWC}
GLDAS-1	NOAH	6.70	0.63	0.01
	VIC	6.35	1.06	0.01
	MOSAIC	6.68	0.70	0.01
	CLM	3.01	0.40	0.00
	Ensemble	5.55	0.67	0.01
GLDAS-2 NOAH		8.15	0.82	0.01

		Sakarya Basin		
		σ_{SM}	σ_{SWE}	σ_{CWC}
GLDAS-1	NOAH	6.98	0.74	0.01
	VIC	7.55	1.51	0.01
	MOSAIC	7.27	0.96	0.01
	CLM	2.86	0.92	0.00
	Ensemble	6.06	1.01	0.01
GLDAS-2 NOAH		8.12	0.74	0.01

		Kızılırmak Basin		
		σ_{SM}	σ_{SWE}	σ_{CWC}
GLDAS-1	NOAH	6.71	0.54	0.01
	VIC	6.11	0.99	0.01
	MOSAIC	6.86	0.79	0.01
	CLM	2.86	0.30	0.00
	Ensemble	5.49	0.64	0.01
GLDAS-2 NOAH		7.98	1.17	0.01

		Yeşilırmak Basin		
		σ_{SM}	σ_{SWE}	σ_{CWC}
GLDAS-1	NOAH	7.19	1.41	0.01
	VIC	7.46	2.58	0.01
	MOSAIC	8.77	1.81	0.01
	CLM	2.66	1.57	0.00
	Ensemble	6.36	1.82	0.00
GLDAS-2 NOAH		8.41	0.88	0.01

		Konya Closed Basin		
		σ_{SM}	σ_{SWE}	σ_{CWC}
GLDAS-1	NOAH	5.87	0.30	0.01
	VIC	5.49	0.65	0.00
	MOSAIC	7.04	0.40	0.01
	CLM	2.84	0.26	0.00
	Ensemble	5.18	0.39	0.00
GLDAS-2 NOAH		7.14	0.47	0.01

		Central Anatolia Basin		
		σ_{SM}	σ_{SWE}	σ_{CWC}
GLDAS-1	NOAH	6.53	0.64	0.01
	VIC	6.38	1.22	0.00
	MOSAIC	7.02	0.86	0.01
	CLM	2.77	0.60	0.00
	Ensemble	5.57	0.81	0.01
GLDAS-2 NOAH		7.78	0.84	0.01

4.5. GRACE GWS Estimates and Validation

GRACE TWS datasets are combined with model-based variables (SM, SWE, and CWC) to find the variations in the GWS. The GRACE observations and the LSM variable estimates are obtained and processed at 1º x 1º grid cells. The model-based variables are obtained from 5 different LSMs provided by GLDAS. Also, the variables from the ensemble average of GLDAS-1 is widely used in the literature. So, 6 different GRACE-based GWS variations are estimated.

These estimates are validated using station-based groundwater level observations, which are observed as point data and later converted into areal averages using two different methods (Average and Thiessen). All of these GWS time series are given separately for Central Anatolia Basin and its subbasins below in Figures 4.13 – 4.18.

In these 5 figures, the shaded area shows the uncertainty of GRACE-derived GWS which is comprised of the error sums of the TWS and SM, SWE and CWC. The errors from GRACE TWS can be seen in Table 4.5. The total error of GRACE TWS decreases as the catchment area increases.

Table 4.5. *GRACE TWS errors*

Basin	Measurement Error (cm)	Leakage Error (cm)	GRACE Total Error (cm)	Catchment Area (km^2)
Akarçay	1.71	2.29	2.86	7,605
Yeşilırmak	1.40	1.65	2.16	36,114
Konya	1.44	2.14	2.58	53,850
Sakarya	1.42	1.10	1.80	58,180
Kızılırmak	1.25	1.30	1.80	78,180
Central Anatolia Basin	1.17	0.91	1.48	233,929

The short term fluctuations in the GRACE-derived GWS may represent the effects of GRACE errors and month-to-month errors in the model parameters. The drawdowns in the GRACE-derived GWS time series correspond to the drought periods as stated in Section 4.3. When the precipitation decreases, hydrologic drought occurs and the groundwater extraction increases in order to supply the precipitation deficits to sustain agricultural production as well as irrigation and drinking water.

The variation in GRACE-derived GWS is less than the changes derived from monitoring wells (Table 4.6). This could be because observation wells are more sensitive to the variations in the associated aquifers. Also, GRACE TWS time series is more smoothened because it represents a much larger area than station-based observations, where the variability at each individual points are expected to be higher.

Table 4.6. *Standard deviations of GLDAS-based and station-based GWS*

	$\sigma_{GRACE\text{-}GWS}$						σ_{Well}	
	GLDAS-1					GLDAS-2	Average	Thiessen
Basin	NOAH	VIC	MOSAIC	CLM	Ensemble	NOAH		
Akarçay Basin	3.24	4.36	3.30	5.34	3.63	4.55	17.57	21.65
Kızılırmak Basin	3.74	4.31	3.79	4.85	3.64	4.75	5.01	9.03
Konya Closed Basin	3.15	4.03	3.06	4.62	3.23	4.32	30.26	32.19
Sakarya Basin	3.48	4.60	3.49	4.95	3.50	4.47	12.69	15.66
Yeşilırmak Basin	5.12	5.60	5.30	6.13	4.84	5.13	15.05	37.58
Central Anatolia Basin	3.46	4.14	3.40	4.89	3.45	4.34	15.39	15.01

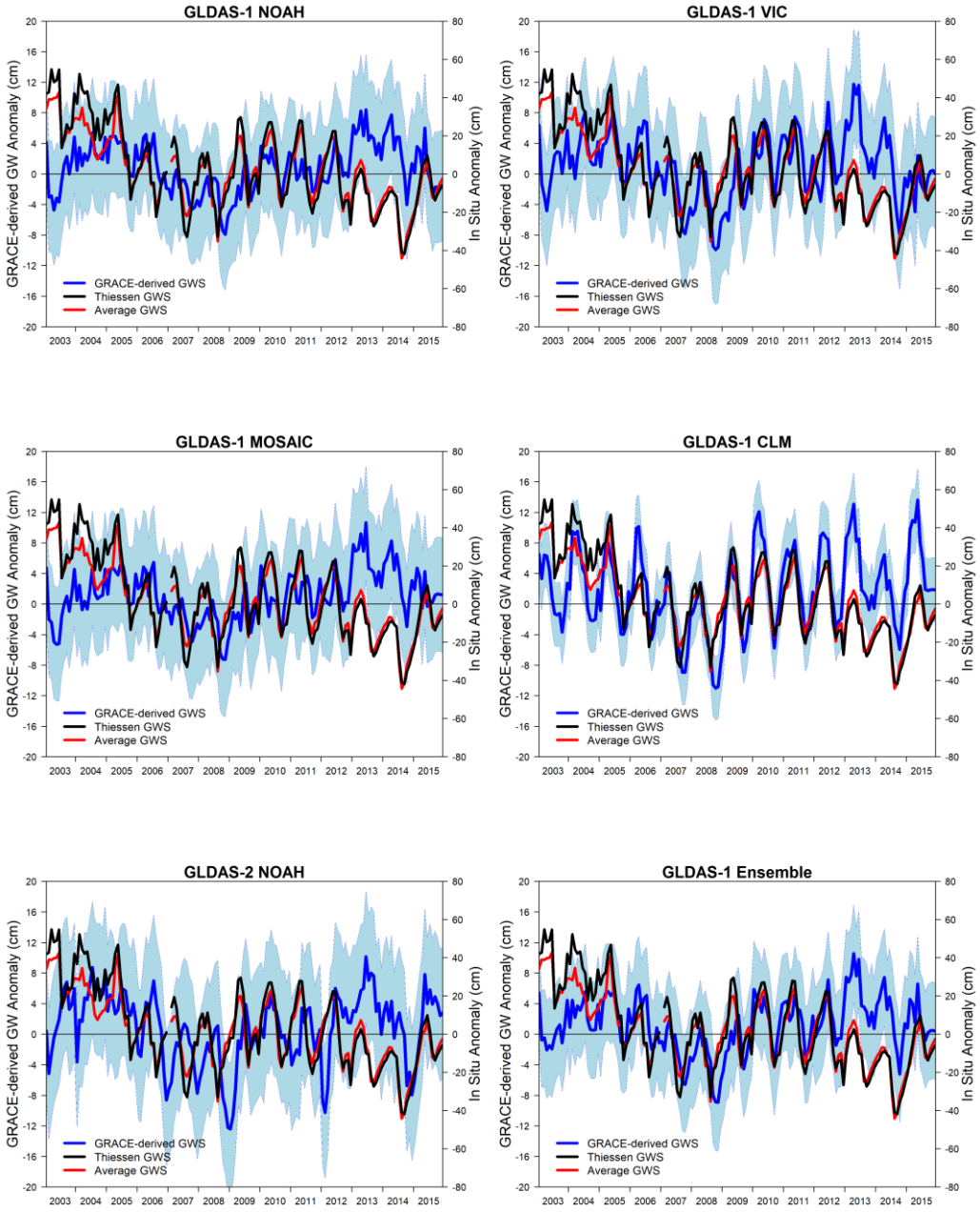

Figure 4.13. Comparison between GWS anomalies derived from GRACE TWS and in situ measurements at Akarçay Basin

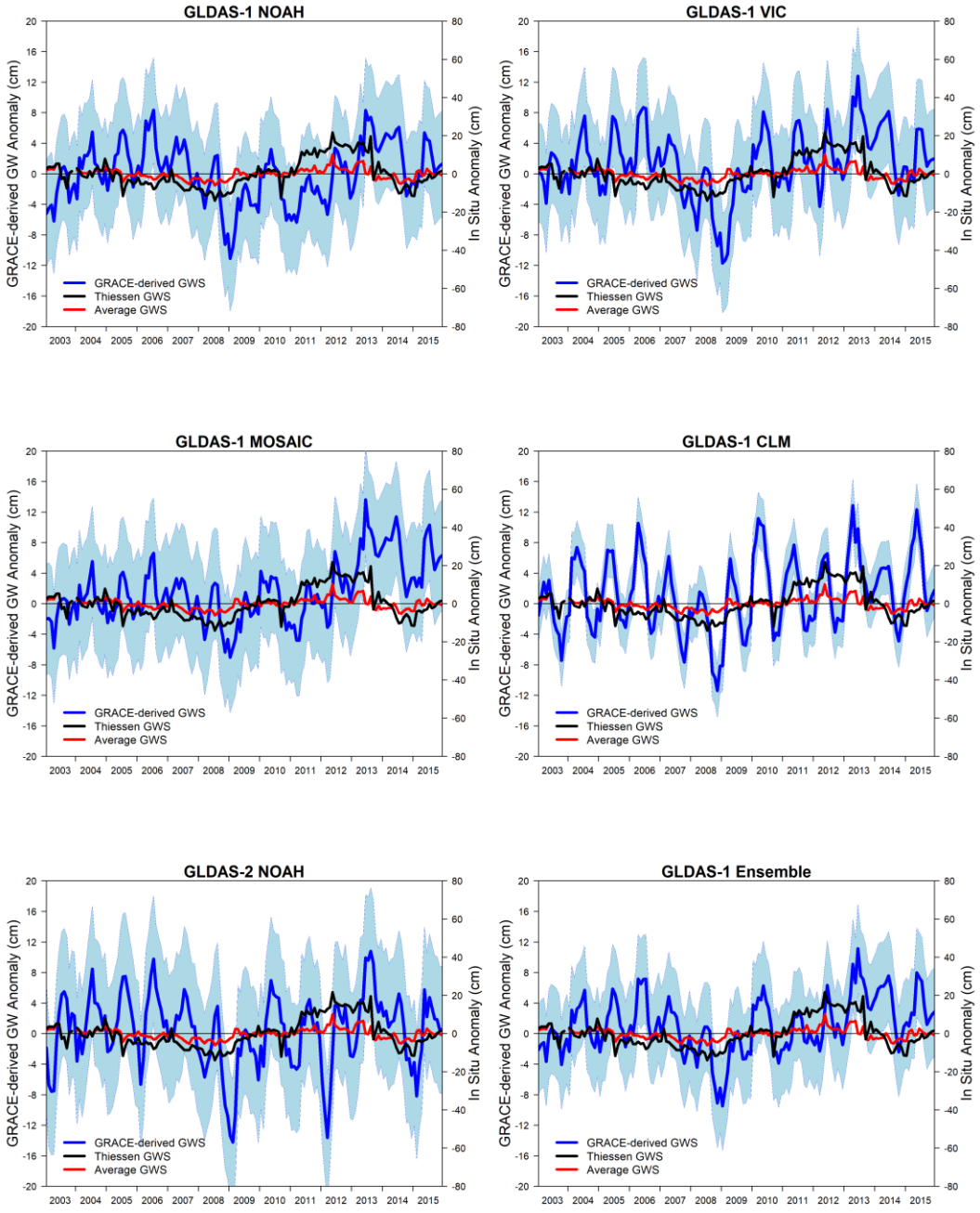

Figure 4.14. Comparison between GWS anomalies derived from GRACE TWS and in situ measurements at Kızılırmak Basin

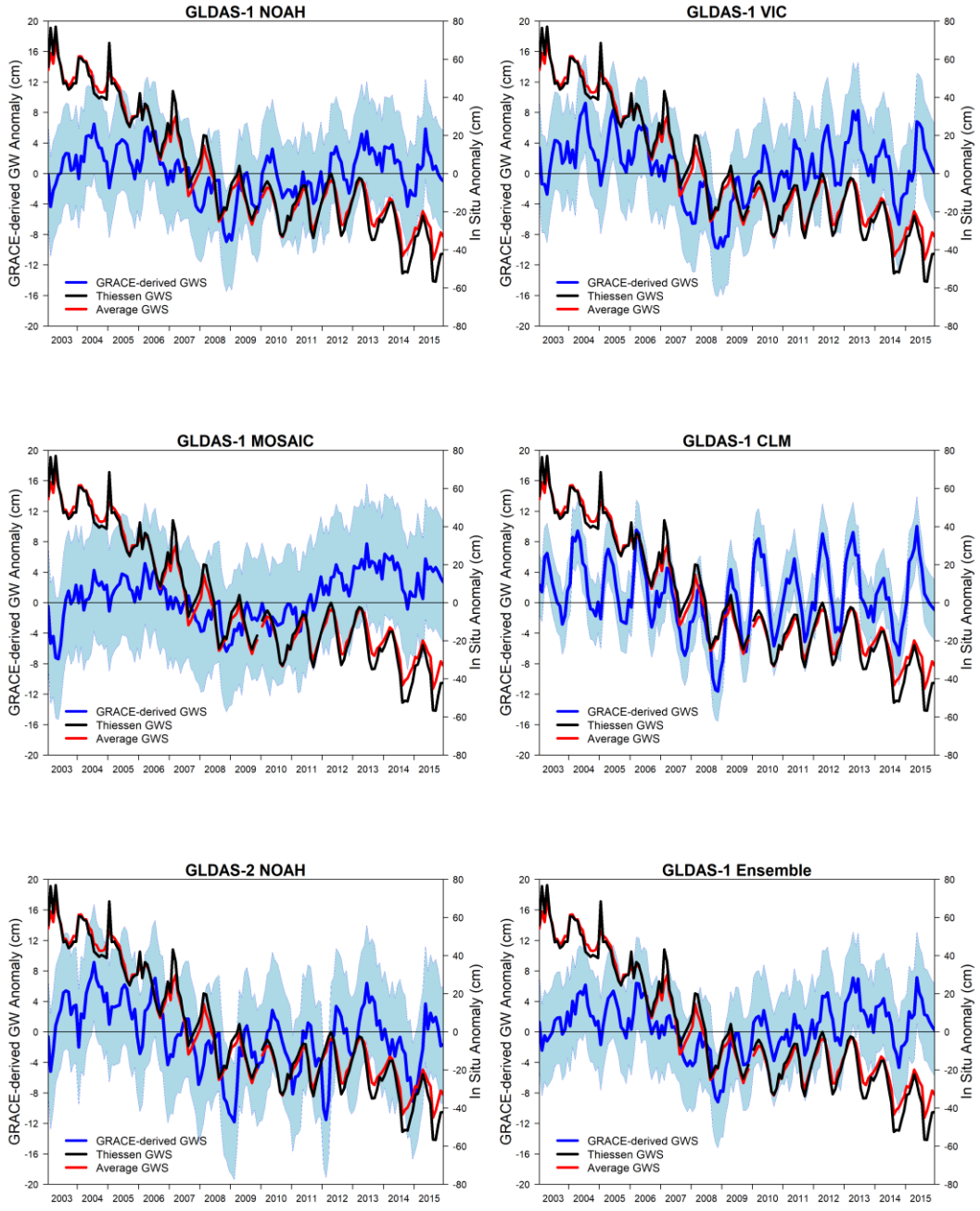

Figure 4.15. Comparison between GWS anomalies derived from GRACE TWS and in situ measurements at Konya Closed Basin

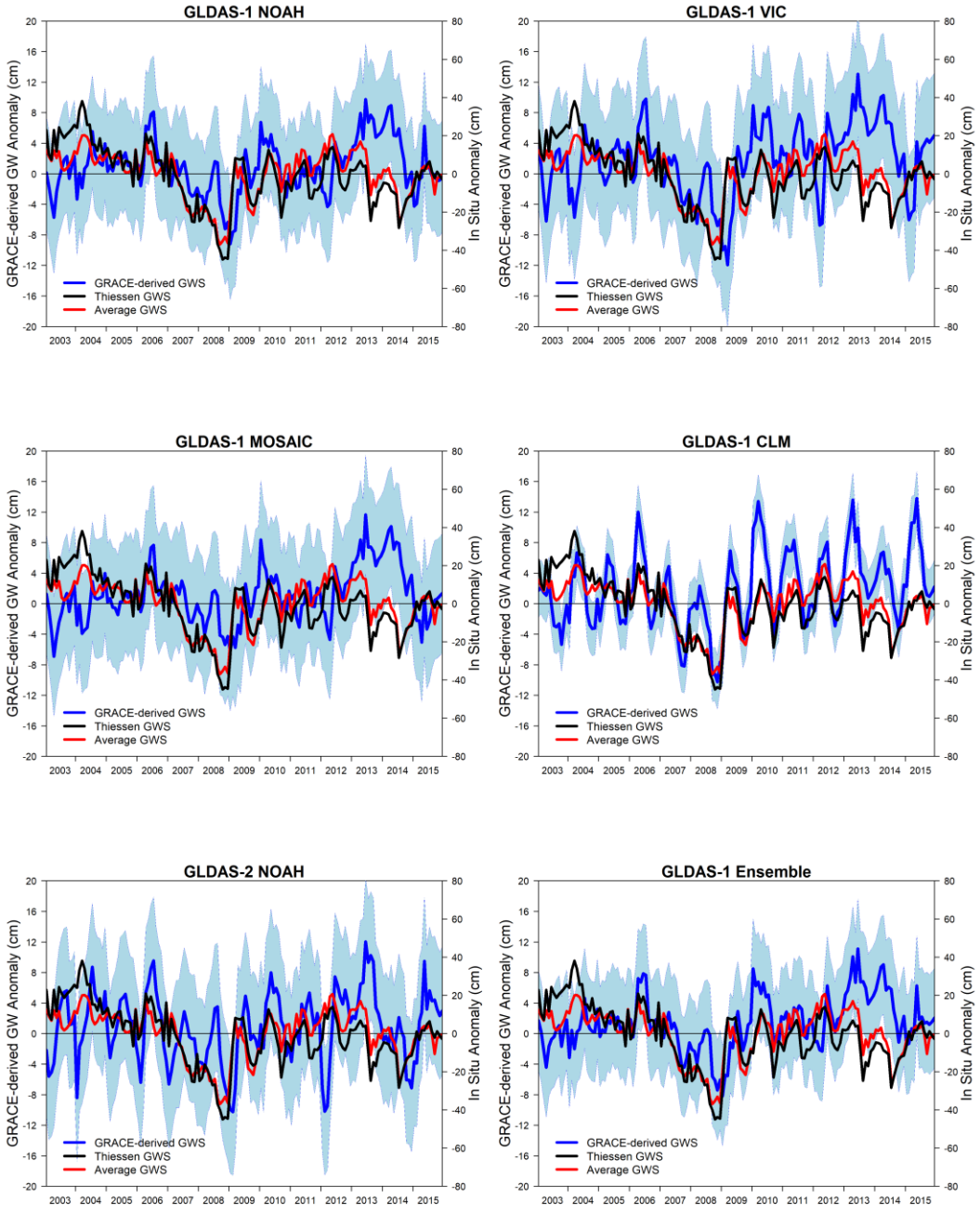

Figure 4.16. Comparison between GWS anomalies derived from GRACE TWS and in situ measurements at Sakarya Basin

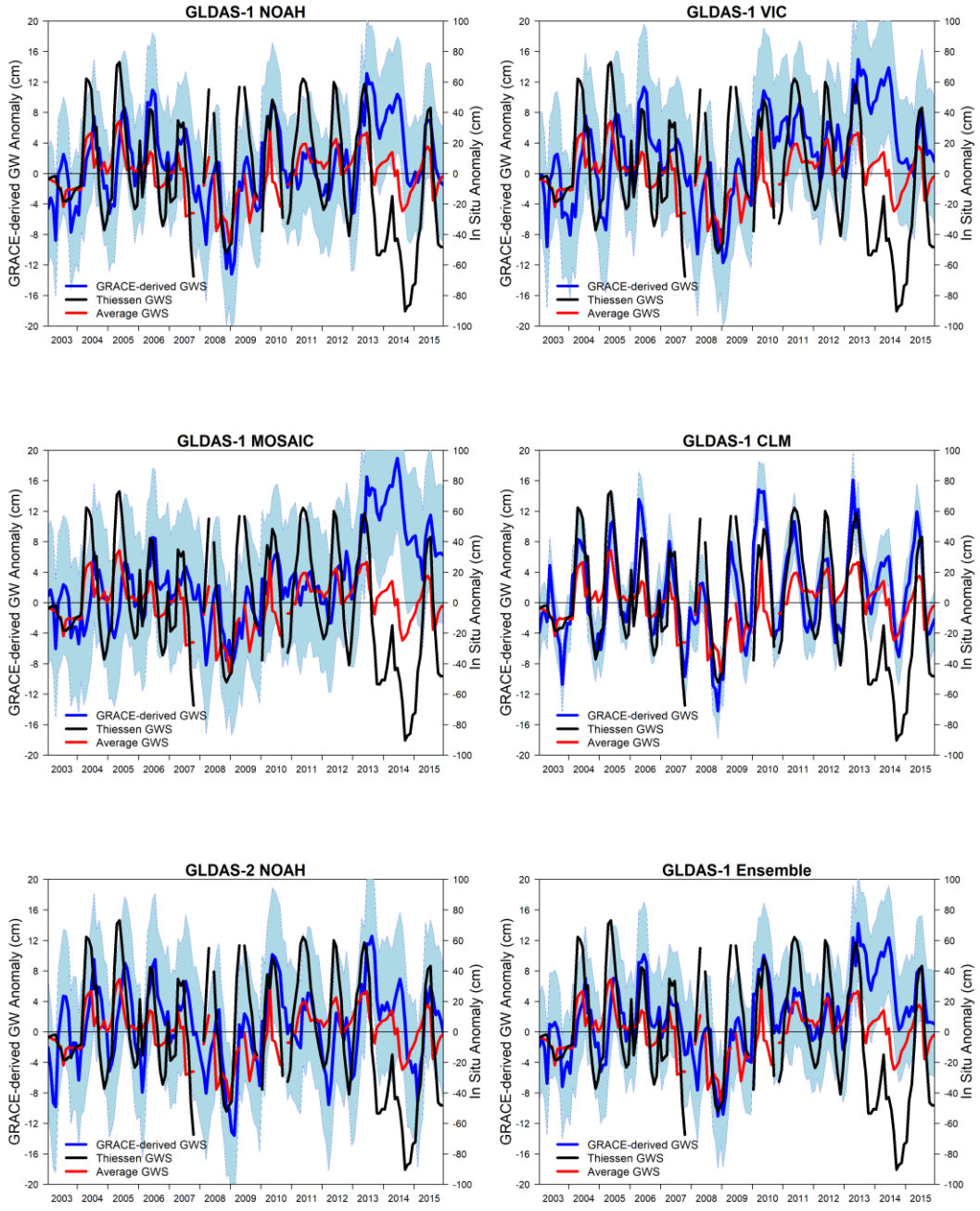

Figure 4.17. Comparison between GWS anomalies derived from GRACE TWS and in situ measurements at Yeşilırmak Basin

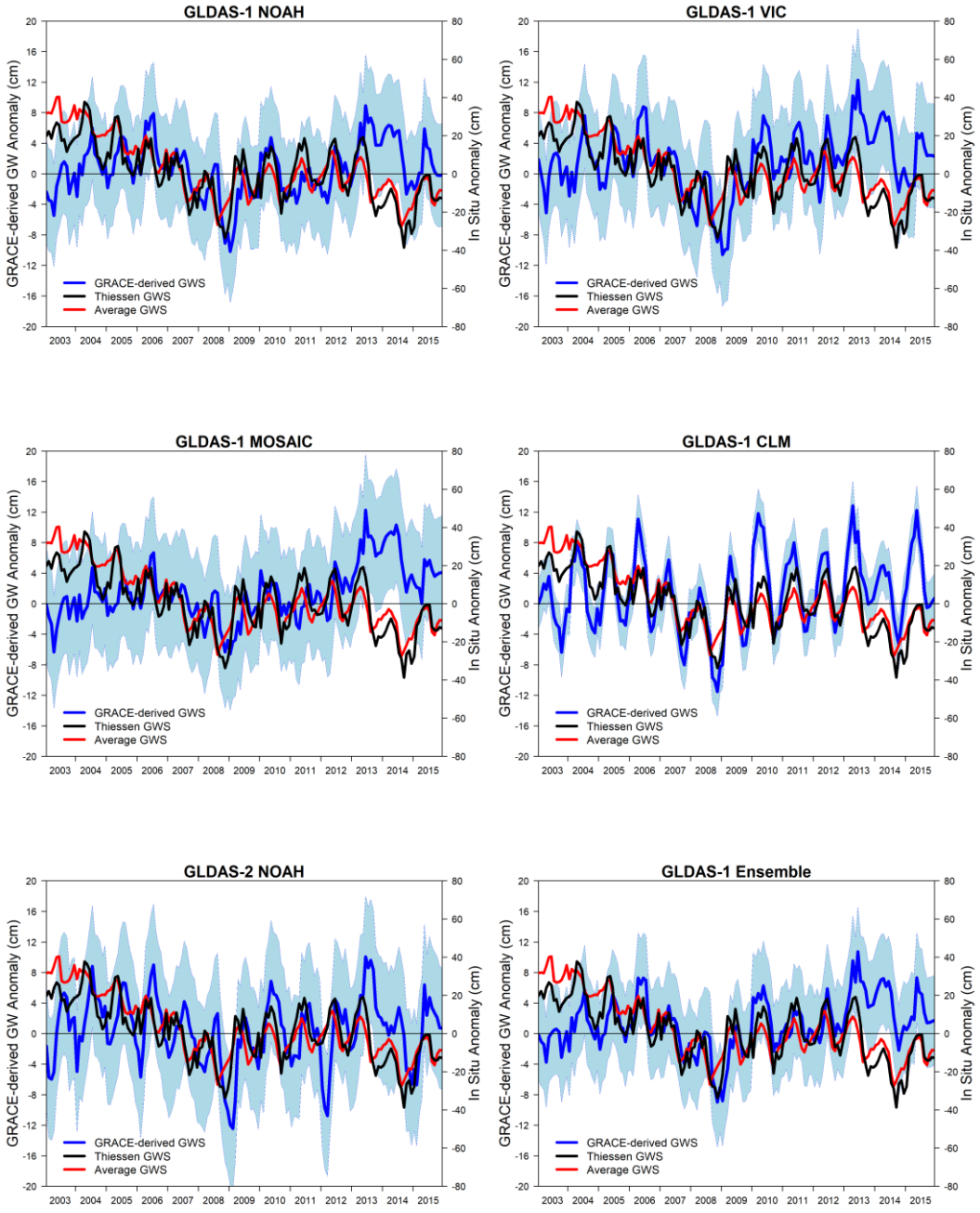

Figure 4.18. Comparison between GWS anomalies derived from GRACE TWS and in situ measurements at Central Anatolia

When the time series of the GRACE GWS are investigated, GLDAS 2 and GLDAS 1 mostly show consistent variability that they capture the drought and the wet periods accurately: the periods 2007-2008 and 2014 exhibit a very sharp decline in GWS over Central Anatolia Basin and all subbasins. There is an exception for this behavior that GLDAS 2 shows below average conditions during early 2012 over almost all regions while GLDAS 1 simulations do not have this behavior. This difference is because of the variations between the forcing datasets of the models that GLDAS 2 forcing data shows exaggerated drought conditions during early 2012 year where in reality the conditions are not as dry as GLDAS 2 depicts.

There are decreasing trends over the study region as far as the station based groundwater level observations are concerned. On the other hand, GRACE and GLDAS combined GWS estimates do not show the same decreasing trends. Overall, the station-based ground data show decreasing and mostly significant trend (Table 4.7 and 4.8), while GRACE-based GWS data does not. Part of the decreasing trend in station-based estimates are due to the seasonality, while removal of this strong impact will reduce the difference between the trends of GRACE GWS and station-based GWS.

Table 4.7. *Trends of GRACE TWS and GWS estimates*

Akarçay	Intercept	Trend	Yearly Change (cm)
GRACE-TWS	2.21	-0.11	-1.38
GLDAS1 NOAH-GW	0.13	0.10	1.24
VIC-GW	1.14	-0.02	-0.22
MOSAIC-GW	-0.51	0.24	2.91
CLM-GW	0.50	0.20	2.44
GLDAS2 NOAH-GW	1.06	-0.04	-0.47
GLDAS1 Ensemble-GW	0.31	0.13	1.59
Well Average	19.89	-2.77	-33.25
Well Thiessen	27.07	-3.58	-42.92

Sakarya	Intercept	Trend	Yearly Change (cm)
GRACE-TWS	0.70	0.15	1.81
GLDAS1 NOAH-GW	-0.28	0.18	2.19
VIC-GW	-0.32	0.34	4.06
MOSAIC-GW	-0.93	0.32	3.80
CLM-GW	-0.66	0.38	4.61
GLDAS2 NOAH-GW	0.18	0.11	1.31
GLDAS1 Ensemble-GW	-0.55	0.31	3.67
Well Average	3.52	-0.55	-6.66
Well Thiessen	10.78	-1.79	-21.42

Kızılırmak	Intercept	Trend	Yearly Change (cm)
GRACE-TWS	1.08	-0.05	-0.55
GLDAS1 NOAH-GW	-0.63	0.10	1.26
VIC-GW	0.00	0.22	2.60
MOSAIC-GW	-1.93	0.53	6.40
CLM-GW	-0.43	0.26	3.08
GLDAS2 NOAH-GW	0.40	-0.01	-0.12
GLDAS1 Ensemble-GW	-0.75	0.28	3.33
Well Average	-0.25	0.02	0.19
Well Thiessen	-3.21	0.50	6.03

Yeşilırmak	Intercept	Trend	Yearly Change (cm)
GRACE-TWS	1.24	-0.13	-1.56
GLDAS1 NOAH-GW	-1.02	0.34	4.06
VIC-GW	-1.55	0.64	7.72
MOSAIC-GW	-2.74	0.86	10.37
CLM-GW	-0.39	0.24	2.93
GLDAS2 NOAH-GW	-0.01	0.11	1.35
GLDAS1 Ensemble-GW	-1.43	0.52	6.27
Well Average	-3.19	0.29	3.42
Well Thiessen	12.62	-2.16	-25.89

Konya	Intercept	Trend	Yearly Change (cm)
GRACE-TWS	3.02	-0.42	-5.02
GLDAS1 NOAH-GW	0.69	-0.08	-0.97
VIC-GW	1.33	-0.10	-1.18
MOSAIC-GW	-1.31	0.32	3.78
CLM-GW	1.23	-0.06	-0.74
GLDAS2 NOAH-GW	2.08	-0.40	-4.84
GLDAS1 Ensemble-GW	0.49	0.02	0.22
Well Average	48.99	-7.21	-86.47
Well Thiessen	52.53	-7.81	-93.74

Central Anatolia	Intercept	Trend	Yearly Change (cm)
GRACE-TWS	1.42	-0.08	-0.99
GLDAS1 NOAH-GW	-0.32	0.13	1.52
VIC-GW	-0.03	0.25	2.95
MOSAIC-GW	-1.61	0.47	5.68
CLM-GW	-0.12	0.22	2.68
GLDAS2 NOAH-GW	0.64	-0.04	-0.46
GLDAS1 Ensemble-GW	-0.52	0.27	3.21
Well Average	22.66	-3.07	-36.80
Well Thiessen	15.98	-2.35	-28.25

Table 4.8. *Significance of GRACE TWS and GWS trends*

Akarçay	p-Value	tau
GRACE-TWS	0.30	-0.05
GLDAS1 NOAH-GW	0.39	0.06
VIC-GW	0.65	-0.03
MOSAIC-GW	0.02	0.17
CLM-GW	0.13	0.08
GLDAS2 NOAH-GW	0.74	-0.02
GLDAS1 Ensemble-GW	0.23	0.08
Well Average	0.00	-0.41
Well Thiessen	0.00	-0.42

Sakarya	p-Value	tau
GRACE-TWS	0.26	0.04
GLDAS1 NOAH-GW	0.09	0.10
VIC-GW	0.00	0.21
MOSAIC-GW	0.00	0.21
CLM-GW	0.00	0.19
GLDAS2 NOAH-GW	0.12	0.06
GLDAS1 Ensemble-GW	0.00	0.22
Well Average	0.06	-0.16
Well Thiessen	0.00	-0.33

Kızılırmak	p-Value	tau
GRACE-TWS	0.37	-0.03
GLDAS1 NOAH-GW	0.33	0.07
VIC-GW	0.04	0.13
MOSAIC-GW	0.00	0.33
CLM-GW	0.00	0.12
GLDAS2 NOAH-GW	0.68	-0.02
GLDAS1 Ensemble-GW	0.00	0.19
Well Average	0.81	-0.02
Well Thiessen	0.30	0.10

Yeşilırmak	p-Value	tau
GRACE-TWS	0.07	-0.05
GLDAS1 NOAH-GW	0.00	0.15
VIC-GW	0.00	0.28
MOSAIC-GW	0.00	0.39
CLM-GW	0.00	0.10
GLDAS2 NOAH-GW	0.15	0.05
GLDAS1 Ensemble-GW	0.00	0.27
Well Average	0.31	0.07
Well Thiessen	0.00	-0.14

Konya	p-Value	tau
GRACE-TWS	0.00	-0.16
GLDAS1 NOAH-GW	0.40	-0.07
VIC-GW	0.43	-0.06
MOSAIC-GW	0.01	0.23
CLM-GW	0.39	-0.05
GLDAS2 NOAH-GW	0.00	-0.24
GLDAS1 Ensemble-GW	0.84	0.02
Well Average	0.00	-0.71
Well Thiessen	0.00	-0.75

Central Anatolia	p-Value	tau
GRACE-TWS	1.42	-0.08
GLDAS1 NOAH-GW	-0.32	0.13
VIC-GW	-0.03	0.25
MOSAIC-GW	-1.61	0.47
CLM-GW	-0.12	0.22
GLDAS2 NOAH-GW	0.64	-0.04
GLDAS1 Ensemble-GW	-0.52	0.27
Well Average	22.66	-3.07
Well Thiessen	15.98	-2.35

The linear relationship between station- and GRACE-derived GWS data for the Central Anatolia Basin and the subbasins are examined by Pearson's correlation coefficient (Table 4.9). On average GRACE TWS correlations are much better than GRACE GWS correlations with station-based groundwater level observations. This is particularly true for NOAH, VIC, and MOSAIC models that the TWS correlation - GWS correlation difference is much larger.

Even though some studies (Joodaki et al., 2014) attribute this to the fact that models only simulate the groundwater conditions in the absence of anthropogenic impacts while satellite also includes such impacts. The degradation of correlation from TWS to GWS is too high to be explained by human impact. This implies that general models are not good at partitioning the TWS information skillfully and degrades the GRACE TWS groundwater predictive skill over the study region.

Table 4.9. *GLDAS TWS and GWS dataset correlation with in-situ groundwater level change*

			TWS		GWS		RMSE	
Basins			**Well Average**	**Well Thiessen**	**Well Average**	**Well Thiessen**	**Well Average**	**Well Thiessen**
Akarçay	GLDAS-1	NOAH	0.67	0.65	0.17	0.19	17.03	21.34
		VIC	0.52	0.52	0.36	0.35	16.20	20.59
		MOSAIC	0.71	0.70	0.08	0.08	17.29	21.67
		CLM	0.72	0.70	0.53	0.53	15.07	19.33
		Ensemble	0.66	0.65	0.36	0.36	16.29	20.65
	GLDAS-2 NOAH		0.52	0.48	0.15	0.21	17.17	21.25
	GRACE TWS		0.65	0.64				
Kızılırmak	GLDAS-1	NOAH	0.46	0.22	-0.10	0.02	4.73	8.20
		VIC	0.32	0.03	0.18	0.33	4.82	7.35
		MOSAIC	0.41	0.13	-0.02	0.19	4.84	7.79
		CLM	0.35	0.10	0.37	0.27	4.75	7.80
		Ensemble	0.40	0.12	0.15	0.24	4.27	7.49
	GLDAS-2 NOAH		0.38	0.14	-0.10	0.06	5.63	8.53
	GRACE TWS		0.45	0.25				
Konya	GLDAS-1	NOAH	0.39	0.43	0.37	0.30	29.43	31.22
		VIC	0.34	0.39	0.38	0.31	29.10	30.96
		MOSAIC	0.53	0.57	-0.06	-0.14	30.74	32.55
		CLM	0.59	0.64	0.37	0.35	29.00	30.65
		Ensemble	0.46	0.50	0.33	0.26	29.51	31.29
	GLDAS-2 NOAH		0.19	0.24	0.48	0.41	28.76	30.63
	GRACE TWS		0.50	0.51				
Sakarya	GLDAS-1	NOAH	0.44	0.39	0.35	0.27	12.06	15.23
		VIC	0.37	0.37	0.31	0.17	12.30	15.79
		MOSAIC	0.50	0.47	0.18	0.05	12.65	16.03
		CLM	0.44	0.43	0.58	0.45	10.85	14.39
		Ensemble	0.44	0.42	0.44	0.30	11.76	15.20
	GLDAS-2 NOAH		0.37	0.29	0.27	0.27	12.37	15.21
	GRACE TWS		0.61	0.51				
Yeşilırmak	GLDAS-1	NOAH	0.37	0.44	0.38	0.32	14.81	35.62
		VIC	0.33	0.46	0.35	0.17	15.26	36.45
		MOSAIC	0.40	0.61	0.20	-0.12	16.07	38.00
		CLM	0.25	0.24	0.62	0.66	13.13	33.20
		Ensemble	0.36	0.49	0.45	0.31	14.59	35.75
	GLDAS-2 NOAH		0.40	0.37	0.26	0.36	15.39	35.38
	GRACE TWS		0.62	0.62				
Central Anatolia Basin	GLDAS-1	NOAH	0.43	0.50	0.17	0.30	15.58	14.67
		VIC	0.41	0.44	0.16	0.32	15.53	14.52
		MOSAIC	0.55	0.62	-0.14	-0.04	16.46	15.80
		CLM	0.57	0.51	0.34	0.56	14.73	13.21
		Ensemble	0.49	0.53	0.18	0.36	15.45	14.43
	GLDAS-2 NOAH		0.33	0.36	0.18	0.32	15.63	14.53
	GRACE TWS		0.50	0.63				

The variations of groundwater from GRACE TWS based and monitoring wells in the basins show diverse results. Overall, the CLM-derived GWS shows the strongest agreement with the basin-wide representations of the in-situ observations in all basins except KCB (Table 4.9). This implies CLM energy and water balance equations reflect the groundwater variability much better than other model equations. In KCB, GWS change calculated from GLDAS-2 NOAH shows the strongest relationship with the station-based observations.

In KCB, between GLDAS 1- and GLDAS 2- NOAH models, GLDAS 1-NOAH TWS has consistently higher correlation coefficient with station-based groundwater observations than GLDAS 2-NOAH TWS. This implies that input atmospheric forcing datasets of GLDAS 1 may have better representation of the TWS components than GLDAS 2 forcing datasets. On the other hand, when these model datasets (SM, SWE, CWC) are combined with GRACE TWS, the linear predictive capability of GLDAS 2-NOAH is higher than the estimates of GLDAS 1-NOAH, implying GLDAS 1-NOAH model water balance partitioning is not very skillful in terms of SM, CWC, SWE component summation.

Even though MOSAIC TWS has the best agreement with GRACE TWS data (Table 4.3) MOSAIC-based GRACE GWS do not have good linear agreement with the station groundwater anomaly data (Table 4.9). The negative correlation coefficients close to zero imply that no relationship exists between the well-based observation. This implies MOSAIC-based GWS deteriorate the temporal consistency existing between the MOSAIC TWS and the station-based GWS; perhaps at a much higher rate than other models. For this reason, MOSAIC-based GWS component may have poor parameterization.

While comparing the GRACE-derived GWS, some problems considered.

Problem 1: The nature of the in situ-based observations is point while the remote sensing datasets are spatial averages.

In order to compare them over the same region of interest, point data are converted into spatial averages. In this study, two different methods are used to implement this conversion and their results are investigated separately to see their relative impact. Except Yeşilırmak Basin and Central Anatolia Basin, averaging the point data yield consistently better correlations and lower errors when compared against the groundwater level observations than the use of Thiessen method (Table 4.9). On the other hand, when these methods are compared with GLDAS TWS is compared against the ground data, then there is no clear difference except in Kızılırmak Basin.

Problem 2: Precipitation that falls over the ground may not immediately increase the groundwater observing station water levels, even though it may immediately impact the GRACE based observations; hence a time lag could be expected between the GRACE GWS and station-based GWS.

Accordingly, the lagged correlation between the GRACE GWS and station-based GWS are calculated (e.g., +1 month lag implies GRACE data for February is matched with station data for January, implies the variabilities are seen in station data 1 month before it can be seen in GRACE data; -2 month lag implies GRACE data for June is matched with station data for August, implies the variabilities are seen in station data 2 months after it can be seen in GRACE data). The cross-correlation analysis for GRACE-derived and in-situ based groundwater shows on average the best correlations are obtained for the lag of 1 - 3 months (Table 4.11) over Central Anatolia Basin. The results of lagged cross-correlations for other basins are given in Appendix G. A possible reason for this lag could be the water extraction because of irrigation that extracted water immediately causes a decrease in the station observations (i.e., particularly the stations measuring at deep layers), while part of the irrigation water infiltrates to the ground and remains as soil moisture which GRACE observations are sensitive to.

Table 4.10. *GRACE and model-based GWS accuracy sensitivity to time lags*

		GWS						GRACE TWS
		GLDAS-1					GLDAS-2	
		NOAH	VIC	MOSAIC	CLM	Ensemble	NOAH	
Well Average	Lag -3	-0.16	-0.14	-0.35	-0.06	-0.19	-0.07	0.19
	Lag -2	-0.12	-0.12	-0.35	0.09	-0.12	-0.07	0.34
	Lag -1	-0.02	-0.02	-0.31	0.23	-0.01	0.01	0.45
	Lag 0	0.11	0.11	-0.21	0.32	0.12	0.15	0.49
	Lag 1	0.24	0.22	-0.12	0.32	0.21	0.29	0.44
	Lag 2	0.32	0.27	-0.05	0.25	0.23	0.42	0.31
	Lag 3	0.35	0.28	-0.03	0.12	0.20	0.51	0.14
Well Thiessen	Lag -3	-0.28	-0.21	-0.44	0.15	-0.19	-0.26	0.44
	Lag -2	-0.12	-0.08	-0.36	0.37	-0.02	-0.13	0.62
	Lag -1	0.05	0.09	-0.25	0.51	0.15	0.06	0.69
	Lag 0	0.23	0.27	-0.12	0.53	0.29	0.28	0.62
	Lag 1	0.37	0.40	-0.01	0.44	0.36	0.49	0.44
	Lag 2	0.40	0.42	0.04	0.24	0.32	0.61	0.18
	Lag 3	0.37	0.39	0.05	0.00	0.22	0.64	-0.08

Overall, the inconsistency between GRACE- and model-based GWS estimates and the ground station-based GWS observations may also stem from observational errors as well in addition to the GRACE- and model-based errors. Although the station data has passed from quality control processes, the amplitude of water levels is high at some well locations.

Problem 3: Groundwater wells are not homogeneously distributed over the basins.

So, the spatial averaging techniques may add bias in terms of GWS estimates. This is particularly true for the regions that have large number of unauthorized and active pumping wells impacting the GWS. Also, ground-based estimates represent individual wells and a variety of local conditions when compared with the GRACE-based estimates, implying the station data has point in nature and may have high representation errors. The fact that specific yield data is taken from literature and not collected in the area may also contribute to the errors of the GWS estimates obtained from GRACE and GLDAS LSM data. For this reason, RMS error is very large (Table

4.9). The reason of high RMS errors might be the misspecification of specific yields, temporal undersampling and anthropogenic factors.

Nevertheless, this impact should be limited as the correlation coefficient is invariant to linear transformations while GRACE and model-based GWS estimates are validated in the literature mostly using correlation coefficient. The temporal and spatial variability of groundwater wells are dependent on several factors including groundwater withdrawals, heterogeneous characteristics of the aquifers. In Central Anatolia Basin, most wells are located in irrigated areas, so, the drawdowns in monitoring wells could be biased due to adjacent pumping wells where high drawdowns are expected. Besides, due to karstic characteristics of the geology over certain locations (i.e. KCB), water leaks through the dissolution holes and fractures. For this reason, high levels of drawdown could be observed. Although the in-situ measurements are derived from point observations, moderate correlation values are obtained.

In order to evaluate the similarity between the station-based groundwater level observations, Pearson's correlation coefficients are calculated. In this table each entry is calculated as the average of cross-correlations for well average and well Thiessen methods; because the groundwater level change calculated using well average and well Thiessen methods over the same subbasin do not yield the same time series, the average cross-correlations over any given subbasin (Table 4.11) is not equal to 1. The mean of average cross-correlations (0.33 – 0.69) between the station-based observations in the subbasins is 0.55; assuming the groundwater system of these subbasins is not directly linked. This implies the common climate over these subbasins on average can explain around half of the variability in the groundwater, while Kızılırmak Basin has the most diverse climate while Akarçay Basin reflect the most common components of the climate.

Table 4.11. *Average cross-correlations between station-based GWS observations over different basins*

Basins	Akarçay	Kızılırmak	Konya	Sakarya	Yeşilırmak	Central Anatolia Basin
Akarçay	0.99	0.21	0.75	0.64	0.44	0.84
Kızılırmak	0.21	0.90	-0.08	0.32	0.41	0.22
Konya	0.75	-0.08	0.99	0.54	0.25	0.81
Sakarya	0.64	0.32	0.54	0.94	0.50	0.77
Yeşilırmak	0.44	0.41	0.25	0.50	0.78	0.56
Central Anatolia Basin	0.84	0.22	0.81	0.77	0.56	0.93
Average	0.64	0.33	0.54	0.62	0.49	0.69

In this study, the accuracy of GRACE and GLDAS-based GWS observations are investigated over 6 basins with various areas (7,605 km^2, 36,114 km^2, 53,850 km^2, 58,180 km^2, 78,180 km^2, and 233,929 km^2). Overall, the correlations found in this study (CLM correlations vary between 0.27 and 0.66) are not as high as the some of the studies in the literature finds (between 0.55 – 0.91). Yet, the Central Anatolia Basin (233.929 km^2) correlations are not higher than the correlations obtained over smaller sub-basins with areas changing between 7.605 km^2 and 78.180 km^2. Considering the GRACE observations are impacted from a large area, the fact that GRACE observations represent the GWS change over smaller regions implies GWS variability is heavily impacted from the climate which may not change over the large region (i.e., Central Anatoli Basin). For this reason, the smaller subbasins are under the impact of similar climate hence similar GWS change. This is consistent with the fact that the mean of cross correlations between the station-based well observations (0.55), implying this much linear relationship could be expected just from the similarity of the climate between the subbasins.

CHAPTER 5

CONCLUSION AND RECOMMENDATIONS

The goal of this study is to evaluate the groundwater level change derived from GRACE satellite and GLDAS LSMs in comparison to the results from monitoring wells over the period 2003-2015 over Central Anatolia Basin and its subbasins having small areas. Although the spatial resolution of the GRACE dataset are relatively coarse, the recent studies show existence of high correlations over small basins. So, the motivation of this study is to investigate the accuracy of GRACE over basins with relatively small areas over Central Anatolia Basin. Additionally, the area of Central Anatolia Basin is large enough to be accepted as suitable for GRACE-based investigation of groundwater change information.

Overall, the correlations are found smaller than some of the studies performed in the literature over regions with similar areas. Ground observations are point data, hence need to be converted into areal averages. In this study, among the different methods performed to convert the point data to areal averages, well average method has very similar performance with well Thiessen method, implying the differences are only marginal. Nevertheless, the GRACE-based GWS correlations accurately the drought periods of the study region; hence proving the capability of GRACE observations over the area.

It is expected that as the basin area increases the accuracy of GRACE increases (Landerer & Swenson, 2012). However, increasing the catchment areas do not give good correlations as expected. Although Akarçay Basin has the lowest surface area, it has a correlation value about 0.53 which is higher than the correlation value of Central Anatolia Basin ($r \approx 0.45$). This shows that GRACE-derived groundwater change levels may be affected by local factors (e.g., groundwater extraction). On average, half of the variability over the small subbasin GWS change can be explained by the climate of the larger Central Anatolia Basin.

TWS estimates from GLDAS models and GRACE show strong correlations ($r \approx 0.83$) implying the water balance of models and GRACE show skillful TWS estimates. These TWS estimates also have moderate capacity ($r \approx 0.60$) to predict the changes in station-based observed GWS values at the ground.

Additionally, the variations in soil moisture from GLDAS models and GRACE TWS show a strong correlation ($r \approx 0.89$) because it highly affects the GRACE signals in the study region. So, the seasonal variations of GRACE may be attributed to SM while the trend may be related to GWS changes within the basins. However, when GLDAS surface datasets (i.e., SM, CWC, SWE) are removed from GRACE TWS to obtain GRACE GWS, then GRACE GWS skill to predict the station-based groundwater level change becomes considerably reduced. Furthermore, other model variables (SWE and CWC) did not show reliable estimates because GRACE satellite alone detects groundwater changes better. Overall, the CLM-derived GWS shows the strongest agreement with the basin-wide representations of the in-situ observations in all basins except KCB.

The results of this study are based on limited data such as specific yield and the missing amount of in-situ groundwater level measurements. Specific yield estimates may be biased because of the mischaracterization of Sy values of the materials which have a great range of values. So, GRACE-derived GWS change and in-situ measurements from monitoring wells show a variety of results both in seasonality and the magnitude of the changes. The results show that the seasonality in ground-based and GRACE-derived groundwater levels follows the same pattern, even though lag has been influencing the prediction of groundwater change at some time.

In this study, surface water is excluded from the equation due to the lack of data. However, surface water variations should be included because the study area has many surface water reservoirs such as Beyşehir Lake, Salt Lake, Kızılırmak, Yeşilırmak and Sakarya rivers and dams. Without considering the effects of large lakes, dams, and other surface water bodies, the estimates in terms of quantity can be misleading.

To conclude, with better information regarding specific yield, more frequent well observation and estimates of surface water storages, it is likely that the relation and the gap between GRACE and ground-based observation results will be improved. Future studies should concentrate on the amount of in-situ measurements that monitor the naturally occuring fluctuations of groundwater and these stations should spread over the entire basin. It is needed because the number of well sites and the amount of the data affect the results. Finally, GRACE mission will continue as GRACE Follow-On which has improved ranging systems that measures the distance in nanometers to increase the spatial resolution.

REFERENCES

Ahi, G. O., & Jin, S. (2019). Hydrologic mass changes and their implications in Mediterranean-climate Turkey from GRACE measurements. *Remote Sensing*, *11*(2), 1–24. https://doi.org/10.3390/rs11020120

Atayer, E., & Aydın, C. (2012). Destriping of GRACE solutions by fitting high–degree polynomials. *Journal of Geodesy and Geoinformation*, *1*(212).

Avsar, N. B., & Ustun, A. (2012). Analysis of Regional Time-Variable Gravity Using GRACE's 10-day Solutions. *FIG Working Week 2012. Knowing to Manage the Territory, Protect the Environment, Evaluate the Cultural Heritage*, (May), 15.

Bayari, C. S., Ozyurt, N. N., & Kilani, S. (2009). Radiocarbon age distribution of groundwater in the Konya Closed Basin, Central Anatolia, Turkey. *Hydrogeology Journal*, *17*, 347–365. https://doi.org/10.1007/s10040-008-0358-2

Bayari, C. S., Pekkan, E., & Ozyurt, N. N. (2008). Obruks, as giant collapse dolines caused by hypogenic karstification in central Anatolia, Turkey: Analysis of likely formation processes. *Hydrogeology Journal*, *17*(2), 327–345. https://doi.org/10.1007/s10040-008-0351-9

Bettadpur, S. (2016). Satellite Gravity : GRACE & GOCE • Global gravity field models derived from satellite data serve as.

Bonan, G. B., Oleson, K. W., Vertenstein, M., Levis, S., Zeng, X., Dai, Y., … Yang, Z.-L. (2002). The Land Surface Climatology of the Community Land Model Coupled to the NCAR Community Climate Model*. *Journal of Climate*, *15*(22), 3123–3149. https://doi.org/10.1175/1520-0442(2002)015<3123:tlscot>2.0.co;2

Bulut, B., & Yılmaz, M. T. (2016). Türkiye'deki 2007 ve 2013 Yılı Kuraklıklarının NOAH Hidrolojik Modeli ile İncelenmesi. *İMO Teknik Dergi*, 7619–7634.

Ceyhan, E. (2016). *Multi-Temporal Water Extent Analysis of a Hypersaline Playa Lake Using Landsat Imagery*. Middle East Technical University.

Chen, J. L., Wilson, C. R., & Tapley, B. D. (2010). The 2009 exceptional Amazon flood and interannual terrestrial water storage change observed by GRACE. *Water Resources Research*, *46*(12), 1–10. https://doi.org/10.1029/2010WR009383

Cleveland, R. B., Cleveland, W. S., McRae, J. E., & Terpenning, I. (1990). STL: A Seasonal-Trend Decomposition Procedure Based on Loess. *Journal of Official Statistics*, *6*(1), 3–73. https://doi.org/10.1007/978-3-642-48425-4_2

Cleveland, W. S., & Loader, C. (1996). Smoothing by Local Regression: Principles and Methods. In *Statistical Theory and Computational Aspects of Smoothing* (pp. 10–49).

DSİ. (2015). *Konya Kapalı Havzası Yeraltısuyu ve Hidrojeoloji Raporu*. *Konya Kapalı Havzası Master Planı Hazırlanması İşi - Hidrojeoloji Etüt Raporu*. Ankara: Devlet Su İşleri Genel Müdürlüğü.

Ek, M. B., Mitchell, K. E., Lin, Y., Rogers, E., Grunmann, P., Koren, V., … Tarpley, J. D. (2003). Implementation of Noah land surface model advances in the National Centers for Environmental Prediction operational mesoscale Eta model. *Journal of Geophysical Research*, *108*(D22), 8851. https://doi.org/10.1029/2002JD003296

Emelyanova, I., Ali, R., Dawes, W., Varma, S., Hodgson, G., & McFarlane, D. (2013). Evaluating the cumulative rainfall deviation approach for projecting groundwater levels under future climate. *Journal of Water and Climate Change*, 317–337. https://doi.org/10.2166/wcc.2013.068

Famiglietti, J. S., Lo, M., Ho, S. L., Bethune, J., Anderson, K. J., Syed, T. H., … Rodell, M. (2011). Satellites measure recent rates of groundwater depletion in California's Central Valley. *Geophysical Research Letters*, *38*(3), 2–5. https://doi.org/10.1029/2010GL046442

Fang, H., Beaudoing, H. K., Rodell, M., Teng, W. L., & Vollmer, B. E. (2008). Global Land Data Assimilation System (GLDAS) Products, Services and Application from NASA Hydrology Data and Information Services Center (HDISC). In *ASPRS 2009 Annual Conference*. Retrieved from https://ntrs.nasa.gov/search.jsp?R=20090005038

Feng, W., Zhong, M., Lemoine, J. M., Biancale, R., Hsu, H. T., & Xia, J. (2013). Evaluation of groundwater depletion in North China using the Gravity Recovery and Climate Experiment (GRACE) data and ground-based measurements. *Water Resources Research*, *49*(4), 2110–2118. https://doi.org/10.1002/wrcr.20192

Ferdowsian, R., J.Pannell, D., McCarron, C., Ryder, A., & Crossing, L. (2001). Explaining groundwater hydrographs: separating atypical rainfall events from time trends. *Australian Journal of Soil Research*, *39*, 861–875.

Frappart, F., & Ramillien, G. (2018). Monitoring groundwater storage changes using the Gravity Recovery and Climate Experiment (GRACE) satellite mission: A review. *Remote Sensing*, *10*(6). https://doi.org/10.3390/rs10060829

Göçmez, G., & İşçioğlu, A. (2004). *Konya Kapalı Havzası'nda Yeraltı Suyu Seviye Değişimleri, Yeraltı suyunun Kullanımı, Problemler ve Çözüm Yolları*.

Han, S. C., Sauber, J., Luthcke, S. B., Ji, C., & Pollitz., F. F. (2008). Implications of postseismic gravity change following the great 2004 Sumatra-Andaman earthquake from the regional harmonic analysis of GRACE intersatellite tracking data. *Journal of Geophysical Research: Solid Earth*, *113*(11), 1–13. https://doi.org/10.1029/2008JB005705

Huang, Z., Pan, Y., Gong, H., Yeh, P. J. F., Li, X., Zhou, D., & Zhao, W. (2015). Subregional-scale groundwater depletion detected by GRACE for both shallow and deep aquifers in North China Plain. *Geophysical Research Letters*, *42*(6), 1791–1799. https://doi.org/10.1002/2014GL062498

Humphrey, V., Gudmundsson, L., & Seneviratne, S. I. (2016). Assessing Global Water Storage Variability from GRACE: Trends, Seasonal Cycle, Subseasonal Anomalies and Extremes. *Surveys in Geophysics*, *37*(2), 357–395. https://doi.org/10.1007/s10712-016-9367-1

Joodaki, G., Wahr, J., & Swenson, S. (2014). Estimating the human contribution to groundwater depletion in the Middle East, from GRACE data, land surface models, and well observations. *Water Resources Research*, *50*(7), 5510–5531. https://doi.org/10.1002/2013WR014910.Received

Kibaroglu, A., Scheumann, W., & Kramer, A. (2011). *Turkey's Water Policy: National Frameworks and International Cooperation*. *Springer London*. https://doi.org/10.1007/978-3-642-19636-2

Klees, R., Zapreeva, E. A., Winsemius, H. C., & Savenije, H. H. G. (2007). The bias in GRACE estimates of continental water storage variations. *Hydrology and Earth System Sciences*, *11*(4), 1227–1241. https://doi.org/10.5194/hess-11-1227-2007

Koster, R. D., & Suarez, M. J. (1996). The Influence of Land Surface Moisture Retention on Precipitation Statistics. *Journal of Climate*, *9*, 2551–2567.

Landerer, F. W., & Swenson, S. C. (2012). Accuracy of scaled GRACE terrestrial water storage estimates. *Water Resources Research*, *48*(4), 1–11.

https://doi.org/10.1029/2011WR011453

Liang, X., Lettenmaier, D. P., Wood, E. F., & Burges, S. J. (1994). A simple hydrologically based model of land surface water and energy fluxes for general circulation models. *Journal of Geophysical Research*, *99*(D7), 14415. https://doi.org/10.1029/94jd00483

Liesch, T., & Ohmer, M. (2016). Comparison of GRACE data and groundwater levels for the assessment of groundwater depletion in Jordan. *Hydrogeology Journal*, *24*(6), 1547–1563. https://doi.org/10.1007/s10040-016-1416-9

Liesch, Tanja, & Ohmer, M. (2016). Comparison of GRACE data and groundwater levels for the assessment of groundwater depletion in Jordan. *Hydrogeology Journal*, *24*(6), 1547–1563. https://doi.org/10.1007/s10040-016-1416-9

Long, D., Scanlon, B. R., Longuevergne, L., Sun, A. Y., Fernando, D. N., & Save, H. (2013). GRACE satellite monitoring of large depletion in water storage in response to the 2011 drought in Texas. *Geophysical Research Letters*, *40*(13), 3395–3401. https://doi.org/10.1002/grl.50655

Longuevergne, L., Wilson, C. R., Scanlon, B. R., & Crétaux, J. F. (2013). GRACE water storage estimates for the middle east and other regions with significant reservoir and lake storage. *Hydrology and Earth System Sciences*, *17*(12), 4817–4830. https://doi.org/10.5194/hess-17-4817-2013

MTA. (2002). 1/500 000 Scale Geological Map of Turkey.

Nicholls, R. J., & Cazenave, A. (2010). Sea-level rise and its impact on coastal zones. *Science*, *328*(5985), 1517–1520. https://doi.org/10.1126/science.1185782

Okay, A. I., & Tüysüz, O. (1999). Tethyan sutures of northern Turkey. *Geological Society, London, Special Publications*, *156*(1), 475–515. https://doi.org/10.1144/gsl.sp.1999.156.01.22

Orhan, H., Delikan, A., Demir, A., Kapan, S., Olgun, K., Özmen, A., … Nazik, A. (2019). Geochemical Evidences of Paleoenvironmental Changes in Late Quaternary Lacustrine Sediments of the Konya Closed Basin (Konya, Turkey). In *Patterns and Mechanisms of Climate, Paleoclimate and Paleoenvironmental Changes from Low-Latitude Regions* (pp. 73–76). https://doi.org/10.1007/978-3-030-01599-2_17

Proulx, R. A., Knudson, M. D., Kirilenko, A., Vanlooy, J. A., & Zhang, X. (2013). Significance of surface water in the terrestrial water budget: A case study in the

Prairie Coteau using GRACE, GLDAS, Landsat, and groundwater well data. *Water Resources Research*, *49*(9), 5756–5764. https://doi.org/10.1002/wrcr.20455

Rodell, M., & Houser, P. R. (2004). Updating a Land Surface Model with MODIS-Derived Snow Cover. *Journal of Hydrometeorology*, *5*, 1064–1075.

Rodell, M, & Famiglietti, J. S. (1999). Detectability of variations in continental water storage from satellite observations of the time dependent gravity field basins ranging in size from 130 , 000 2 and uses estimates of uncertainty in, *35*(9), 2705–2723.

Rodell, Matthew, Chen, J., Kato, H., Famiglietti, J. S., Nigro, J., & Wilson, C. R. (2007). Estimating groundwater storage changes in the Mississippi River basin (USA) using GRACE. *Hydrogeology Journal*, *15*(1), 159–166. https://doi.org/10.1007/s10040-006-0103-7

Sakumura, C., Bettadpur, S., & Bruinsma, S. (2014). Ensemble prediction and intercomparison analysis of GRACE time-variable gravity field models. *Geophysical Research Letters*, *41*(5), 1389–1397. https://doi.org/10.1002/2013GL058632

Scanlon, B. R., Longuevergne, L., & Long, D. (2012). Ground referencing GRACE satellite estimates of groundwater storage changes in the California Central Valley, USA. *Water Resources Research*, *48*(4), 1–9. https://doi.org/10.1029/2011WR011312

Scanlon, B. R., Zhang, Z., Save, H., Wiese, D. N., Landerer, F. W., Long, D., … Chen, J. (2013). Global evaluation of new GRACE mascon products for hydrologic applications. *The Journal of Real Estate Research*, *35*(4), 393–406. https://doi.org/10.1002/2016WR019494.Received

Sensoy, S., Demircan, M., Ulupınar, Y., & Balta, İ. (2008). Türkiye İklimi.

Seyoum, W. M., & Milewski, A. M. (2016). Monitoring and comparison of terrestrial water storage changes in the northern high plains using GRACE and in-situ based integrated hydrologic model estimates. *Advances in Water Resources*, *94*, 31–44. https://doi.org/10.1016/j.advwatres.2016.04.014

Sheffield, J., Goteti, G., & Wood, E. F. (2006). Development of a 50-year high-resolution global dataset of meteorological forcings for land surface modeling. *Journal of Climate*, *19*(13), 3088–3111. https://doi.org/10.1175/JCLI3790.1

Siebert, S., Burke, J., Faures, J. M., Frenken, K., Hoogeveen, J., Döll, P., & Portmann, F. T. (2010). Groundwater use for irrigation - A global inventory. *Hydrology and Earth System Sciences*, *14*(10), 1863–1880. https://doi.org/10.5194/hess-14-1863-2010

Simav, M., Yıldız, H., & Arslan, E. (1989). GRACE Uydu Verileri ile Yer Sistemi İçerisindeki Kütle Değişimlerinin İzlenmesi, 15–27.

Strassberg, G., Scanlon, B. R., & Chambers, D. (2009). Evaluation of groundwater storage monitoring with the GRACE satellite: Case study of the High Plains aquifer, central United States. *Water Resources Research*, *45*(5), 1–10. https://doi.org/10.1029/2008WR006892

Strassberg, Gil, Scanlon, B. R., & Rodell, M. (2007). Comparison of seasonal terrestrial water storage variations from GRACE with groundwater-level measurements from the High Plains Aquifer (USA). *Geophysical Research Letters*, *34*(14), 1–5. https://doi.org/10.1029/2007GL030139

Sun, A. Y., Green, R., Rodell, M., & Swenson, S. (2010). Inferring aquifer storage parameters using satellite and in situ measurements: Estimation under uncertainty. *Geophysical Research Letters*, *37*(10), 1–5. https://doi.org/10.1029/2010GL043231

Swenson, S., & Wahr, J. (2003). Estimated accuracies of regional water storage variations inferred from the Gravity Recovery and Climate Experiment, *39*(8). https://doi.org/10.1029/2002WR001808

Todd, D. K., & Mays, L. W. (2005). *Groundwater Hydrology* (3rd Editio).

Velicogna, I. (2009). Increasing rates of ice mass loss from the Greenland and Antarctic ice sheets revealed by GRACE. *Geophysical Research Letters*, *36*(19), 2–5. https://doi.org/10.1029/2009GL040222

Voss, K. A., Famiglietti, J. S., Lo, M., De Linage, C., Rodell, M., & Swenson, S. C. (2013). Groundwater depletion in the Middle East from GRACE with implications for transboundary water management in the Tigris-Euphrates-Western Iran region. *Water Resources Research*, *49*(2), 904–914. https://doi.org/10.1002/wrcr.20078

Wahr, J., Swenson, S., & Velicogna, I. (2006). Accuracy of GRACE mass estimates. *Geophysical Research Letters*, *33*(March 2006), 1–5. https://doi.org/10.1029/2005GL025305

WWF-Turkey. (2014). *Konya'da Suyun Bugünü Raporu*.

Xiao, R., He, X., Zhang, Y., Ferreira, V. G., & Chang, L. (2015). Monitoring groundwater variations from satellite gravimetry and hydrological models: A comparison with in-situ measurements in the mid-atlantic region of the United States. *Remote Sensing*, *7*(1), 686–703. https://doi.org/10.3390/rs70100686

Yesertener, C. (2008). Assessment of the declining groundwater levels in the Gnangara Groundwater Mound. *Government of Western Australia, Department of Water, Hydrogeology Report No: HR199*.

APPENDICES

A. GROUNDWATER MONITORING WELLS

Akarçay Basin

Well Number	Well ID/Owner	Location		Altitude (m)	Well Depth (m)	Province	Lithological Unit
		Longitude	Latitude				
1	35596	291603	4255478	1171	107	Afyon	Alluvial Deposits - Tuff - Agglomerate
2	21848	368374	4244646	996	130	Konya	Alluvial Deposits
3	33926	377812	4238796	1032	160	Konya	Alluvial Deposits
4	55176-A	289926	4259822	1121	147	Afyon	Alluvial Deposits - Limestone
5	19065	286628	4266694	1135	134	Afyon	Alluvial Deposits - Limestone
6	37625	290226	4273279	1155	200	Afyon	Alluvial Deposits - Limestone
7	58864	294369	4243426	1080	250	Afyon	Alluvial Deposits
8	41011	293691	4244419	1079	250	Afyon	Alluvial Deposits
9	49003	297318	4291513	1040	150	Afyon	Alluvial Deposits - Limestone
10	52973	302128	4282654	1023	130	Afyon	Alluvial Deposits
11	45811	277816	4300366	1018	80	Afyon	Alluvial Deposits
12	35142	339320	4269899	1096	152	Afyon	Alluvial Deposits
13	60264	308988	4286309	985	126	Afyon	Alluvial Deposits
14	50639	270635	4290764	1090	160	Afyon	Alluvial Deposits
15	50544	253948	4295582	1162	140	Afyon	Alluvial Deposits - Limestone
16	11156	272316	4294351	1066	160	Afyon	Tuff
17	47619	277280	4316193	1074	188	Afyon	Alluvial Deposits - Limestone
18	49621	285733	4318502	1068	128	Afyon	Alluvial Deposits - Tuff
19	28372	329648	4284888	983	100	Afyon	Alluvial Deposits
20	39288	372832	4248942	985	178	Konya	Alluvial Deposits
21	42335	365665	4246994	992	144	Konya	Alluvial Deposits
22	9540	290178	4285933	1000	150	Afyon	Alluvial Deposits - Limestone

Table A-1. Attributes of groundwater monitoring wells of Akarçay Basin.

Kızılırmak Basin

Well Number	Well ID/Owner	Location		Altitude (m)	Well Depth (m)	Province	Lithological Unit
		Longitude	Latitude				
23	52908	276750	4359775	1230	47	Sivas	Alluvial Deposits
24	39416	578800	4557550	710	40	Çankırı	Alluvial Deposits
25	10583	622875	4553150	380	230	Çorum	Alluvial Deposits
26	59842	536834	4590147	878	50	Kastamonu	Alluvial Deposits
27	59841	539388	4595250	900	45	Kastamonu	Alluvial Deposits
28	59850	543431	4592037	840	35	Kastamonu	Alluvial Deposits
29	59849	546098	4592242	843	35	Kastamonu	Alluvial Deposits
30	59840	561463	4589665	735	70	Kastamonu	Alluvial Deposits
31	59837	564156	4589788	724	40	Kastamonu	Alluvial Deposits
32	59844	567856	4588676	699	40	Kastamonu	Alluvial Deposits
33	59838	569833	4588535	707	50	Kastamonu	Alluvial Deposits
34	59845	570534	4589615	693	40	Kastamonu	Alluvial Deposits
35	59839	576368	4592615	675	40	Kastamonu	Alluvial Deposits
36	59846	580647	4593854	641	40	Kastamonu	Alluvial Deposits
37	59847	585851	4592809	605	40	Kastamonu	Alluvial Deposits
38	59836	597788	4595606	561	70	Kastamonu	Alluvial Deposits
39	59835	600823	4596383	546	40	Kastamonu	Alluvial Deposits
40	59848	610260	4604175	480	40	Kastamonu	Alluvial Deposits
41	19076	610727	4342565	1160	117	Kırşehir	Alluvial Deposits - Limestone
42	54173	705358	4285672	1034	38	Kayseri	Bazalt
43	54171	704535	4284606	1038	37	Kayseri	Bazalt
44	54170	703467	4284907	1041	29	Kayseri	Bazalt
45	55062	701434	4286021	1032	50	Kayseri	Bazalt
46	53205	700009	4282857	1040	40	Kayseri	Bazalt
47	55061	700644	4282579	1070	83	Kayseri	Bazalt
48	53207/B	699770	4282750	1041	74	Kayseri	Bazalt
49	53207/A	698291	4282097	1038	33	Kayseri	Bazalt
50	32438	688678	4223475	1249	54	Niğde	Alluvial Deposits
51	34937	683162	4214099	1562	39	Niğde	Marble

Table A-2. Attributes of groundwater monitoring wells of Kızılırmak Basin.

Konya Closed Basin

Well Number	Well ID/Owner	Location		Altitude (m)	Well Depth (m)	Province	Lithological Unit
		Longitude	Latitude				
52	34798	647679	4260446	1438	150	Nevşehir	Alluvial Deposits - Tuff
53	37302	482403	4253327	981.535	129	Konya	Neogene Limestone - Claystone
54	52265	485012	4236752	980.968	100	Konya	Neogene Clayey Limestone - Conglomerate
55	52770	400882	4185130	1220.52	140	Konya	Neogene Marl
56	53705	481957	4315358	973.167	76	Konya	Alluvial Deposits
57	53704	487746	4277618	992.265	100	Konya	Alluvial Deposits
58	52267 (13312)	492190	4148976	1021.18	76	Konya	Neogene Clayey Limestone
59	182	478757	4154871	1014.28	138	Konya	Neogene Limestone
60	52268	516350	4156270	1025	125	Konya	Neogene Clayey Limestone
61	181	478036	4163883	1011.23	250	Konya	Neogene Limestone
62	5649	471830	4157179	1020.09	139	Konya	Neogene Limestone
63	52259	621200	4176098	1058.77	100	Konya	Alluvial Deposits
64	9749/A	604848	4184473	1051.88	150	Konya	Alluvial Deposits
65	28719	481548	4128078	1060.58	148	Konya	Neogene Limestone
66	52258	541540	4174661	1024	173	Konya	Neogene Limestone
67	53707	508977	4317992	997.213	150	Konya	Alluvial Deposits - Flysch
68	62564 (221)	476661	4224054	987.998	83	Konya	Neogene Clayey Limestone
69	52266 (35735)	537437	4228075	1015	104	Aksaray	Neogene Limestone
70	17167 (52264)	623923	4249625	1215	N/A	Aksaray	Neogene Tuff - Agglomerate
71	1167	496389	4120118	1046.67	106	Karaman	Alluvial Deposits - Neogene Limestone
72	13314	550735	4143651	1034.76	119	Karaman	Alluvial Deposits - Paleozoic Limestone
73	52260 (212)	518923	4117728	1017.75	110	Karaman	Neogene Limestone
74	52261	641667	4190219	1146.96	86	Niğde	Neogene Limestone - Tuff
75	7801	656288	4232391	1314.48	183	Niğde	Alluvial Deposits
76	49615	656639	4229248	1327.2	150	Niğde	Alluvial Deposits
77	Niğde Merkez DSİ Şb Müd. İçi	647635	4202401	1204.65	145	Niğde	Tuff

Table A-3. Attributes of groundwater monitoring wells of Konya Closed Basin.

Sakarya Basin

Well Number	Well ID/Owner	Location		Altitude (m)	Well Depth (m)	Province	Lithological Unit
		Longitude	Latitude				
78	38147	361625	4464250	785	50	Ankara	Alluvial Deposits
79	35337	421475	4482450	828	30	Ankara	Alluvial Deposits
80	36029	478150	4452175	890	52	Ankara	Alluvial Deposits - Limestone
81	36031	478650	4452375	897	50	Ankara	Alluvial Deposits - Limestone
82	36032	478950	4452450	900	50	Ankara	Alluvial Deposits - Limestone
83	36033	479200	4452550	898	50	Ankara	Alluvial Deposits - Limestone
84	49418	481698	4419960	859	35	Ankara	Alluvial Deposits
85	59858	481700	4418450	875	40	Ankara	Alluvial Deposits
86	61018	481600	4418150	855	44	Ankara	Alluvial Deposits
87	43093	320127	4416437	811	227	Eskişehir	Alluvial Deposits - Neogene Units
88	35322/B	358375	4394150	745	35	Eskişehir	Alluvial Deposits
89	61363/A	326644	4408050	762	62	Eskişehir	Alluvial Deposits
90	61363/B	326641	4408050	762	152	Eskişehir	Marl
91	39362/A	354754	4406182	815	110	Eskişehir	Alluvial Deposits - Claystone
92	61344	321892	4412530	776	104	Eskişehir	Alluvial Deposits - Marl
93	61364	317898	4418997	860	154	Eskişehir	Alluvial Deposits - Flysch
94	61342	315770	4404967	791	102	Eskişehir	Alluvial Deposits - Marl
95	61365	332115	4402624	768	150	Eskişehir	Marl
96	61362/A	337440	4408677	808	150	Eskişehir	Marl
97	61362/B	337445	4408677	808	21	Eskişehir	Alluvial Deposits
98	7553	330412	4400032	760	177	Eskişehir	Alluvial Deposits - Neogene Units
99	31515	299892	4384528	975	162	Eskişehir	Neogene Units
100	56500	311355	4442956	290	65	Eskişehir	Limestone - Flysch
101	5588	264411	4411997	823	45	Eskişehir	Alluvial Deposits - Conglomerate
102	10663	304389	4381787	939	55	Eskişehir	Alluvial Deposits - Limestone
103	15488	326440	4355317	884	306	Eskişehir	Alluvial Deposits - Marl - Conglomerate
104	6548-II	284958	4507115	55	268	Sakarya	Alluvial Deposits - Conglomerate
105	41006	348650	4322406	938	198	Afyon	Alluvial Deposits - Limestone
106	28763	357692	4324298	898	136	Afyon	Alluvial Deposits - Limestone
107	52257 (30419)	402109	4286896	932.289	100	Konya	Neogene Limestone
108	52884	737014	4373836	1056	196	Kütahya	Alluvial Deposits - Limestone - Tuffite

Table A-4. Attributes of groundwater monitoring wells of Sakarya Basin.

Yeşilırmak Basin

Well Number	Well ID/Owner	Location		Altitude (m)	Well Depth (m)	Province	Lithological Unit
		Longitude	Latitude				
109	15981/A	247781	4496930	622	67	Amasya	Alluvial Deposits
110	21378	257838	4495559	735	43	Amasya	Alluvial Deposits
111	14579	685626	4527109	827	68	Amasya	Alluvial Deposits
112	20546	688850	4526250	771	70	Amasya	Alluvial Deposits
113	58802	692300	4517900	760	100	Amasya	Alluvial Deposits
114	58804	692980	4525280	735	82	Amasya	Alluvial Deposits
115	58805	706580	4527180	722	100	Amasya	Alluvial Deposits
116	38710	744900	4494850	510	91	Amasya	Alluvial Deposits
117	50360	689222	4523611	736	140	Amasya	Alluvial Deposits
118	61499	697656	4523677	675	120	Amasya	Alluvial Deposits
119	61817	686329	4513627	875	44	Amasya	Alluvial Deposits
120	1714	702460	4520230	596	140	Amasya	Alluvial Deposits

Table A-5. Attributes of groundwater monitoring wells of Yeşilırmak Basin.

B. CORRELATIONS OF GRACE TWS SOLUTIONS

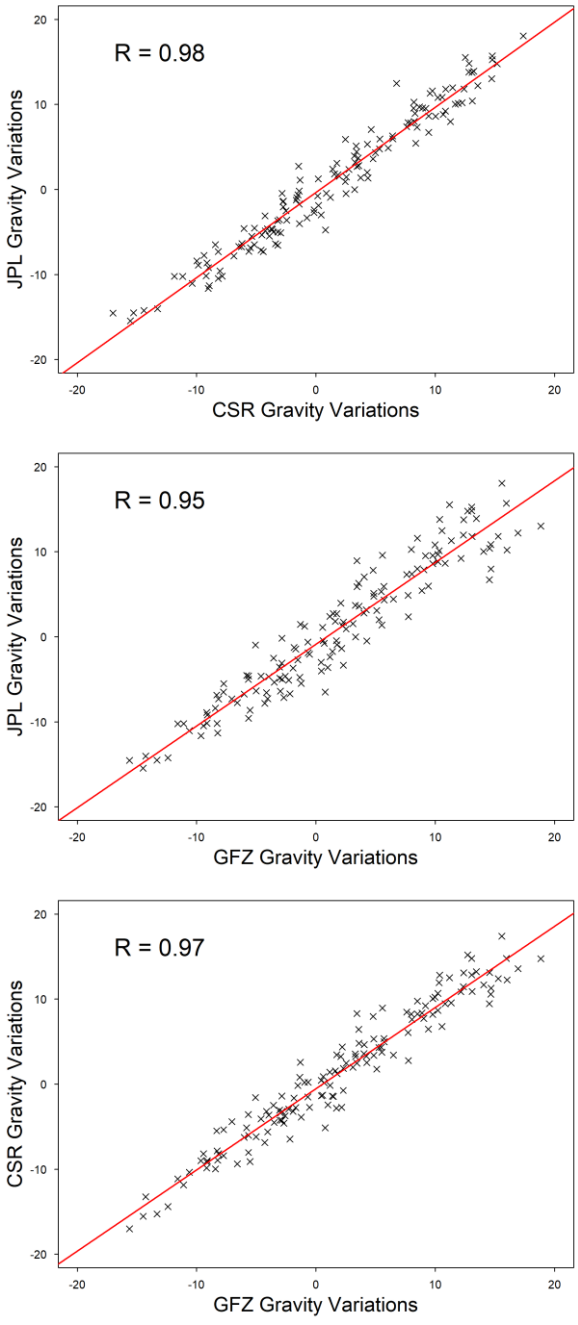

Figure B-1. Correlations of 3-centers solution over Akarçay Basin

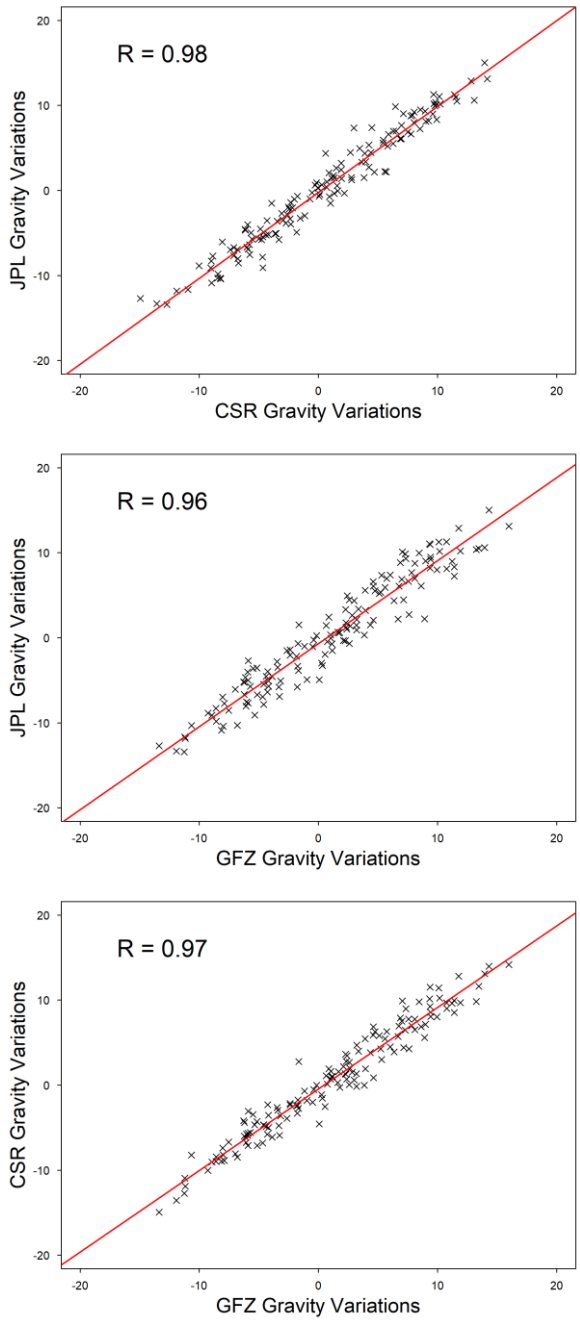

Figure B-2. Correlations of 3-centers solution over Kızılırmak Basin

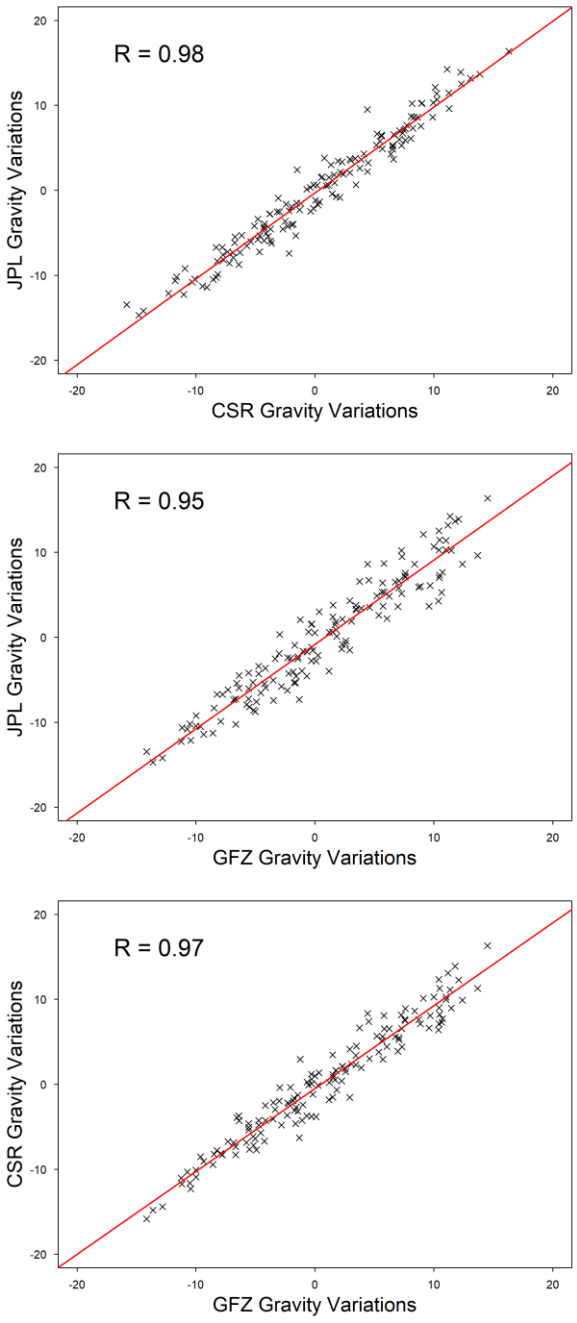

Figure B-3. Correlations of 3-centers solution over Konya Closed Basin

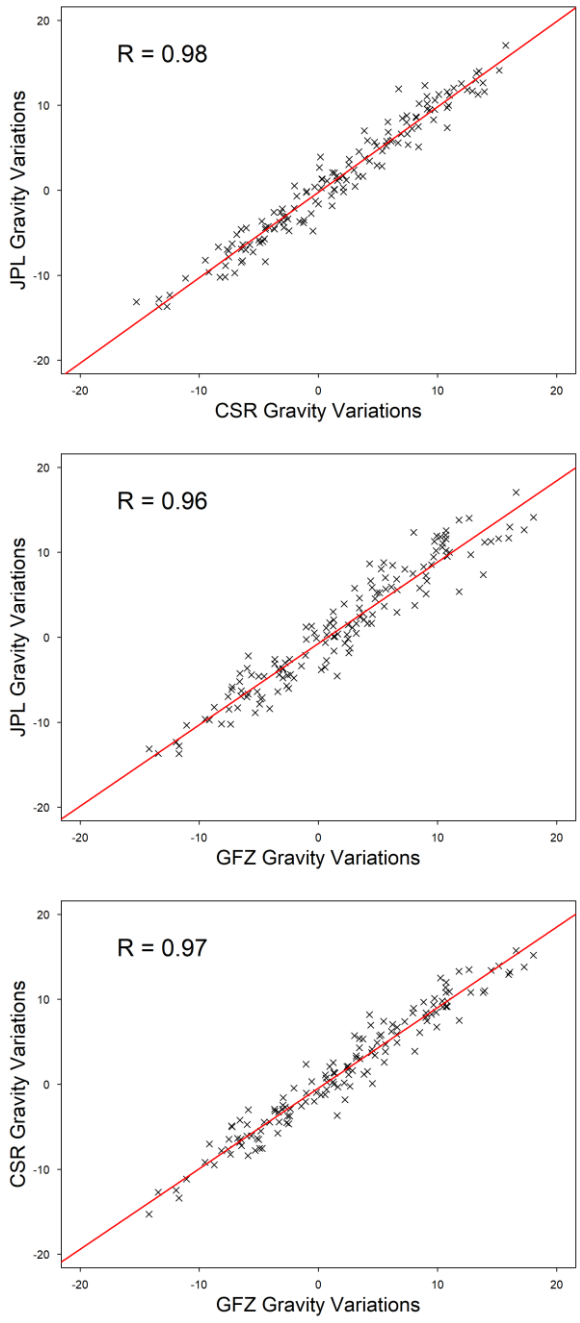

Figure B-4. Correlations of 3-centers solution over Sakarya Basin

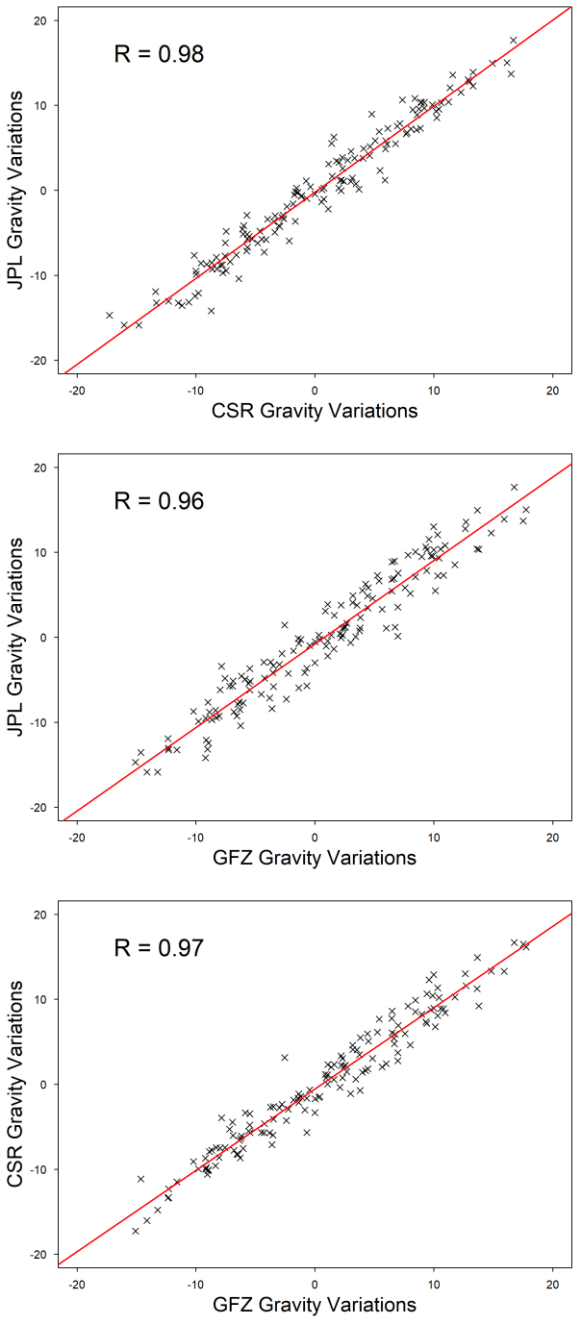

Figure B-5. Correlations of 3-centers solution over Yeşilırmak Basin

C. COMPARISON OF SCALED AND UNSCALED GRACE TWS TIME SERIES

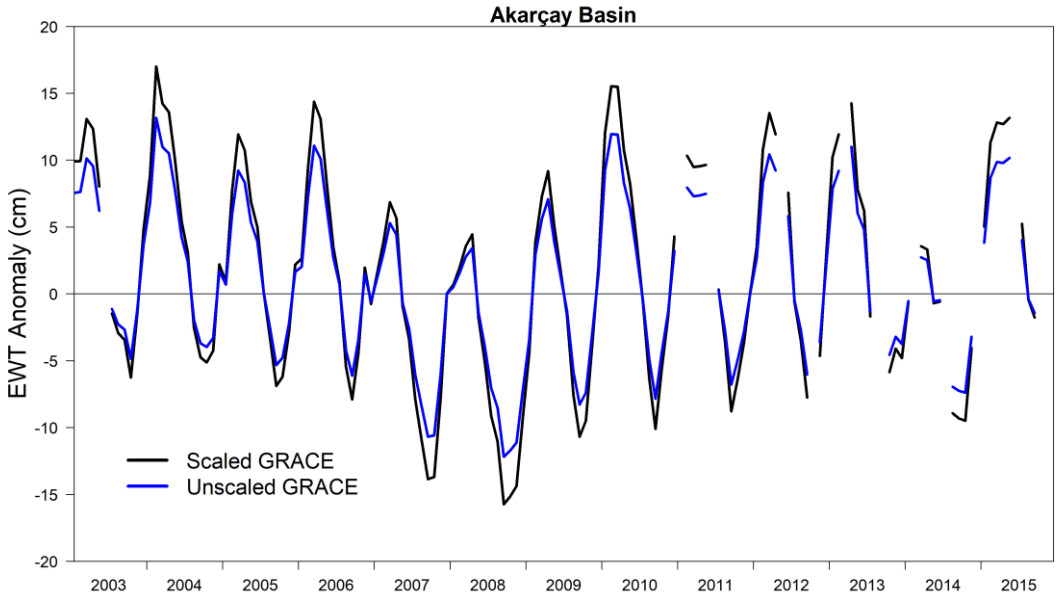

Figure C-1. Scaled and unscaled GRACE TWS time series of Akarçay Basin

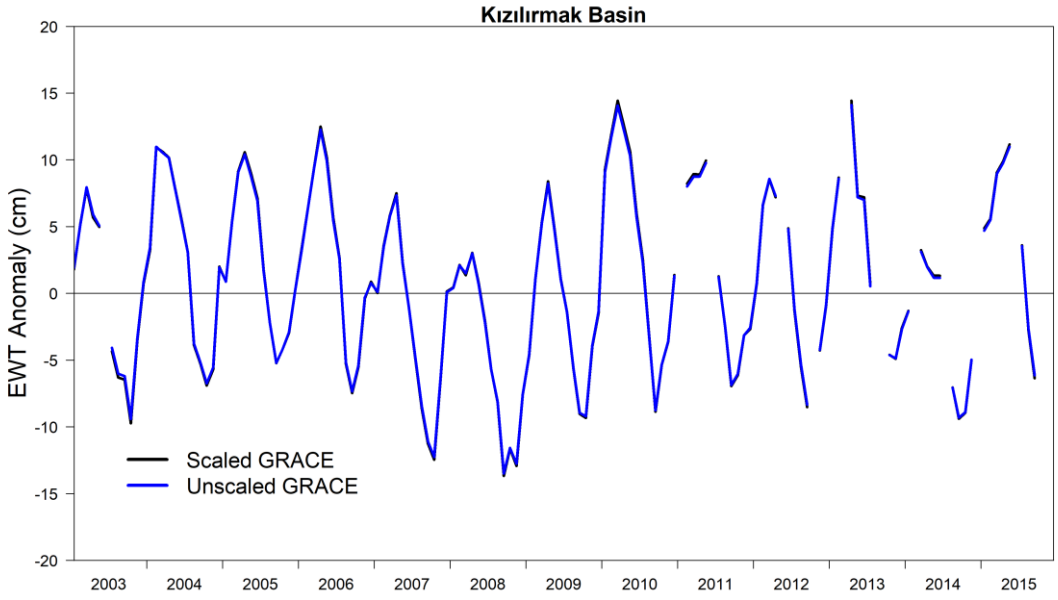

Figure C-2. Scaled and unscaled GRACE TWS time series of Kızılırmak Basin

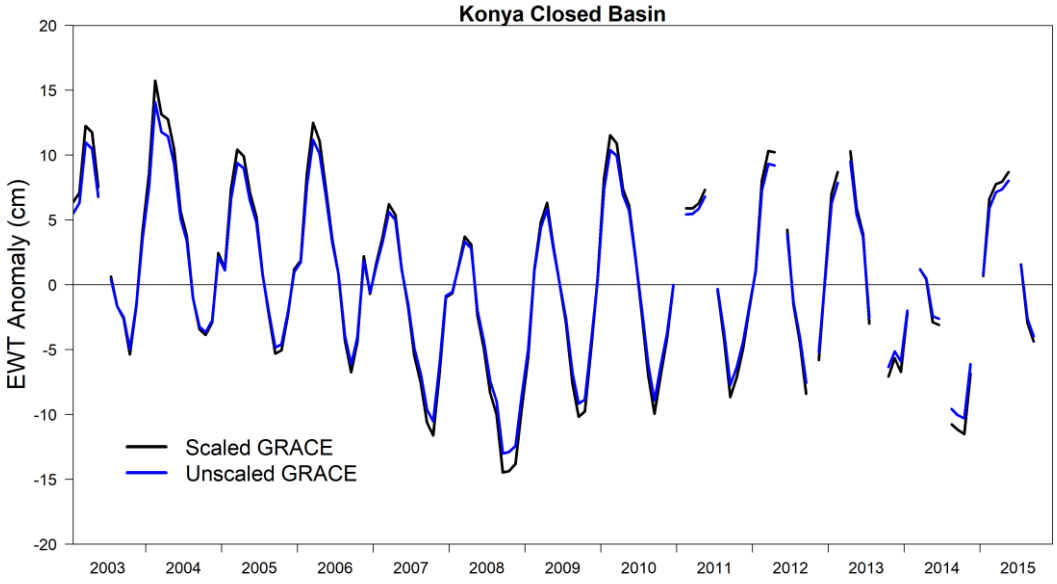

Figure C-3. Scaled and unscaled GRACE TWS time series of Konya Closed Basin

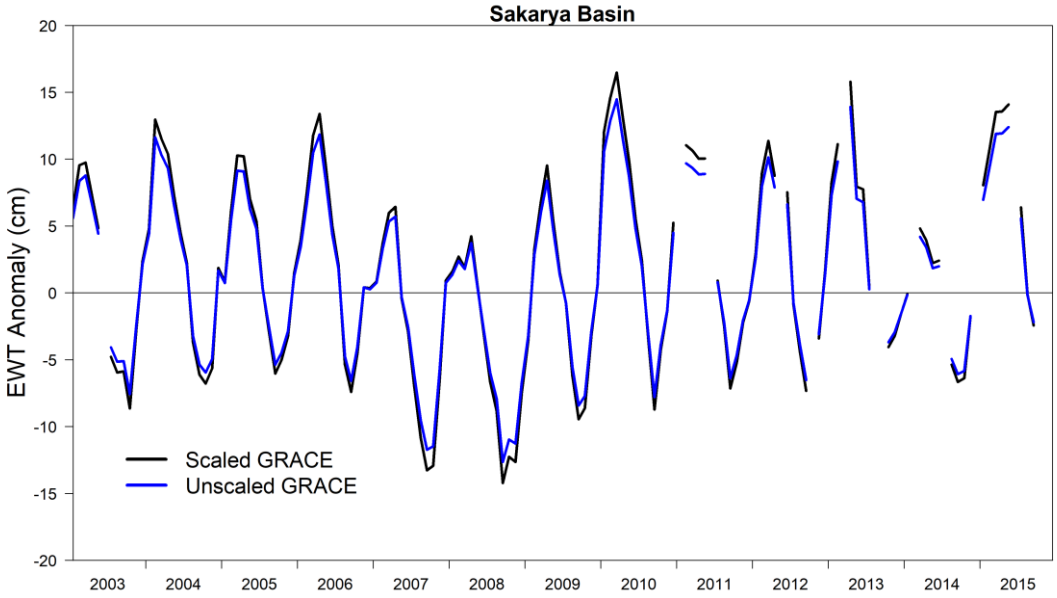

Figure C-4. Scaled and unscaled GRACE TWS time series of Sakarya Basin

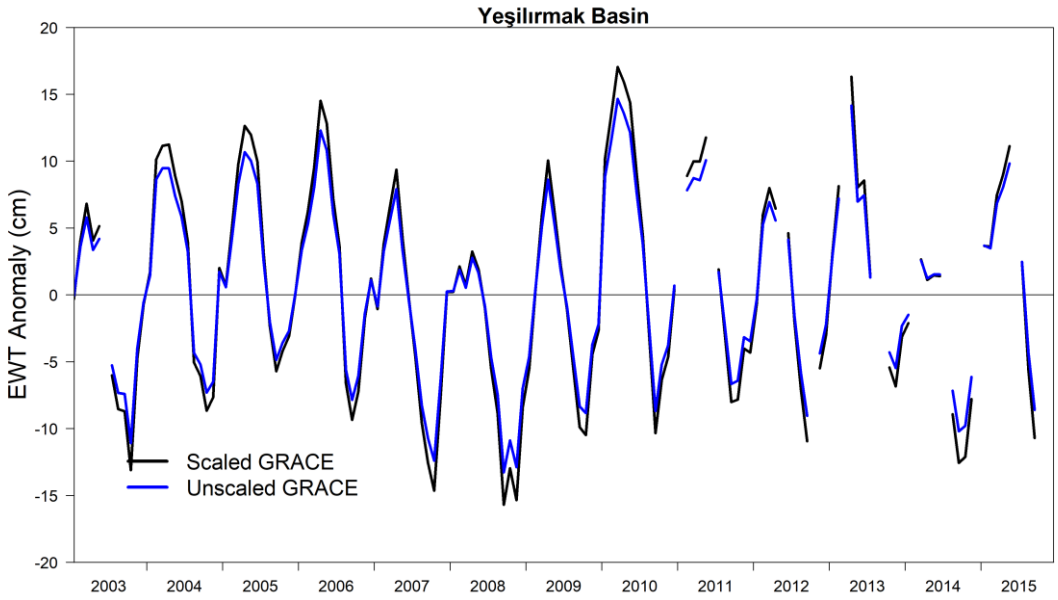

Figure C-5. Scaled and unscaled GRACE TWS time series of Yeşilırmak Basin

D. DECOMPOSITION OF GRACE TWS TIME SERIES

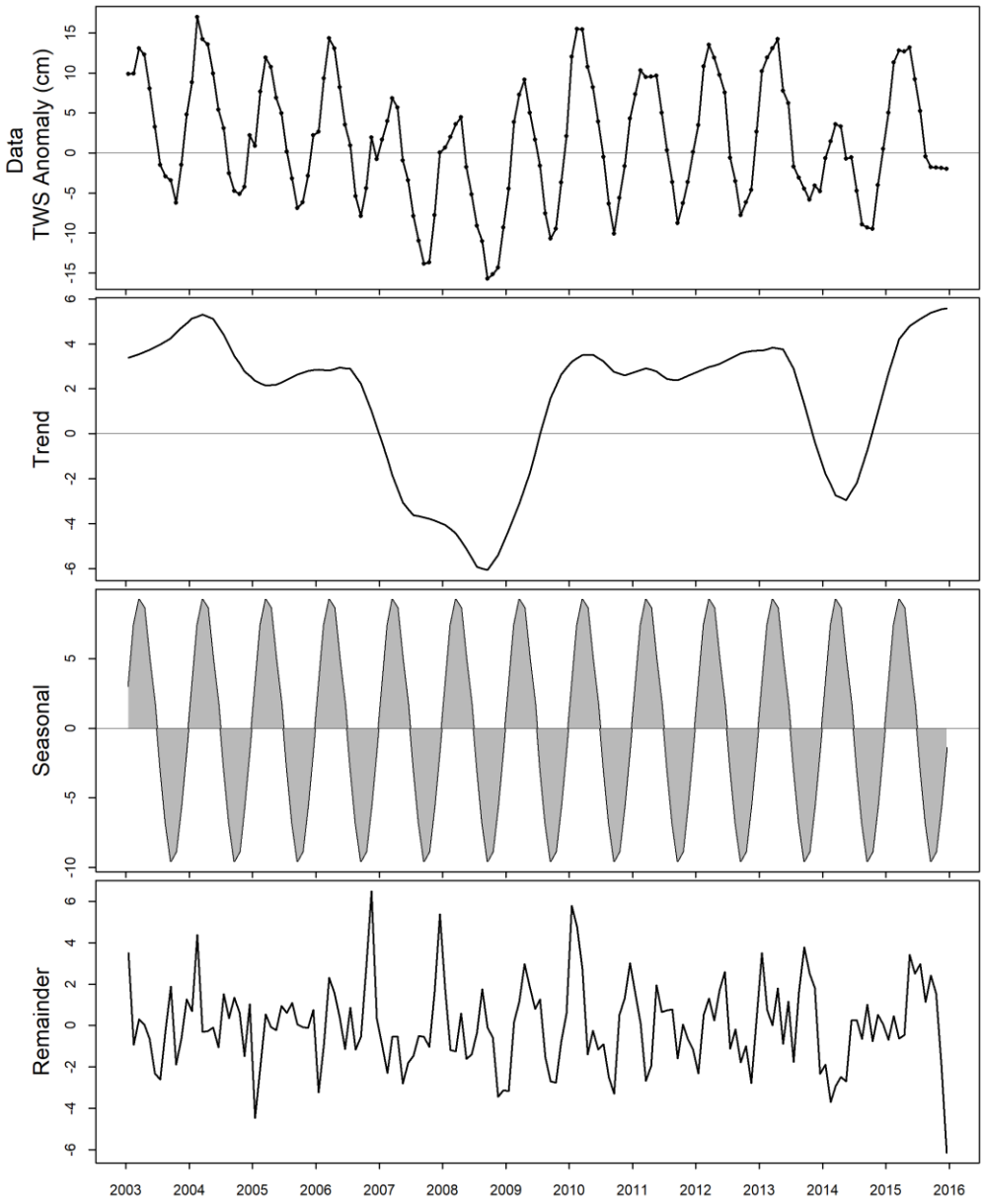

Figure D-1. GRACE TWS time series decomposition of Akarçay Basin

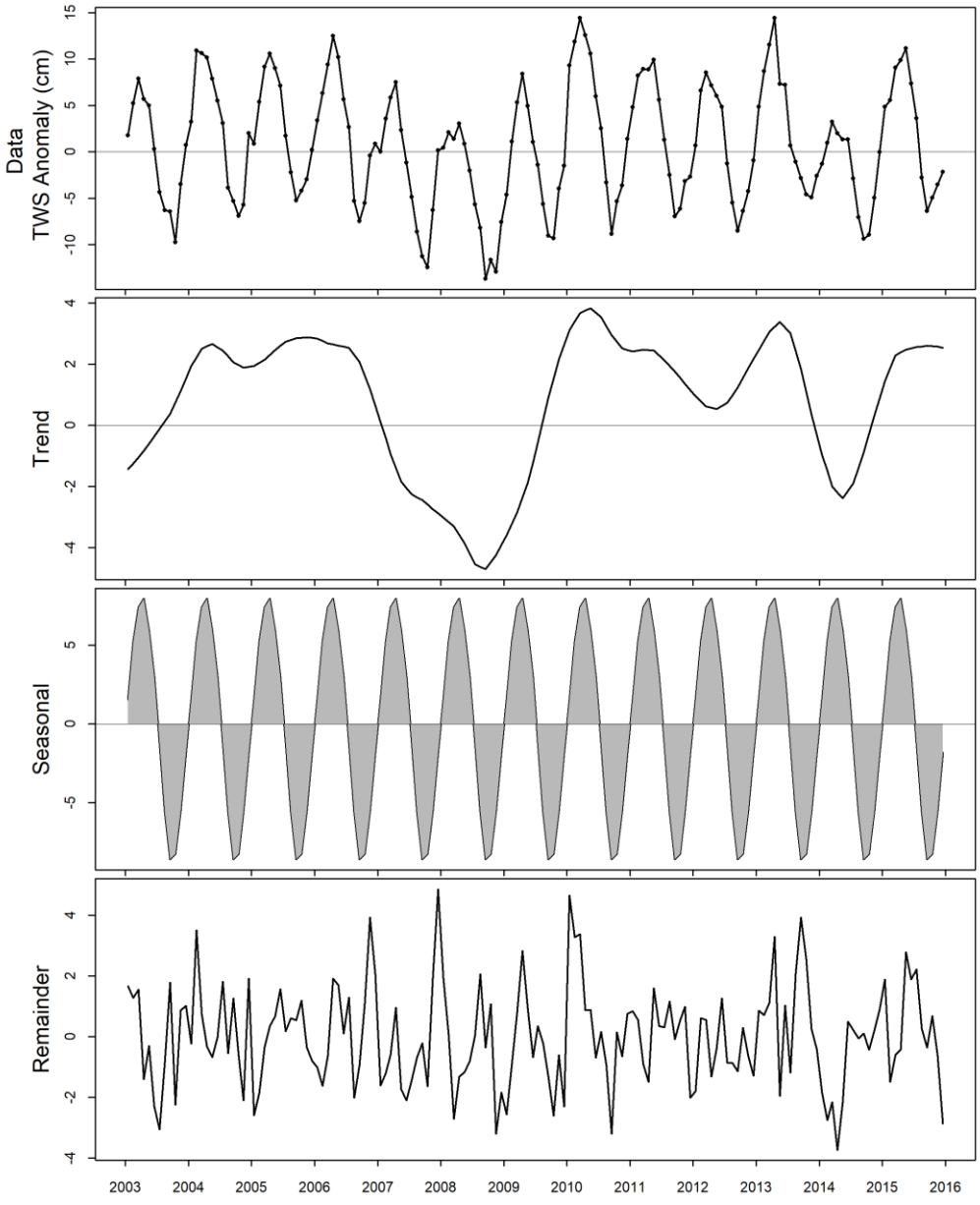

Figure D-2. GRACE TWS time series decomposition of Kızılırmak Basin

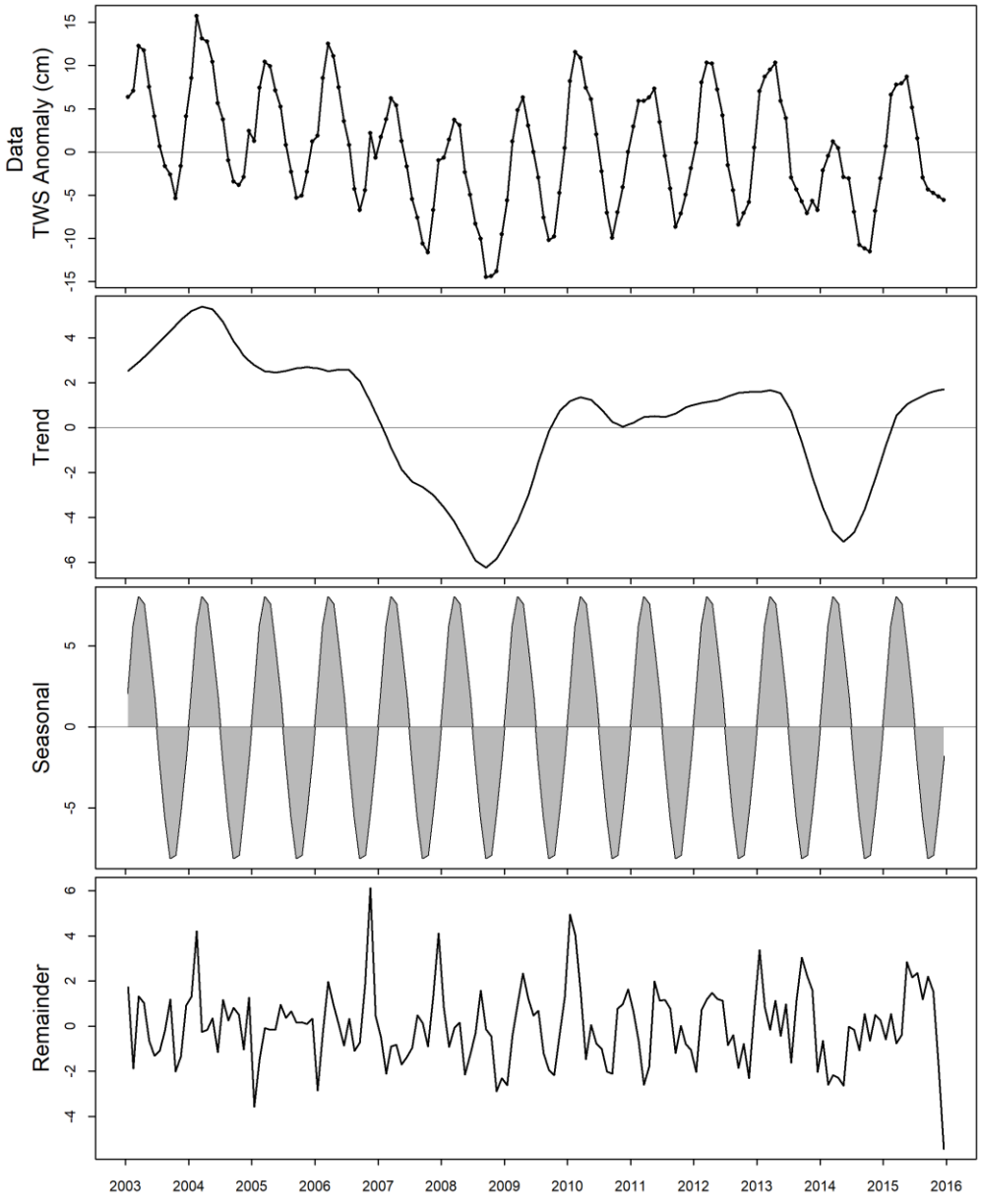

Figure D-3. GRACE TWS time series decomposition of Konya Closed Basin

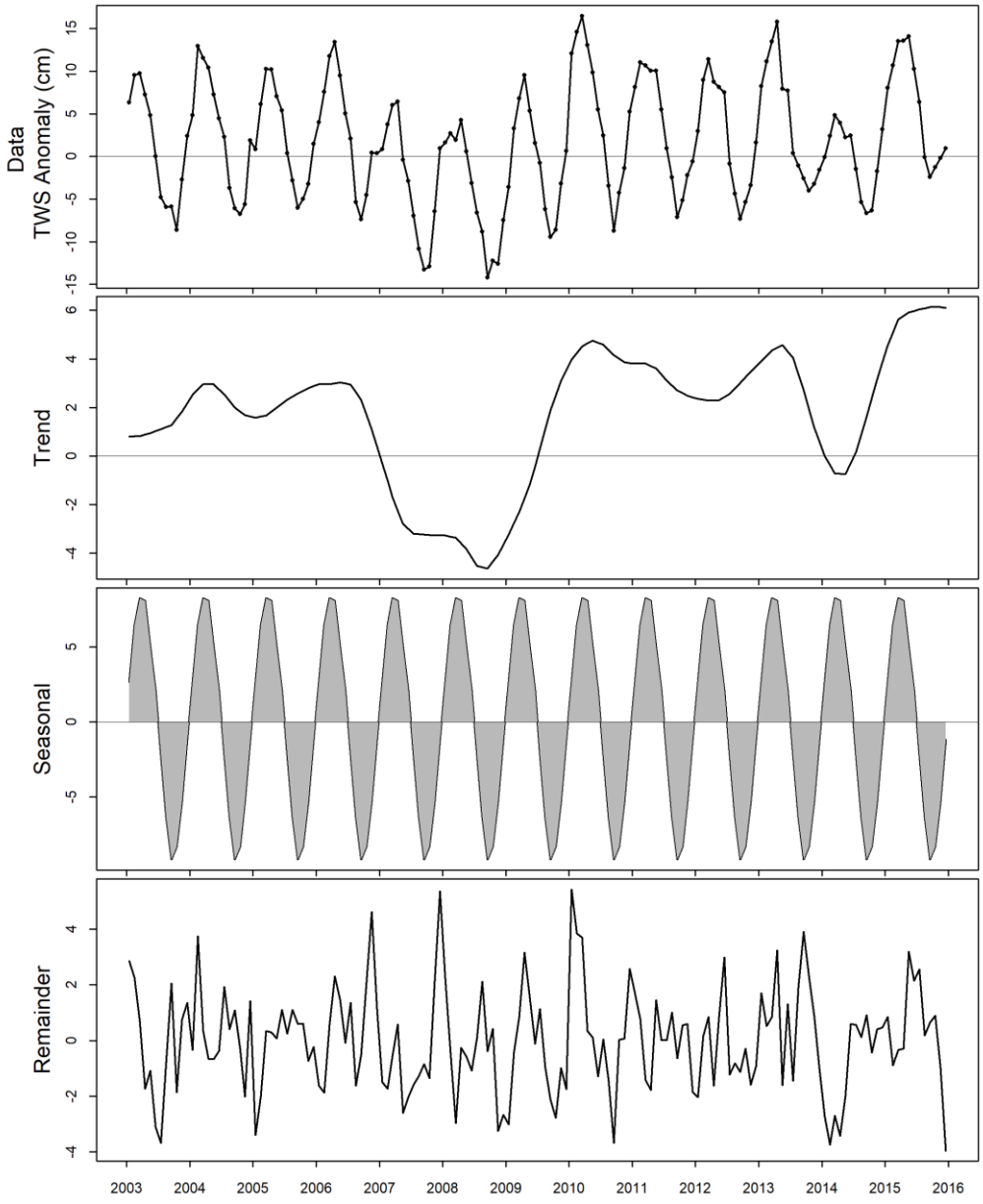

Figure D-4. GRACE TWS time series decomposition of Sakarya Basin

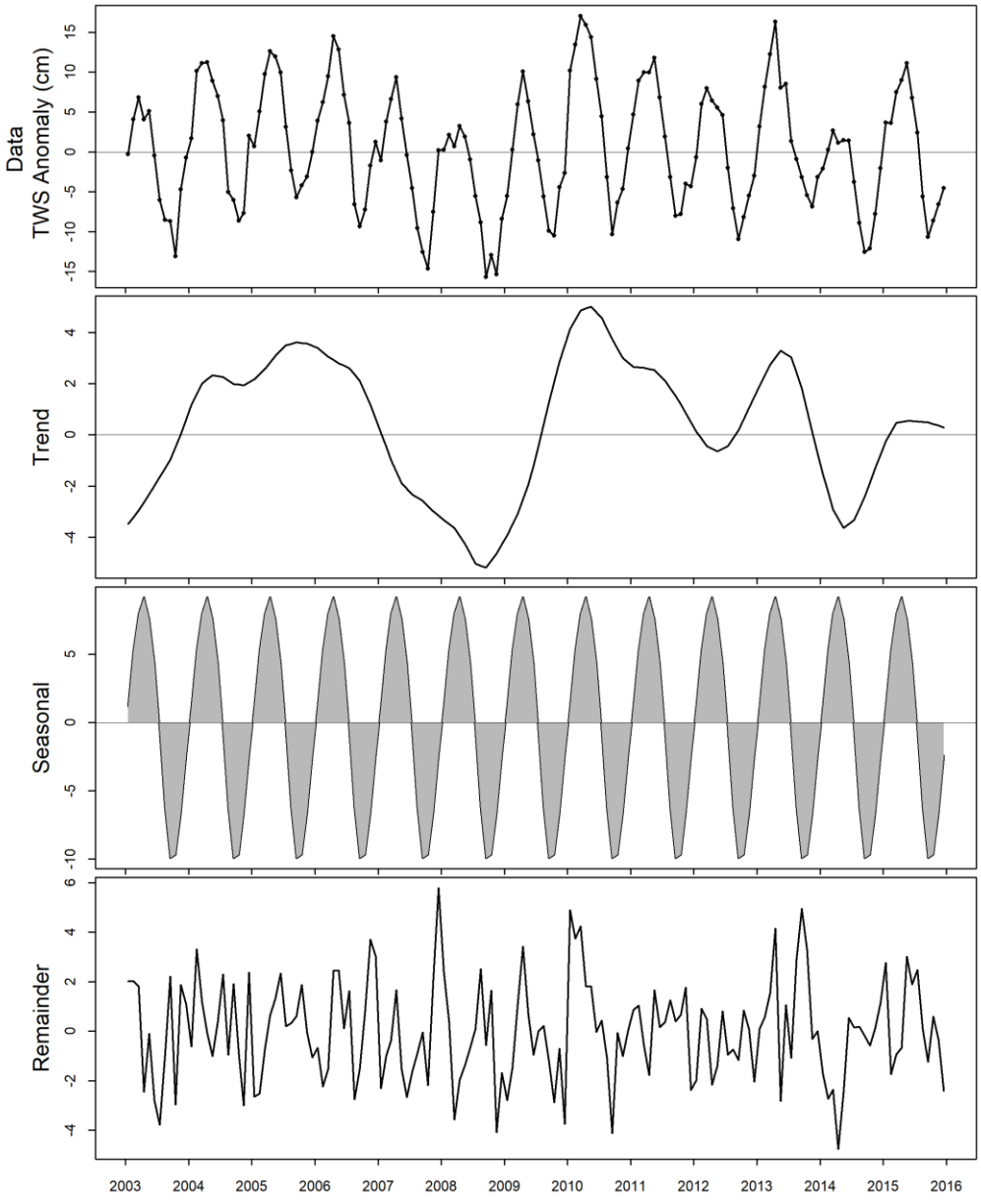

Figure D-5. GRACE TWS time series decomposition of Yeşilırmak Basin

E. COMPARISON OF DESEASONALIZED GRACE TWS AND CDFM PRECIPITATIONS

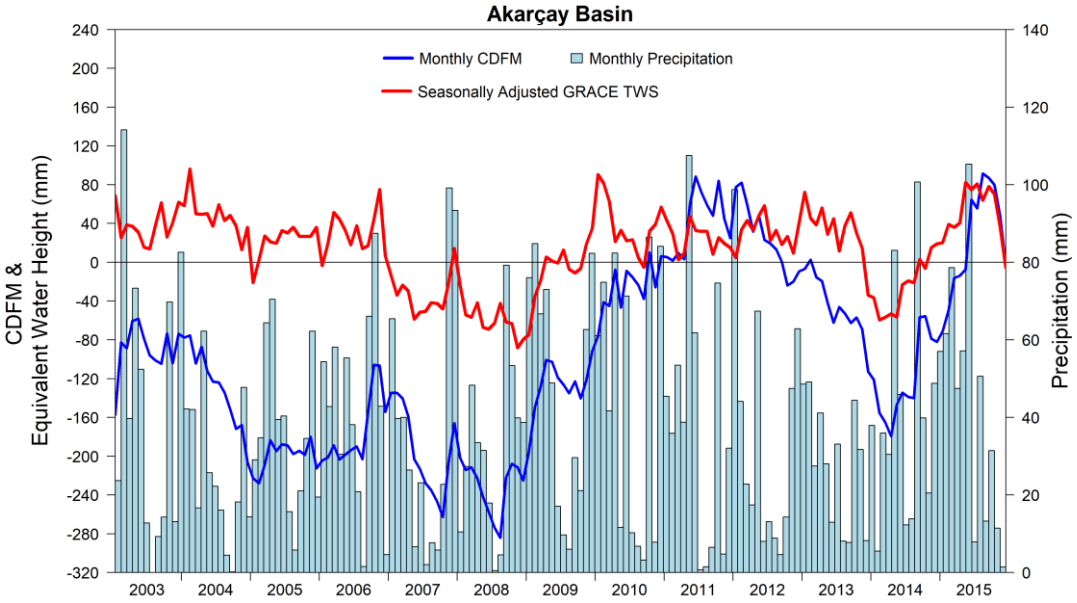

Figure E-1. CDFM and deseasonalized GRACE comparison over Akarçay Basin

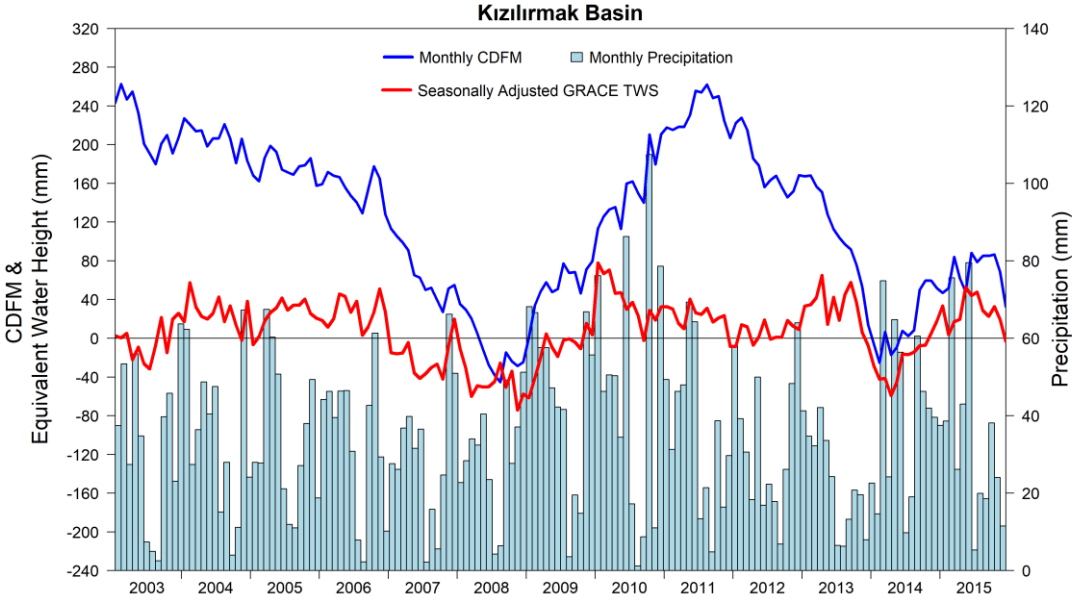

Figure E-2. CDFM and deseasonalized GRACE comparison over Kızılırmak Basin

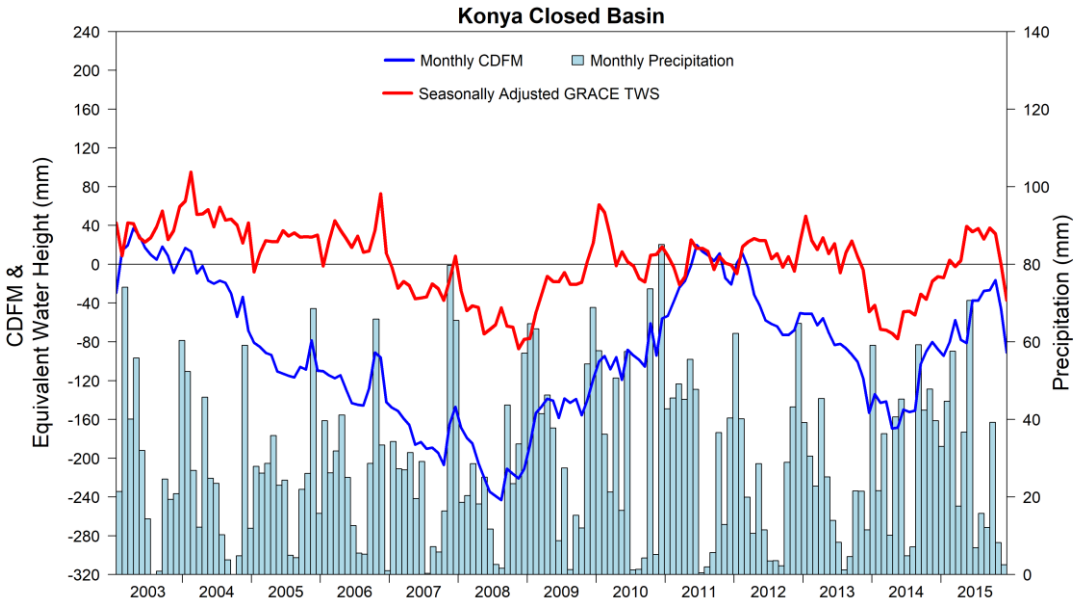

Figure E-3. CDFM and deseasonalized GRACE comparison over Konya Closed Basin

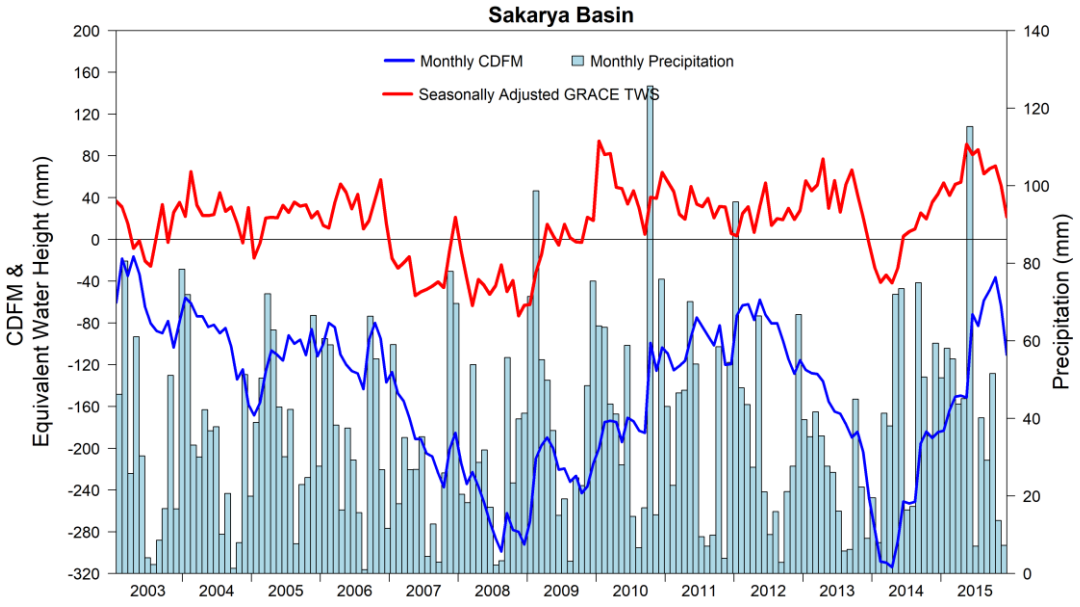

Figure E-4. CDFM and deseasonalized GRACE comparison over Sakarya Basin

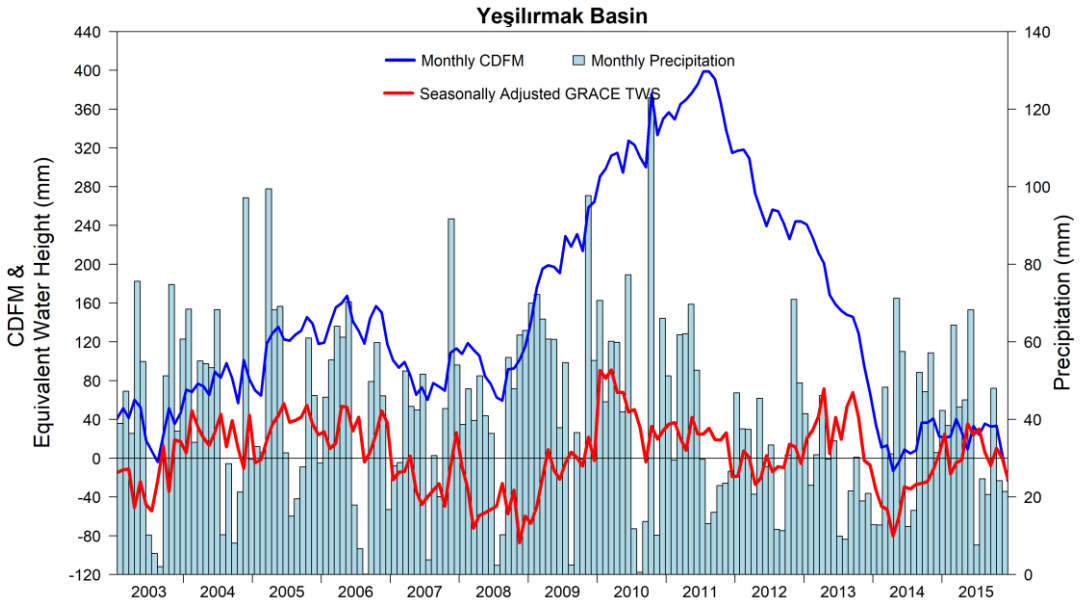

Figure E-5. CDFM and deseasonalized GRACE comparison over Yeşilırmak Basin

F. COMPARISON OF GLDAS MODEL VARIABLES

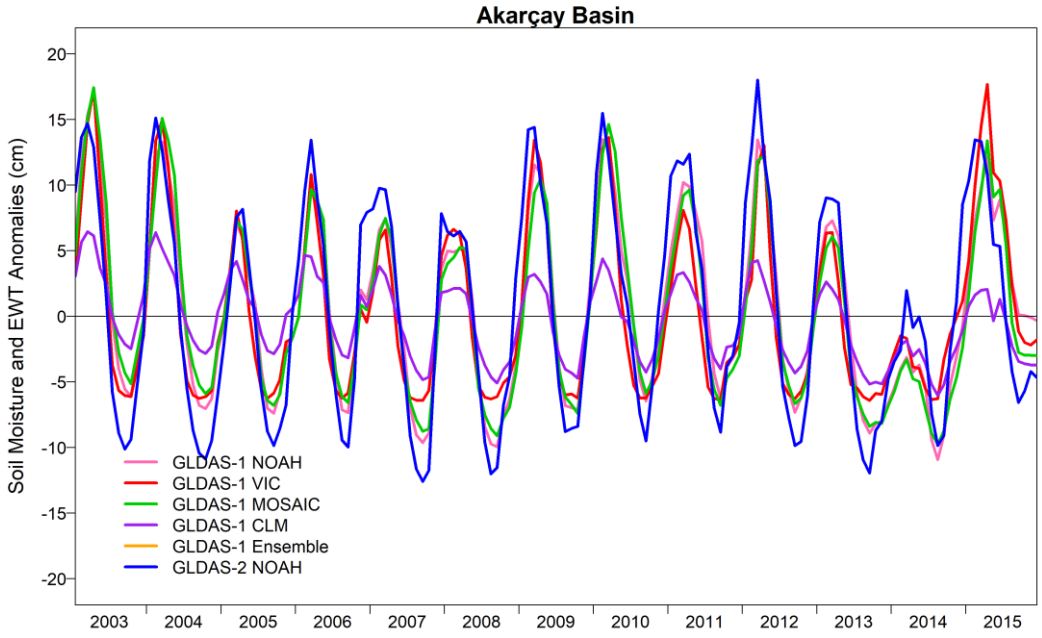

Figure F-1. Anomaly of soil moisture components over Akarçay Basin

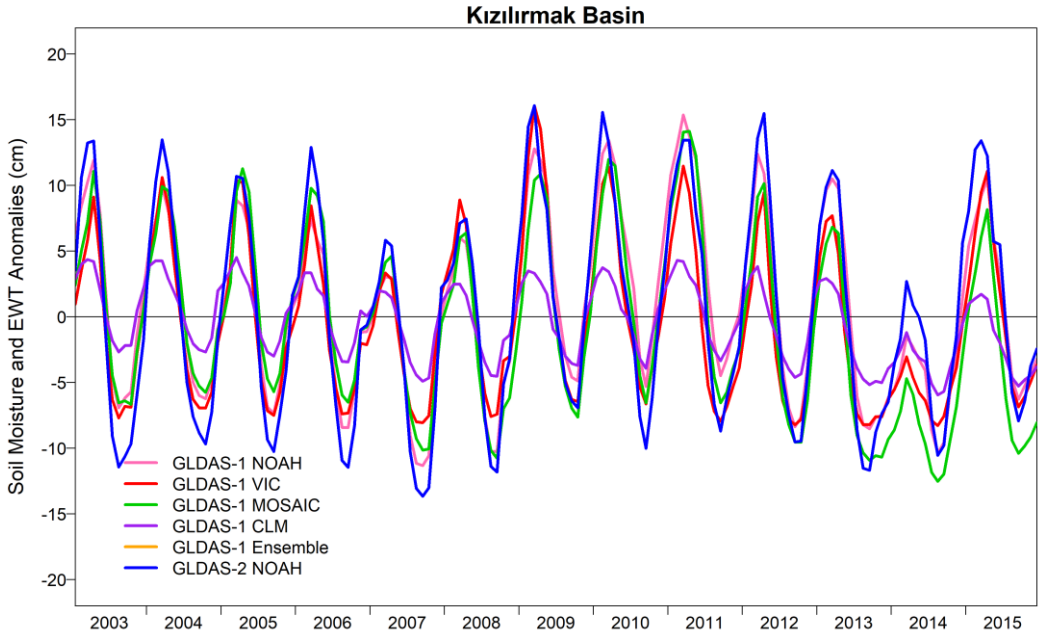

Figure F-2. Anomaly of soil moisture components over Kızılırmak Basin

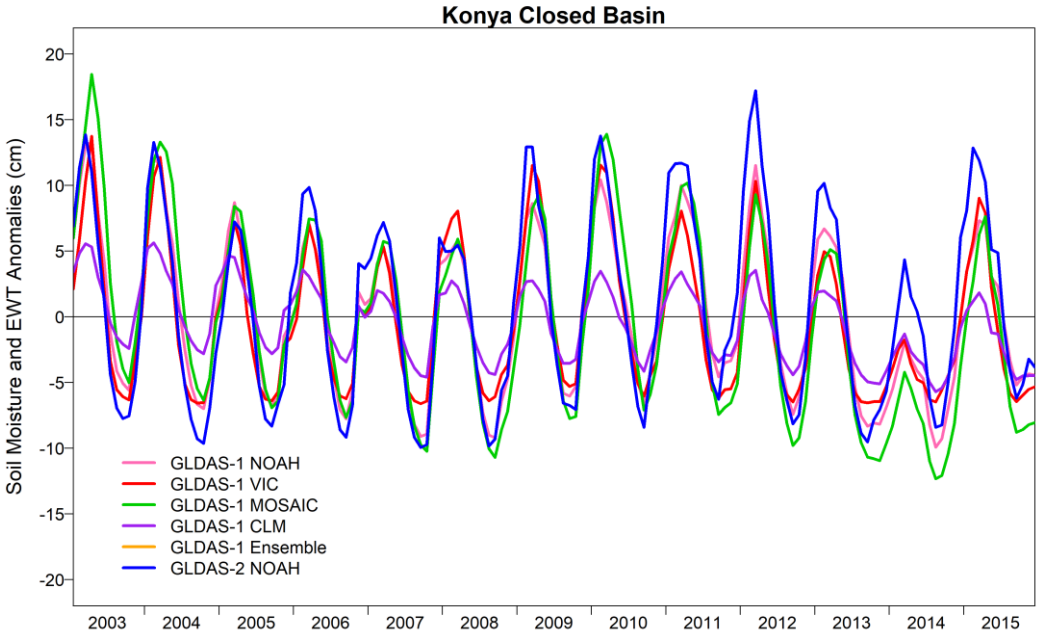

Figure F-3. Anomaly of soil moisture components over Konya Closed Basin

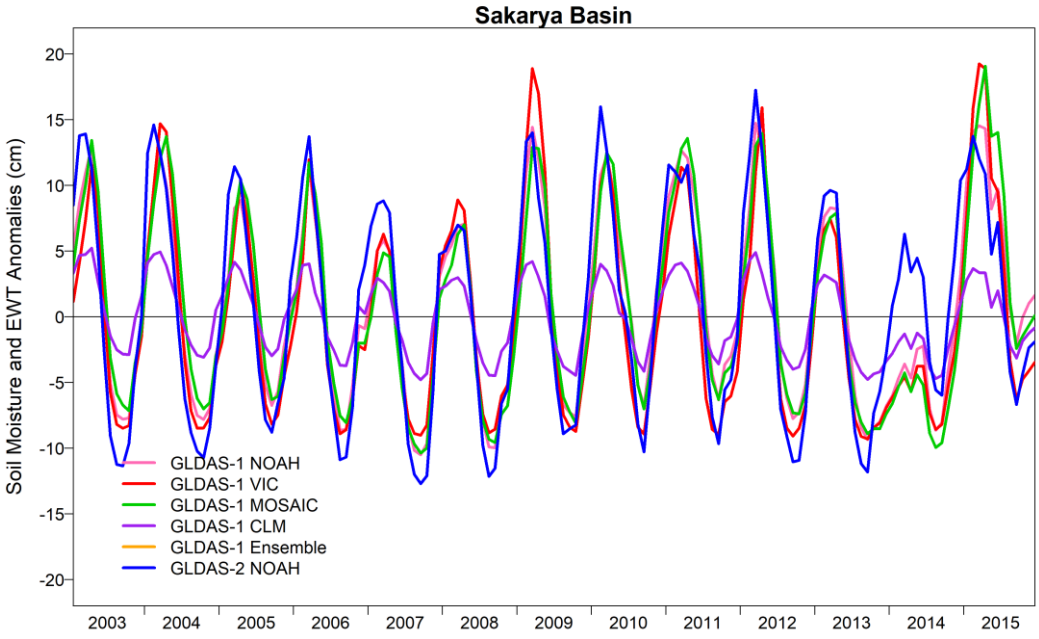

Figure F-4. Anomaly of soil moisture components over Sakarya Basin

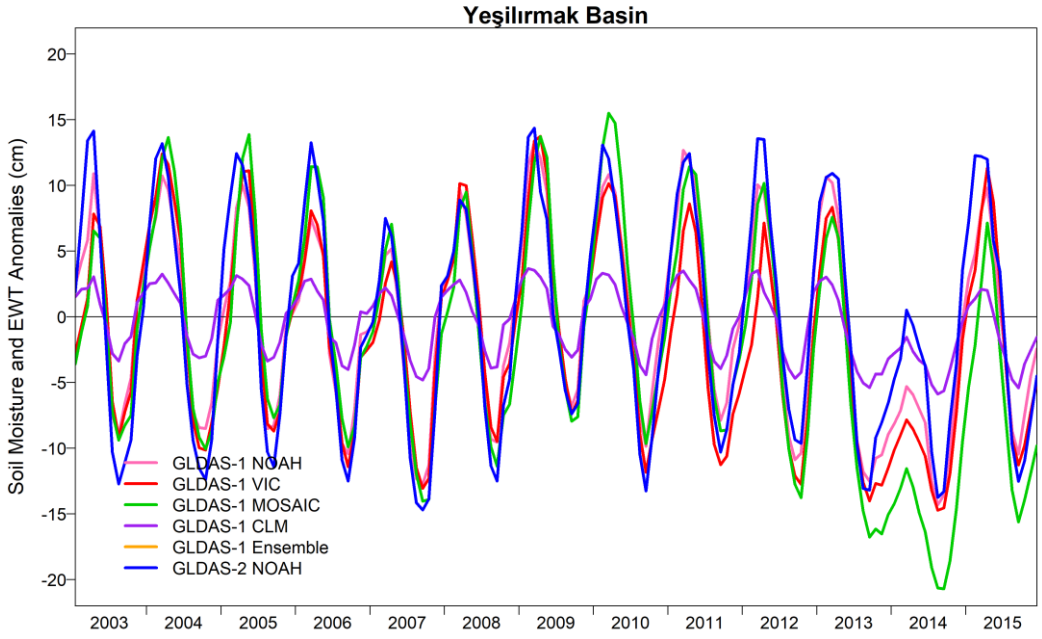

Figure F-5. Anomaly of soil moisture components over Yeşilırmak Basin

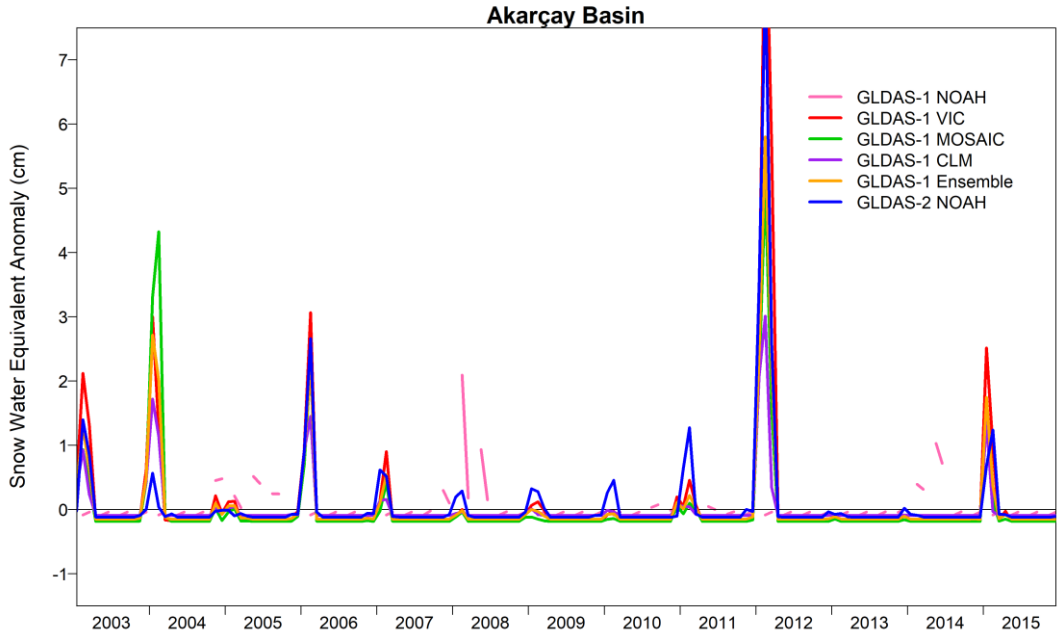

Figure F-6. Anomaly of snow water equivalent components over Akarçay Basin

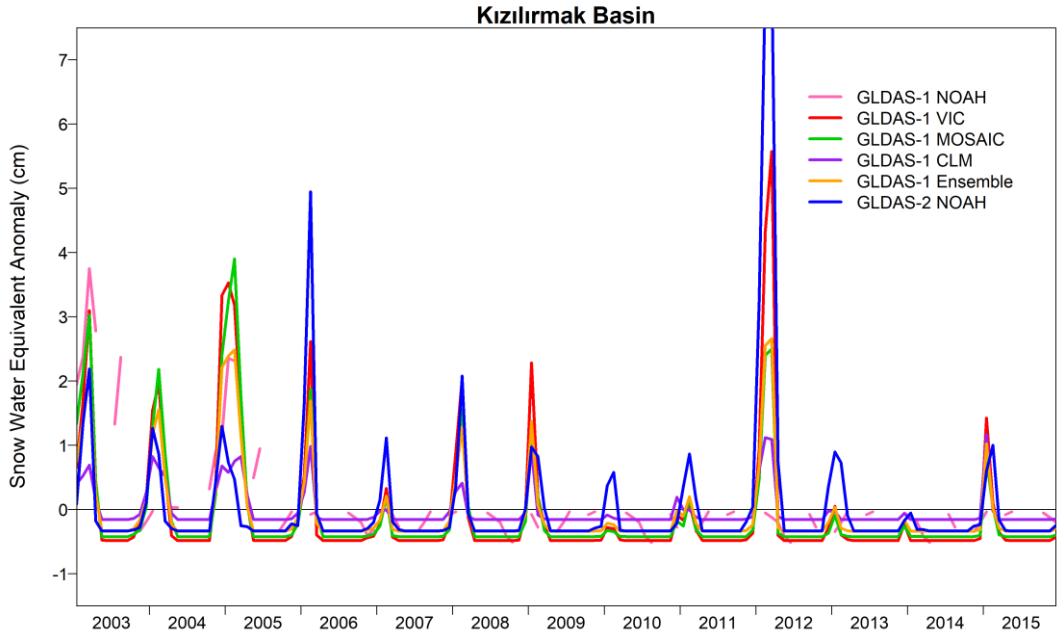

Figure F-7. Anomaly of snow water equivalent components over Kızılırmak Basin

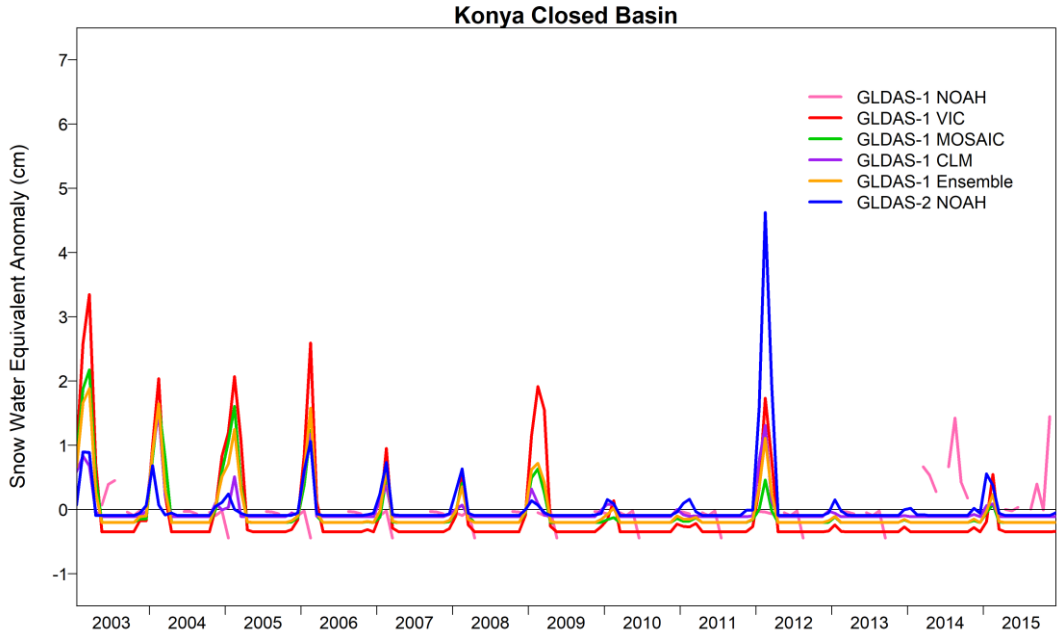

Figure F-8. Anomaly of snow water equivalent components over Konya Closed Basin

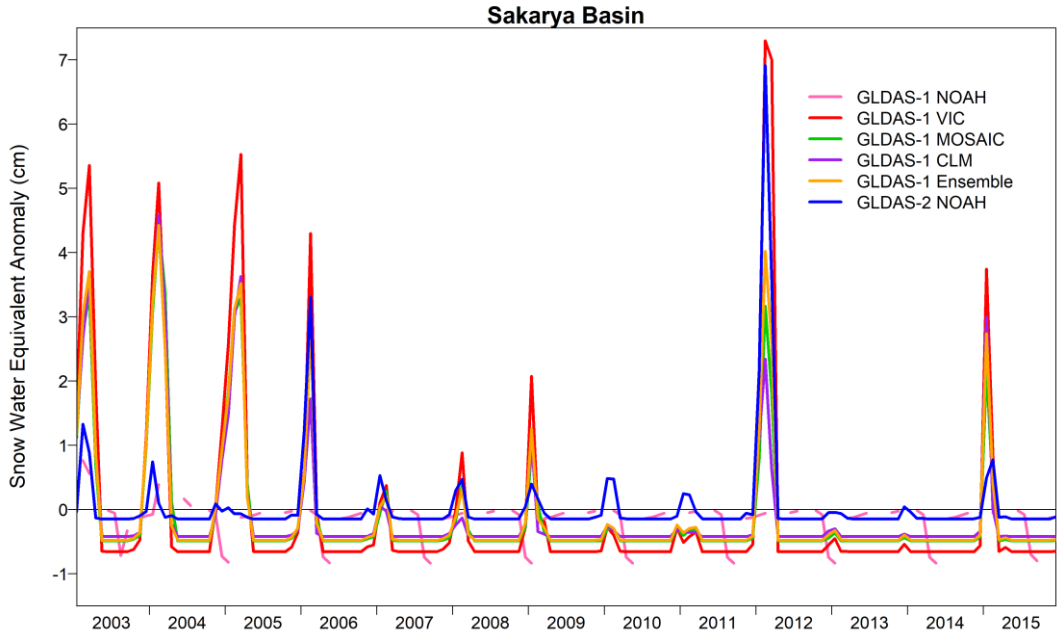

Figure F-9. Anomaly of snow water equivalent components over Sakarya Basin

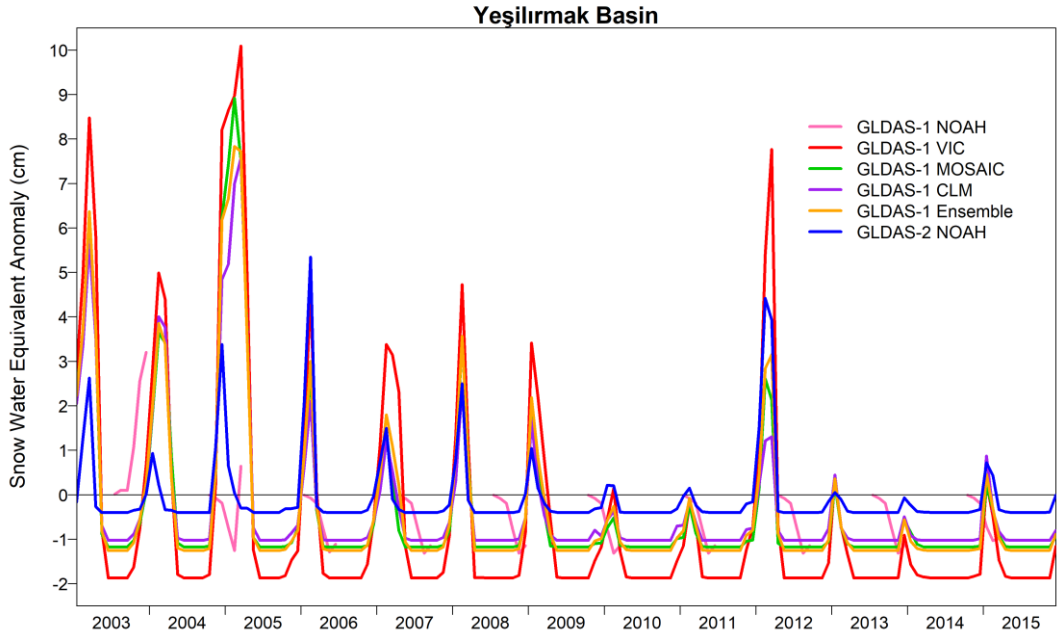

Figure F-10. Anomaly of snow water equivalent components over Yeşilırmak Basin

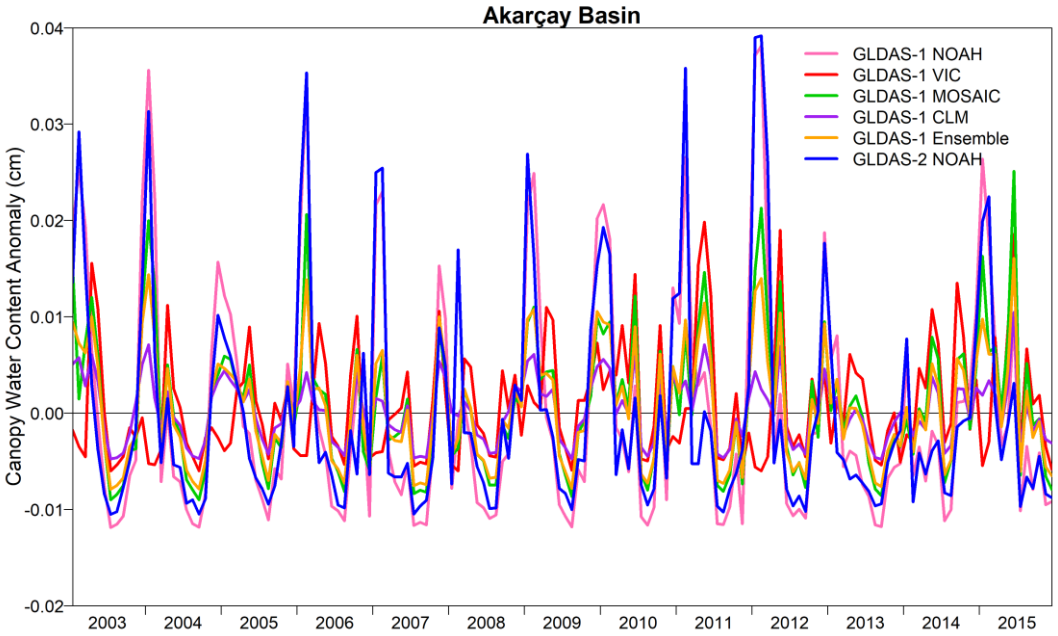

Figure F-11. Anomaly of canopy water content components over Akarçay Basin

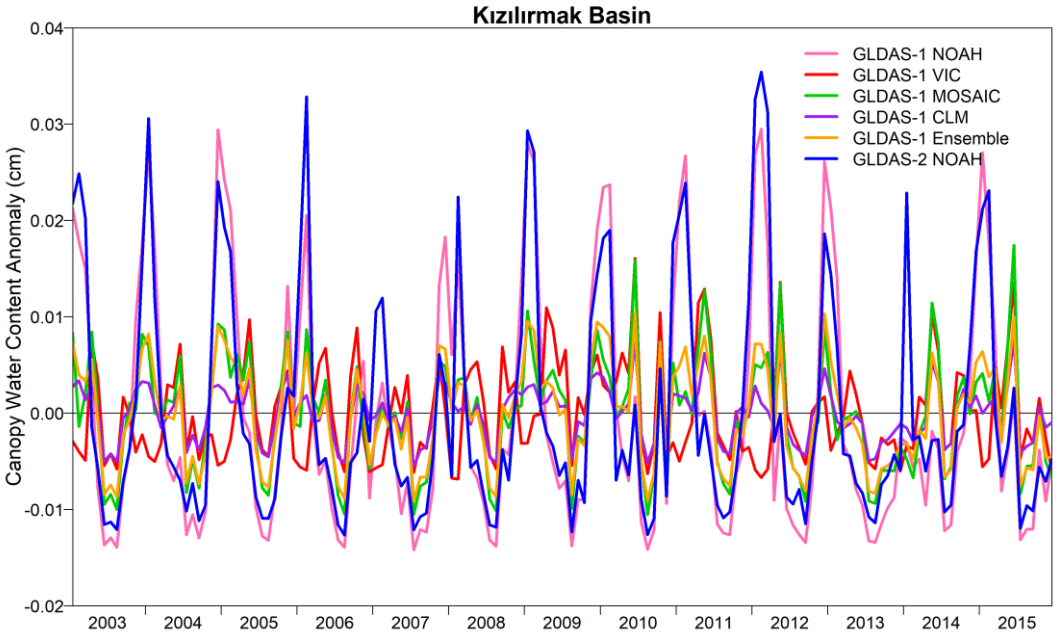

Figure F-12. Anomaly of canopy water content components over Kızılırmak Basin

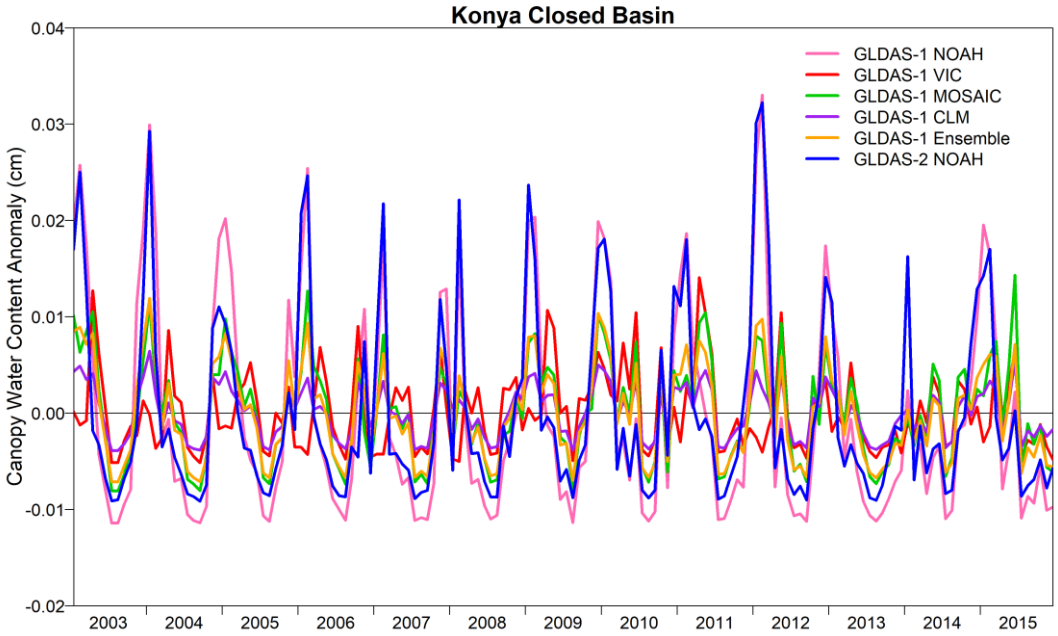

Figure F-13. Anomaly of canopy water content components over Konya Closed Basin

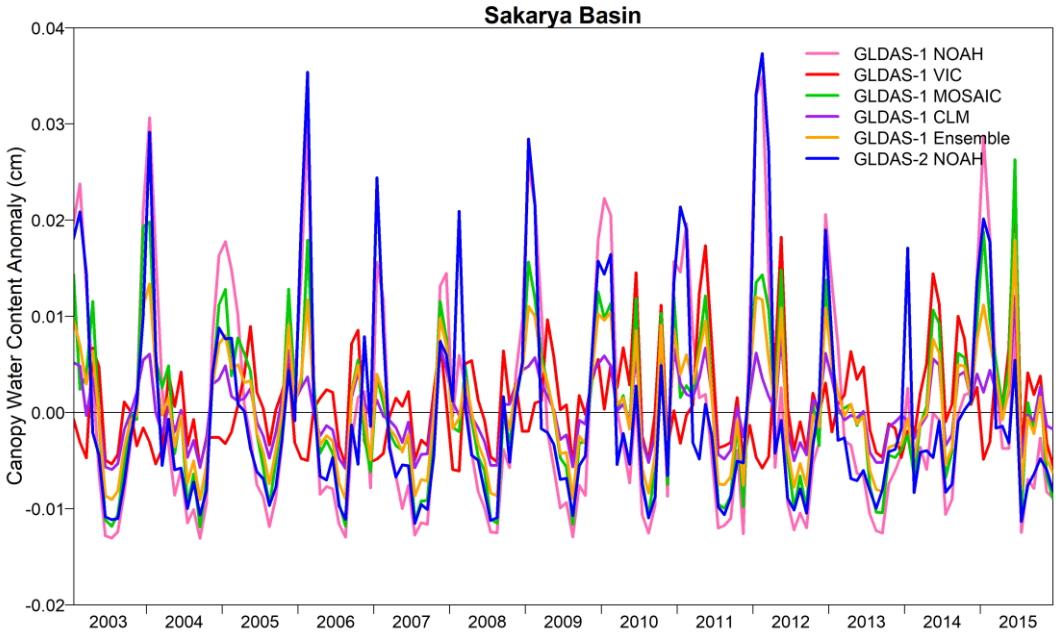

Figure F-14. Anomaly of canopy water content components over Sakarya Basin

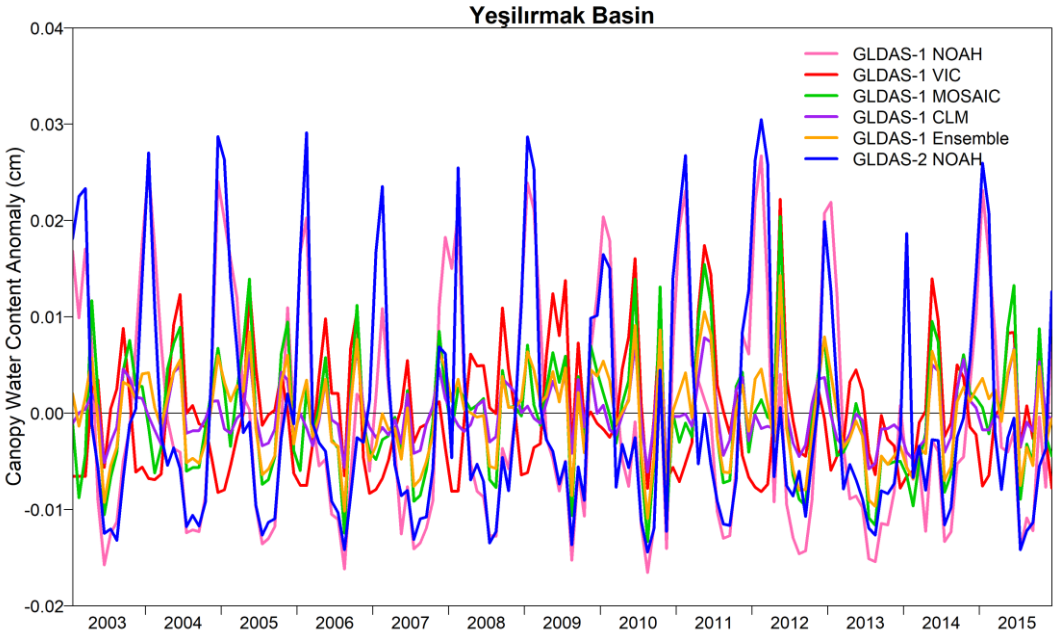

Figure F-15. Anomaly of canopy water content components over Yeşilırmak Basin

G. LAGGED CROSS-CORRELATIONS OF GWS ESTIMATES

		GWS						GRACE TWS
		GLDAS-1					GLDAS-2	
		NOAH	VIC	MOSAIC	CLM	Ensemble	NOAH	
Well Average	Lag -3	-0.14	-0.10	-0.17	0.07	-0.08	-0.15	0.26
	Lag -2	-0.07	0.00	-0.13	0.28	0.06	-0.12	0.48
	Lag -1	0.03	0.17	-0.05	0.45	0.21	-0.02	0.62
	Lag 0	0.09	0.34	0.01	0.50	0.31	0.11	0.64
	Lag 1	0.13	0.42	0.04	0.44	0.33	0.27	0.54
	Lag 2	0.16	0.43	0.04	0.30	0.28	0.43	0.35
	Lag 3	0.13	0.34	-0.03	0.08	0.15	0.51	0.10
Well Thiessen	Lag -3	-0.08	-0.06	-0.13	0.11	-0.02	-0.12	0.30
	Lag -2	-0.01	0.04	-0.08	0.32	0.11	-0.07	0.50
	Lag -1	0.05	0.18	-0.05	0.46	0.22	0.02	0.62
	Lag 0	0.12	0.32	0.00	0.50	0.31	0.16	0.63
	Lag 1	0.13	0.39	0.01	0.41	0.30	0.30	0.51
	Lag 2	0.16	0.40	0.01	0.26	0.25	0.45	0.31
	Lag 3	0.12	0.33	-0.04	0.05	0.13	0.52	0.07

Figure G-1. Cross correlation between groundwater components over Akarçay Basin

		GWS						GRACE TWS
		GLDAS-1					GLDAS-2	
		NOAH	VIC	MOSAIC	CLM	Ensemble	NOAH	
Well Average	Lag -3	-0.33	-0.06	-0.19	0.02	-0.15	-0.26	0.16
	Lag -2	-0.30	-0.06	-0.19	0.15	-0.10	-0.28	0.29
	Lag -1	-0.23	0.03	-0.15	0.27	0.00	-0.22	0.38
	Lag 0	-0.09	0.19	-0.01	0.38	0.15	-0.08	0.44
	Lag 1	0.10	0.36	0.15	0.44	0.32	0.13	0.44
	Lag 2	0.20	0.42	0.21	0.37	0.35	0.25	0.32
	Lag 3	0.27	0.42	0.25	0.27	0.35	0.34	0.18
Well Thiessen	Lag -3	-0.17	0.16	0.00	0.15	0.05	-0.07	0.17
	Lag -2	-0.11	0.21	0.06	0.21	0.12	-0.02	0.21
	Lag -1	-0.06	0.25	0.09	0.24	0.16	0.02	0.23
	Lag 0	0.03	0.34	0.18	0.28	0.25	0.09	0.25
	Lag 1	0.13	0.41	0.26	0.30	0.32	0.17	0.24
	Lag 2	0.19	0.42	0.30	0.27	0.34	0.21	0.20
	Lag 3	0.23	0.43	0.33	0.24	0.35	0.25	0.14

Figure G-2. Cross correlation between groundwater components over Kızılırmak Basin

		GWS						GRACE TWS
		GLDAS-1					GLDAS-2	
		NOAH	VIC	MOSAIC	CLM	Ensemble	NOAH	
Well Average	Lag -3	0.18	0.20	-0.15	0.12	0.11	0.36	0.29
	Lag -2	0.22	0.24	-0.15	0.22	0.17	0.36	0.39
	Lag -1	0.28	0.30	-0.15	0.31	0.23	0.40	0.47
	Lag 0	0.34	0.35	-0.13	0.36	0.29	0.46	0.50
	Lag 1	0.40	0.40	-0.10	0.36	0.33	0.54	0.47
	Lag 2	0.44	0.42	-0.06	0.31	0.33	0.62	0.39
	Lag 3	0.45	0.41	-0.03	0.22	0.31	0.66	0.28
Well Thiessen	Lag -3	0.10	0.13	-0.22	0.05	0.03	0.30	0.24
	Lag -2	0.14	0.16	-0.23	0.16	0.09	0.29	0.36
	Lag -1	0.21	0.22	-0.22	0.27	0.17	0.33	0.46
	Lag 0	0.27	0.29	-0.21	0.34	0.22	0.39	0.51
	Lag 1	0.34	0.34	-0.17	0.36	0.28	0.48	0.49
	Lag 2	0.40	0.37	-0.14	0.31	0.29	0.57	0.41
	Lag 3	0.41	0.37	-0.10	0.21	0.27	0.63	0.28

Figure G-3. Cross correlation between groundwater components over Konya Closed Basin

		GWS						GRACE TWS
		GLDAS-1					GLDAS-2	
		NOAH	VIC	MOSAIC	CLM	Ensemble	NOAH	
Well Average	Lag -3	0.05	0.10	-0.01	0.20	0.11	0.01	0.32
	Lag -2	0.08	0.09	-0.01	0.35	0.17	0.02	0.48
	Lag -1	0.16	0.15	0.03	0.48	0.27	0.11	0.58
	Lag 0	0.29	0.27	0.13	0.56	0.39	0.25	0.61
	Lag 1	0.41	0.38	0.21	0.54	0.47	0.39	0.52
	Lag 2	0.46	0.45	0.25	0.42	0.47	0.50	0.36
	Lag 3	0.48	0.48	0.27	0.26	0.44	0.57	0.15
Well Thiessen	Lag -3	-0.08	-0.10	-0.19	0.12	-0.06	-0.09	0.32
	Lag -2	-0.01	-0.08	-0.17	0.27	0.03	-0.03	0.44
	Lag -1	0.08	0.00	-0.11	0.38	0.12	0.09	0.52
	Lag 0	0.20	0.12	-0.03	0.42	0.23	0.23	0.50
	Lag 1	0.30	0.23	0.05	0.38	0.29	0.37	0.40
	Lag 2	0.35	0.29	0.09	0.25	0.29	0.47	0.23
	Lag 3	0.36	0.33	0.11	0.09	0.26	0.50	0.05

Figure G-4. Cross correlation between groundwater components over Sakarya Basin

		GWS						GRACE TWS
		GLDAS-1					GLDAS-2	
		NOAH	VIC	MOSAIC	CLM	Ensemble	NOAH	
Well Average	Lag -3	-0.08	0.00	-0.03	0.10	0.00	-0.17	0.28
	Lag -2	0.03	0.06	-0.02	0.32	0.12	-0.10	0.48
	Lag -1	0.20	0.19	0.06	0.53	0.29	0.06	0.61
	Lag 0	0.37	0.35	0.19	0.63	0.45	0.25	0.62
	Lag 1	0.56	0.51	0.35	0.63	0.59	0.45	0.52
	Lag 2	0.63	0.59	0.44	0.48	0.61	0.56	0.29
	Lag 3	0.61	0.60	0.49	0.26	0.55	0.59	0.03
Well Thiessen	Lag -3	-0.46	-0.47	-0.60	0.18	-0.37	-0.50	0.54
	Lag -2	-0.23	-0.30	-0.50	0.47	-0.14	-0.28	0.75
	Lag -1	0.04	-0.08	-0.34	0.65	0.09	0.02	0.79
	Lag 0	0.27	0.13	-0.17	0.66	0.26	0.30	0.64
	Lag 1	0.38	0.27	-0.04	0.48	0.32	0.49	0.34
	Lag 2	0.38	0.33	0.03	0.21	0.27	0.55	-0.01
	Lag 3	0.27	0.29	0.04	-0.10	0.14	0.50	-0.31

Figure G-5. Cross correlation between groundwater components over Yeşilırmak Basin